INTRODUCTION TO
Photon Science and Technology

INTRODUCTION TO
Photon Science and Technology

David L. Andrews
David S. Bradshaw

SPIE PRESS
Bellingham, Washington USA

Library of Congress Cataloging-in-Publication Data

Names: Andrews, David L., author | Bradshaw, David S., author.
Title: Introduction to photon science and technology / David L. Andrews and David S. Bradshaw.
Description: Bellingham, Washington, USA : SPIE Press, [2018] | Includes bibliographical references and index.
Identifiers: ISBN 9781510621954 (soft cover) | ISBN 1510621954 (soft cover) | ISBN 9781510621961 (PDF) | ISBN 1510621962 (PDF) | ISBN 9781510621978 (ePub) | ISBN 1510621970 (ePub) | ISBN 9781510621985 (Kindle) | ISBN 1510621989 (Kindle)
Subjects: LCSH: Photonics.
LC record available at https://lccn.loc.gov/2018026666

Published by
SPIE
P.O. Box 10
Bellingham, Washington 98227-0010 USA
Phone: +1 360.676.3290
Fax: +1 360.647.1445
Email: books@spie.org
Web: http://spie.org

Printed in the United States of America.
First printing.
For updates to this book, visit http://spie.org and type “PM293” in the search field.

Cover image courtesy of Shutterstock.

Dedicated to all who seek truth in the pursuit of light.

Contents

Preface

Photonics is a technology that has rapidly gained recognition as one of the most important areas of modern development. Worldwide, this enterprise generates over 500 billion dollars of annual trade, which since 2015 has been accounting for employment figures of more than two million individuals.[1] In funding circles, photonics is now widely accepted as a "key enabling domain," in which entirely new scientific and technological spheres of application are keenly anticipated. Indeed, it is often remarked that the present century will become—if it is not already—one in which light and photonics will supplant the previous role of electricity and electronics in modern society. It is entirely fitting that this should be so: the term "photonics" was originally introduced to the technical community by Eugen Sänger, with just such a vision in mind.[2] Acceptance of the term was accelerated when, in 1982, the trade publication previously entitled *Optical Spectra* changed its name to *Photonics Spectra*; its consolidation in academic circles came with the 1991 publication of Saleh and Teich's masterwork.[3]

Today, photonics is a field that has opened up a host of new avenues for research and applications, to the extent that in a typical year there are numerous scientific and technical conferences taking place around the globe, including major conventions such as Photonics West. While scientific advances race on in fields including quantum optics, cavity photonics, nonlinear optics, plasmonics, and metamaterials, other areas of application are emerging in solid-state lighting and displays, optical interconnect technology, and electronic chips, alongside new platforms for quantum computing, bio-imaging, solar energy capture, and many more.

True to form, just as electronics has in the past led to microelectronics, so photonics now leads to microphotonics and nanophotonics. Topics such as these, once considered a fringe of the subject, have already become the core of modern photonics. This is not simply the result of a drive towards increasing miniaturization, pursued for its own ends; it also reflects the distinctive mechanisms that become operative at sub-micron scales.[4] Almost all of the recent innovations involving photonics would have been impossible without the disruptive breakthroughs at micron and sub-micron scales. As miniature lasers and microfabrication methods have continually evolved, parallel growth in the optical

fiber industry has helped spur the continued push towards the long-sought goal of total integration in optical devices.

So, with a broad spectrum of activity and progress typifying the whole sphere of photonics, one might ask where the nature of the photon itself fits. We know that light is made of photons.[5] How important is it that light is not simply represented as a continuous sinusoidal waveform, as seen in most optics textbooks? Even some research areas headlined as "photonics" can generate accounts that pay scant heed to the quantum nature of light—it is not hard to find work, even in this subject, in which the word "photon" fails to appear. Nonetheless, some areas, such as the burgeoning field of quantum optics and informatics, hinge upon the discrete nature of photons:[6] indeed, the sciences of color, spectroscopy, and photochemistry, and much of the technology of optical materials, depend on this simple premise. With an increasing number of phenomena that absolutely require full use of the photon concept, it is appropriate to look into the full meaning and significance of the photon.

The content of this book is now outlined. In Chapter 1, we begin with an overview of the history that eventually led to a photon-based understanding of optical phenomena, paving the way for the later development of the fully-fledged quantum theory of light. Chapter 2 then presents a broad perspective on the properties of the photon, and the associated characteristics of photon propagation both in free space and within dispersive and complex media. This is where links to modern photonics technology first begin to feature. Chapter 3 draws out some of the most striking quantum aspects of photon science, introducing a simple operator formalism that enables links to be shown with current developments in quantum communication, computation, and informatics.

Chapter 4 introduces and develops the modern field theory that underpins our whole understanding of light, relevant across the full range of optical and electrodynamic applications. Revisiting some of the simple concepts such as energy, linear momentum, and angular momentum in full quantum operator form provides a basis to understand the principles of not only conventional light, but also structured light such as optical vortices. The formal field theory also furnishes the feature known as vacuum fluctuations, whose nature and significance are far more pervasive than is commonly recognized, and whose effects have to be built into the design of nanoscale electromechanical systems.

Photonic aspects of light–matter interaction, encompassing both active and passive optical systems, are then addressed in Chapter 5. Here, it is not only the more distinctively photon-based features that prove to require the application of a quantum field treatment; this is because semiclassical descriptions fail to correctly describe even simple processes such as photoemission. The route to develop theory for arbitrary kinds of interaction is clearly spelled out. Coverage extends from linear to nonlinear optics, where links with specifically quantum features once again emerge. This chapter also addresses near-field interactions that arise in the vicinity of a material source and introduces specifically quantum-based opto-mechanical effects, such as those used in cold atom physics (again linking with the

technology of platforms for quantum computation). We conclude with a brief summary and outlook.

Throughout the chapters that follow, we have been at pains to develop and deploy a representation of theory that is internally consistent across very different fields of optics—whose basis is to be found at the heart of an even more diverse range of modern technologies. We have aimed to deliver, in a slender volume, a treatment that is fresh, concise, expedient, and reasonably complete, showcasing a huge interconnectivity with a firm focus on the key concepts, principles, and mechanisms. One of the greatest challenges has been to keep to an accessible level of theory that is also sufficient for readers to follow the latest lines of research.

We have imposed on ourselves a strict limitation, resisting numerous inclinations to go further into individual topics. In the effort to present a very concise introduction to a subject as large as this, the selection of citations to primary sources is an invidious task, and we crave forgiveness from countless scientists whose pioneering studies are not explicitly cited. Undoubtedly, many readers will want to learn more about specific topics, and to this end we have included more than 250 references, supplemented by suggestions for further reading. While the responsibility for any errors or omissions is our own, we are truly grateful to colleagues and friends who have made time to read the draft and provide feedback. In particular, we thank Kayn Forbes, Jack Ford, Jesper Glückstad, Roger Grinter, and Garth Jones.

David L. Andrews
David S. Bradshaw
Norwich, Norfolk
June 2018

List of Symbols

a	Lowering ladder operator
a	Separation between plates (Section 4.6)
$a^\dagger$	Raising ladder operator
$\mathbf{B}$	Magnetic field vector (classical)
$\mathbf{B}$, $\mathbf{B}(\mathbf{r})$	Magnetic field operator (quantum)
$\hat{\mathbf{B}}$	Unit vector of $\mathbf{B}$
c	Speed of light
CNOT	Controlled-NOT gate
$\mathbf{e}$	Electric polarization unit vector
$\hat{\mathbf{E}}$	Unit vector of E
$\mathbf{E}$, $\mathbf{E}(\mathbf{r})$, $\mathbf{E}(\mathbf{R})$	Electric field operator (quantum)
$\mathbf{E}$, $\mathbf{E}(\mathbf{R})$	Electric field vector (classical)
E_0	Molecular ground state energy
E_I	Energy of initial system state
E_r	Molecular intermediate state energy
E_R, E_S, E_T	Energy of virtual intermediate states
e_x, e_y, e_z	Cartesian components of the electric field unit vector
$E_\parallel$	Longitudinal component of the electric field
$E_\perp$	Transverse component of the electric field
$f_{l,p}(\mathrm{r})$	Normalized radial function
$g^{(M)}$	Degree of M^{th}-order coherence
h	Planck constant
H	Hadamard transform (Sections 3.5 and 3.6)
H	Hamiltonian operator of a system
H	Horizontal plane polarization
H_0	Hamiltonian operator of an unperturbed system
H_{int}	Interaction Hamiltonian operator
H_{mat}	Matter Hamiltonian operator
H_{rad}	Radiation Hamiltonian operator
h.c.	Hermitian conjugate
$\hbar$	Reduced Planck constant (Dirac constant)
I, $I(\mathbf{r})$	Irradiance (intensity) of a light beam
$\overline{I}$	Mean (time-averaged) irradiance
I_ω	Irradiance per unit frequency
$\mathbf{J}_{\text{rad}}$	Total angular momentum operator of radiation

k	Magnitude of the wavevector
$\mathbf{k}$	Wavevector
$\hat{\mathbf{k}}$	Unit vector of $\mathbf{k}$
l	Topological charge (or winding number) of a vortex beam
L	Left-handed circularly polarized light
$\mathbf{L}_{\text{rad}}$	Orbital angular momentum operator of radiation
M	Mean number of photons
m_0	Rest mass
M_{FI}	Matrix element
n, n_ω	Refractive index
N	Number of photons
$N^{(\eta)}(\mathbf{k})$	Number operator
p	Degree of polarization (Section 2.3)
p	Magnitude of linear momentum
p	Radial index (Sections 4.2 and 4.4)
$\mathbf{p}$	Linear momentum
P	Inward pressure (Section 4.6)
P	Radiation pressure (Section 5.5)
$\mathbf{P}$	Electric polarization of a material
$\mathbf{P}_{\text{rad}}$	Linear momentum operator of radiation
q	Position coordinate
$\mathbf{r}$	Position vector
r	Complex reflection coefficient
r	Off-axis radial distance (Section 4.4)
R	Right-handed circularly polarized light
$\mathbf{R}$	Displacement from the source
R	Reflectance
R	Reflectivity (Section 5.5)
r_b	Radius of beam ring
$\mathbf{S}$	Intrinsic spin
$\mathbf{S}_{\text{rad}}$	Spin angular momentum operator of radiation
t	Complex transmission coefficient (Sections 2.4 and 3.1)
t	Time
T	Transmittance
T_0	Resolvent operator
tr()	Trace of a matrix
V	Vertical plane polarization
V	Volume
X	Bit flip
z	Axial position
Z	Phase flip

$\langle\ \rangle$	Expectation (average) value
$\|0\rangle$	Electronic ground state
$\|e\rangle$	Excited state of a two-level atom
$\|f\rangle$	Electronic excited state
$\|F\rangle$	Final system state
$\|g\rangle$	Ground state of a two-level atom
$\|I\rangle$	Initial system state
$\|N\rangle$	Number (Fock) state
$\|r\rangle$	Virtual intermediate state of a molecule
$\|R\rangle$,$\|S\rangle$,$\|T\rangle$	Virtual intermediate states
$\|\alpha\rangle$	Coherent state
$\|\Psi\rangle$	State of a qubit
(S_0, S_1, S_2, S_3)	Stokes parameters
($\|0\rangle$, $\|1\rangle$)	Standard basis (Sections 3.3–3.6)
($\|+\rangle$, $\|-\rangle$)	Sign basis
(θ, ϕ)	Spherical polar angular coordinates (Sections 2.3 and 3.4)
α	Scalar polarizability
α_0, α_1	Probability amplitudes for the standard basis
$\alpha_{ij}(\omega)$, $\boldsymbol{\alpha}(\omega)$	Molecular polarizability tensor
$\beta_{ijk}\left(\omega\right)$	Molecular hyperpolarizability tensor
Γ	Rate
ΔU	Potential energy
∇	Gradient operator (differential with respect to **r**)
ε_0	Permittivity of free space
ε_r	Relative electric permittivity
η	Polarization state
$\theta^{(\eta)}(\mathbf{k})$	Phase operator
λ	Wavelength of light in a medium
λ_0	Wavelength of light in vacuum
$\boldsymbol{\mu}$	Electric dipole moment operator
$\boldsymbol{\mu}^{f0}$	Transition electric dipole moment (between the ground and excited state)
μ_r	Relative magnetic permittivity
ν	Optical frequency
$\bar{\nu}$	Wavenumber
v_g	Group velocity
v_p	Phase velocity
ρ, ρ_F	Density of states
ρ_N	Density number
$\boldsymbol{\tau}$	Optical torque
ϕ	Azimuthal angle (Section 4.4)

ϕ	Optical phase
$\chi^{(1)}$	Linear electric susceptibility
$\boldsymbol{\chi}^{(q)}$	q^{th}-order electric susceptibility tensor
ω	Circular frequency
ω_0	Circular frequency at the center of a bandgap

List of Figures

Chapter 1
Origins and Development of Photon Science

1.1 Light in the Ancient and Modern Era

In the beginning, God said, "Let there be light," and there was light. God saw that the light was good. However, ever since the sixth day of the heavens and the earth, the human understanding of the nature of light has been keenly contested. The very earliest ideas are lost to history, no doubt influenced by natural phenomena such as sunlight, starlight, lightning, and fire. The first recorded thoughts on light were offered by the ancient Greeks. In the sixth century BCE, Pythagoras (570–495 BCE) reasoned that sight required visual rays to leave our eyes and shine upon an object. Expanding on this notion, the philosopher Empedocles (490–430 BCE) believed the eye to be composed of the four basic elements (water, earth, air, and fire), with the fire of the eye facilitating vision. An outcome of this notion is the ability to see in the dark; to counter this difficulty, Plato (428–348 BCE) supposed that the fire of the eye mixes with daylight to enable a link between man and the external world. Around 300 BCE, the mathematician Euclid (325–265 BCE) provided a geometric description of visual rays and proclaimed that "light travels in a straight line."[7] Much later, in 499 CE, the Indian astronomer Aryabhata (476–550) recognized that objects are seen by reflected light. In his virtually unknown work, he wrote that celestial objects do not shine through their own intrinsic effulgence but through the light from the Sun that they reflect.[8] The Arab mathematician and physicist Ibn Al-Haytham (965–1039) noted that extremely bright light injures the eye, and he concluded that "[…] light comes to the surface of the eye from the light of the visible object."[9]

In the early modern period, the philosopher and mathematician René Descartes (1596–1650) postulated the idea of luminiferous (light-bearing) aether, i.e., a medium for the propagation of light that is imperceptible by human senses. He suggested that the speed of light is infinite, traveling from one place to another in an instant;[10] however, in 1676, this idea was dispelled by the astronomer Ole Rømer (1644–1710), who estimated a finite speed of light by observing the eclipses of Jupiter's moon Io. Christiaan Huygens (1629–1695) and Robert Hooke (1635–1703) supported the idea of light as a vibratory motion of the aether, much like ripples propagating on the surface of water. However, most scientists around that time accepted the corpuscular theory of light advocated by Isaac Newton (1643–1727), primarily owing to the great reverence placed on Newton's accomplishments and the deficiencies of experimental apparatus in the 18th century. According to the theory of corpuscles, luminous objects eject tiny

particles of light that are governed by Newton's laws of motion. The color was thought to vary with its size, where red is the largest particle and violet the smallest. Although Newton accepted the concept of an aether, he did not believe that it acted as a medium for propagating light.

In 1801, the late modern period, Thomas Young (1773–1829) seemingly disproved the corpuscular theory of light with his two-slit experiment. As shown in Fig. 1, following the passage of a light beam through two parallel slits, the interference pattern (a series of light and dark patches) predicted by Huygens' principle is observed on the screen—not the two bands expected from the particle theory of light. Despite the importance of this experiment to modern physics, Young's contemporaries showed little interest in his work. However, within 50 years, the wave theory of light was generally accepted, mainly due to the extension of the theory by Augustine-Jean Fresnel (1788–1827).[11] He overturned the prevailing idea that light is a longitudinal wave, which greatly troubled Newton, by suggesting that the vibrations of light (in the aether) were transverse to the direction of propagation; a universally acceptable explanation of light polarization followed. Following the discovery of electromagnetic induction by Michael Faraday (1791–1867), it was realized by James Clerk Maxwell (1831–1879) that the propagation speed of electromagnetic waves and the speed of light—at the time, measured by the Fizeau–Foucault apparatus with reasonable accuracy—are very similar. He concluded in 1865 that "the agreement of the results seems to show that light and magnetism are affections of the same substance, and that light is an electromagnetic disturbance propagated through the field according to electromagnetic laws."[12] Identical to every major scientific figure that followed Descartes, Maxwell believed in an aether. However, the existence of such a "substance" was irrevocably dispelled by the experiment conducted by Albert Michelson (1852–1931) and Edward Morley (1838–1923) in 1887.

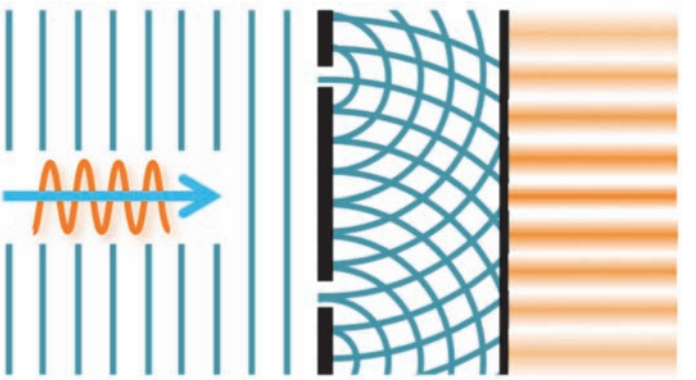

Figure 1 When light, in the form of a plane electromagnetic wave, passes through two slits in a screen, it diffracts and creates bright and dark fringes on a detector screen (screen and pattern shown on the right-hand side). The effect is commonly explained in terms of constructive and destructive interference of the diffracted wave at different positions.

1.2 Photons in the Quantum Era

At the end of the 19th century, the battle over the understanding of light was ostensibly won: light is a self-propagating, electromagnetic wave that does not require a medium. One of the few mysteries in physics at the time was the phenomena called "blackbody" radiation, and its solution led to new insights into the nature of light.

The term "blackbody" was introduced in 1860 by Gustav Kirchhoff (1824–1887).[13,14] It describes an idealized material that is both a perfect absorber and emitter of radiation. Closely matching this ideal system was an experiment proposed by Kirchhoff, which he called Hohlraumstrahlung (translated as cavity or "hollow space" radiation). This involved inserting a tiny hole into one side of a large box so that any radiation that enters cannot escape and will (eventually) be absorbed by the non-transparent box. For similar reasons, the box also acts as a perfect emitter. Analogous to visible light, the scientists of the day realized that infrared, thermal radiation is also an electromagnetic wave. Their classical theory was able to predict, to some extent, the emission intensities from a blackbody in the infrared frequency range (Fig. 2). However, they were unable to obtain results comparable to experimental observations at low wavelengths. This problem was called the "ultraviolet catastrophe." In an act of desperation,[15] Max Planck (1858–1947) introduced the idea that electromagnetic radiation is emitted or absorbed in discrete packets known later as quanta,[16] although this appeared to contradict Maxwell's assertion that light is electromagnetic radiation. Thus, in terms of Kirchhoff's box, the blackbody radiation within the cavity is quantized. By inclusion of this important physical insight into his formula, he was able to attain perfect agreement with precise experiments. Developed in 1900, this idea became known as Planck's law, and it represents the beginning of the quantum revolution.

Another phenomenon unexplained by classical theory is the photoelectric effect, which involves the release of electrons from the surface of a material when irradiated with high-frequency light. The effect is attributed to the transfer of energy from the light to the electrons. In the wave model of light, this meant that higher light intensities should release electrons with higher kinetic energies. In practice, it is not the case; electrons are emitted from the surface only when the irradiating light has a sufficiently large frequency, irrespective of the intensity. In 1905, by treating light as quanta, Albert Einstein (1879–1955) was able to provide a complete explanation of the effect.[17] He determined that energy transfer to the electrons depends on the frequency of the quanta—electrons are only released from the surface when the frequency matches or exceeds the work function of the metal. This understanding also provided a link with the explanation of atomic spectra by Niels Bohr (1885–1962) in 1913. A further, conclusive piece of evidence for particle-like behavior of light arrived in 1923: Arthur Compton (1892–1962) observed, in the results of inelastic scattering of light by an electron, features that could not be explained with classical theory where light is a wave.[18] These discoveries led to the quantum mechanical notion that light is both a wave

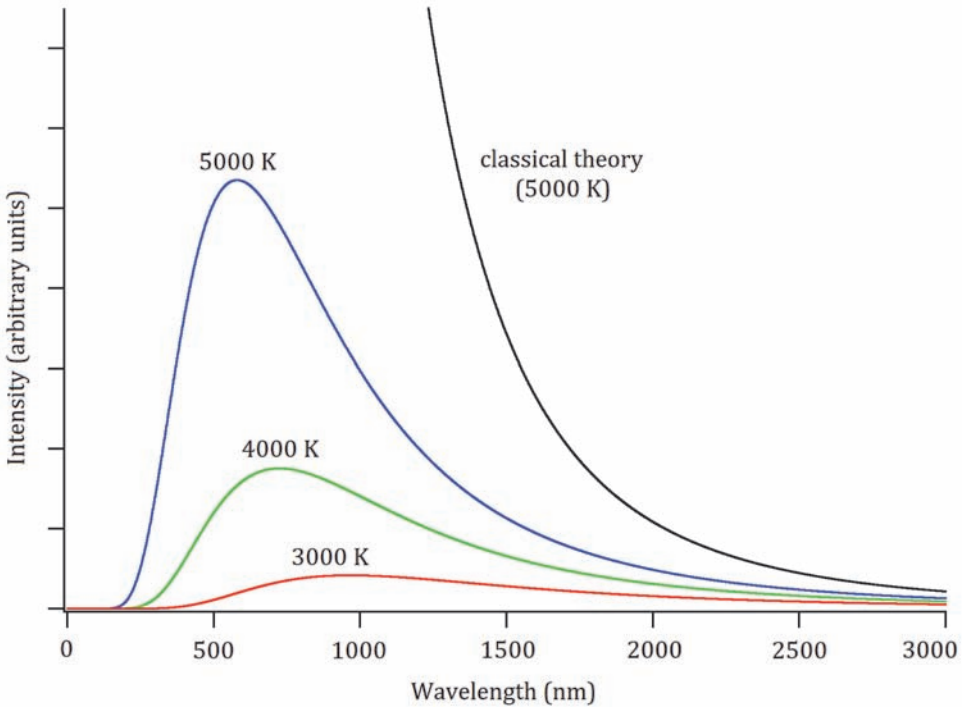

Figure 2 Graph showing the intensities of emitted radiation from a blackbody against the wavelength of the light. It is clear that the classical theory does not agree with the experiment (5000 K) at short wavelengths.

and a particle, depending on the circumstance. In short, light is a photon.* The first use of the word "photon" is credited to Gilbert Lewis (1875–1946) in 1926;[5] however, with a different meaning to quantized light, four other authors used the term as much as ten years beforehand.[19]

By the 1860s, it was known that electromagnetic waves have a linear momentum,[20,21] which was experimentally confirmed by Lebedev[22] and by Nichols and Hull[23] in 1901. Later, Louis de Broglie (1892–1987) was able to relate the linear momentum of light to its wavelength via Planck's constant h and proposed that electrons exhibit wave-like behavior.[24] While quantities such as linear momentum and polarization were contemplated in classical theory, the concept of spin (angular momentum) has no classical counterpart. The integer spin of a photon, in units of $h/2\pi$, was suggested by Satyendra Nath Bose (1894–1974), in whose honor photons are now categorized as bosons (as opposed to half-integer spin fermions, named after Enrico Fermi (1901–1954)), and experimental attempts to verify such a spin soon followed in 1931.[25,26] Five years later, Beth linked photon spin to circularly polarized light.[27] In much more recent times, it has been established that spin angular momentum is only half the story. The photons

* The name "photon" derives from the Greek word for light (*phōtos*), and the suffix *-on* indicates an elementary particle, such as a proton, electron, or neutron.

comprising structured light beams can carry *orbital* angular momentum.[28] Even today, we are still learning and debating about the nature of a photon; a wide variety of descriptions continues to be offered,[29] varying from the insightful to the eccentric. Yet, at heart, it is the observations of relatively simple phenomena that provide the most strongly persuasive reasons to accept the central, conventional tenets for the quantization of light.[30]

1.3 Quantum Electrodynamics: Photon Interactions with Matter

The theory of photon interactions with matter is known as quantum electrodynamics (QED), i.e., a complete quantum description in which the electromagnetic radiation is quantized. The first publication on the subject is credited to Paul Dirac (1902–1984), who wrote, in 1927, a description of quantum theory for the emission and absorption of radiation;[31] an image of Dirac is shown in Fig. 3. Three years later, Dirac completed his book *The Principles of Quantum Mechanics*; the fourth edition remains a standard textbook on the subject.[32] This early form of QED produced infinite results for some elementary physical quantities, such as the mass and charge of particles. In the 1940s, using the renormalization method, this problem was separately resolved by Sin'ichirō Tomonaga[33,34] (1906–1979), Julian Schwinger[35,36] (1918–1994) and Richard Feynman[37,38] (1918–1988). These independent discoveries were shown to be equivalent by Freeman Dyson (1923–).[39] This covariant (relativistic) form of QED produces extremely accurate predictions and acts as a foundation for other quantum field theories. Slow-moving electrons bound to atoms or molecules can be described by non-relativistic (molecular) QED. This framework was first developed by Edwin Power (1928–2004) and Sigurd Zienau (1921–1976) in the late 1950s,[40] and later consolidated by Power and "Thiru" Thirunamachandran (1932–2008) in a number of publications.[41–45]

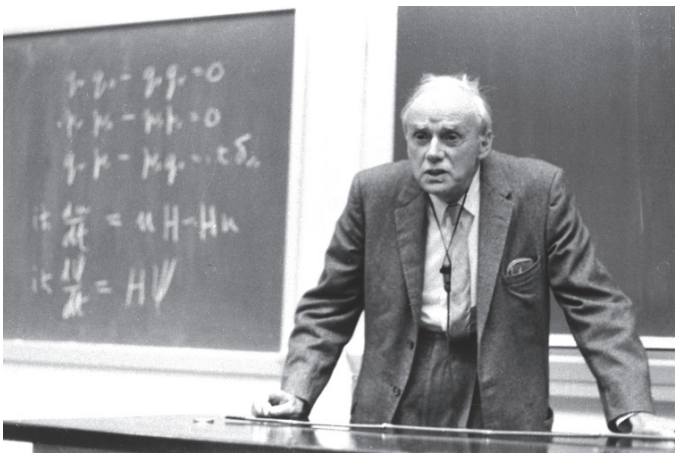

Figure 3 Photograph of Paul Dirac, the founding father of quantum electrodynamics. © Florida State University.

1.4 Photons in Free Flight

Before 1960 and the creation of the first laser,[46] quantum electrodynamical notions (such as photon creation and annihilation operators) were rarely applied to the problems of optics, which still relied on classical or semiclassical ideas. As a result, the quantum depiction of an electromagnetic beam remained underdeveloped until the ascent of quantum optics and its photon statistical concepts. Seminal to the field of quantum optics is the intensity interferometer developed by Robert Hanbury Brown (1916–2002) and Richard Twiss (1920–2005).[47] This experiment demonstrates photon bunching in incoherent light beams, i.e., photons in a seemingly uncorrelated chaotic beam tend to arrive in clusters (not at random times) at photodetectors in close proximity. While this phenomenon can be explained classically, photon antibunching is only understandable in terms of a quantized electromagnetic field.[48]

Although the coherence of light has no direct connection to photon bunching or antibunching (and neither occurs in a laser), the Hanbury Brown–Twiss experiment led to an enhanced interest in the coherent properties of light in general.[49] A quantum description presented in 1963 by Roy Glauber (1925–) introduced the concept and mathematical structure of a coherent state (or minimum uncertainty state, in which neither the number of photons nor phase is precisely defined) as a representation of laser light.[50] A related state, with properties unexplained by classical theory, is known as a squeezed state.[51,52] Here, one of the quantities (either the photon number or the phase) has less uncertainty at the expense of the other. In polarization correlation experiments pioneered by Alain Aspect (1947–) and others,[53] it was subsequently verified that light satisfies quantum principles that are unequivocally at odds with classical predictions, thus providing incontrovertible proof of the existence of light in the form of photons. Emerging from such studies, quantum optics has grown into a vast subject. Highly regarded books on the topic include those authored by Leonard Mandel (1927–2001) and Emil Wolf (1922–2018),[54] and Rodney Loudon (1934–).[55]

Today, the concept of the photon is as firmly entrenched in science and technology as any other major tenet of established physics. The fact that many of the principles and mechanisms of modern optics and photonics entirely hinge upon it is exemplified in numerous topics covered in the following chapters. Nonetheless, the history outlined in this chapter reveals a progression, and a depth, that is far richer and deeper than could ever have been anticipated at the outset. Some of the most recent developments—structured light in particular—have raised new questions about the nature of the photon and so led to the further refinement and extension of theory. Perhaps the story is not yet over: we shall return to a summary review at the end of book.

Chapter 2
Properties of a Photon

In this chapter, we examine some of the principal attributes of electromagnetic radiation that feature in photons. At the outset, it is worth asserting that the photon concept owes its legitimacy to the quantum theory of light. As we shall see in later chapters, the photon is formally regarded as a quantum of excitation of any specific optical mode. In the literature, one can find occasional mentions of photons qualified by an adjective, such as dipole photons, electric photons, ballistic photons, etc.[56,*] These should be regarded as potentially misleading[57] because each alludes to a property that is more correctly associated with a particular kind of phenomenon. Even if the distinction between "real" and "virtual" photons represents one of the most widely used descriptors, it does not signify a clear-cut difference.[58] We thus begin by listing the following photon properties, all of which can be involved in specific forms of optical interaction, with the exception of the first.

2.1 Intrinsic Photon Properties

1. *Mass.* Photons are elementary particles with zero mass, necessarily so because no particle with a finite mass can move at the speed of light. This is a conclusion that follows from special relativity. Occasional representations of theory introduce a contrived "effective mass of the photon" for certain applications—for example, in connection with superconductivity and polariton propagation—but even then it is a concept that is neither necessary nor especially commendable.

2. *Velocity.* Photons propagate with a velocity whose absolute magnitude is normally quoted as the speed c in vacuum, with refractive corrections to be applied as appropriate for passage through material media. In free space, light travels in a straight line, and the direction of its well-defined velocity is usually denoted by the unit vector $\hat{\mathbf{k}}$. On propagation through a medium of refractive index n, individual photons travel at a speed known as the *phase velocity* $v_p = c/n$. Although it is possible to produce pulses of light that appear to exhibit "superluminal" features,[59] it has been

[*] A distinction that has sometimes been drawn between "ballistic" and "snake-like" photons is truly a post-event interpretation of propagation history, rather than an intrinsic difference between kinds of photon. While most photons propagating through an optically dense, heterogeneous medium experience multiple scattering, and hence might be considered to have a sinuous, snake-like path, statistics may allow a small number to pass through without encountering a scatterer, and their rectilinear pathway might seem to have been ballistic.

shown that none of the individual photons within these pulses travels faster than c. Section 2.4 returns to this topic to discuss media effects.

3. *Electromagnetic fields.* The charge of the photon is self-evidently zero, but the photon nonetheless conveys oscillatory electric and magnetic fields, which are vector quantities denoted by **E** and **B**, respectively. In free propagation, these vector quantities are oriented such that the unit vectors ($\hat{\mathbf{E}}$, $\hat{\mathbf{B}}$, $\hat{\mathbf{k}}$) form a right-handed, orthogonal set. The absence of any constituent charge (together with the absence of mass) means that photons cannot interact between themselves; any engagement of two or more photons requires its mediation by interaction with matter.

4. *Frequency.* The optical frequency ν expresses the number of wave cycles, at a fixed point in space, per unit time. Also commonly used in quantum optics is the circular frequency $\omega = 2\pi\nu$ (radians per unit time).

5. *Wavelength.* The wavelength λ_0 of the electric and magnetic waves, for light traveling in vacuum, is given by c/ν. It is the closest distance along the propagation direction between any two positions with the same optical phase. In applications such as spectroscopy, reference is commonly made to its inverse, the wavenumber $\bar{\nu} = 1/\lambda_0 = \nu/c$, usually expressed in cm^{-1}. Photons propagating within a medium of refractive index n have a modified wavelength $\lambda = \lambda_0/n$, such that the product $\lambda\nu$ still equals the propagation speed.

6. *Energy.* Photons convey electromagnetic energy from one piece of matter to another. Their energy links to optical frequency ν through the Planck relation $E = h\nu$ (where Planck's constant $h = 6.6261 \times 10^{-34}$ J s) or, equally, $E = \hbar\omega$, where $\hbar = h/2\pi$ is known as the reduced Planck's constant (or Dirac constant). The lower the optical frequency is, the greater the number of photons for a given amount of energy, and hence the more their behavior approaches that of a classical wave (an instance of the "large numbers" hypothesis of quantum theory). For this reason, electromagnetic radiation becomes increasingly wave-like at low frequencies; thus, we tend to think of radiofrequency and microwave radiation primarily in terms of waves rather than particles.

7. *Linear momentum.* Despite having no mass, each photon carries a linear momentum **p**, a vector of magnitude $h/\lambda = \hbar\omega/c$ in the direction of propagation. This follows from the relativistic energy-momentum equation $E^2 = p^2c^2 + m_0^2c^4$, with a rest mass $m_0 = 0$. It is often convenient to define a wavevector or propagation vector $\mathbf{k} = (\omega/c)\hat{\mathbf{k}} = (2\pi/\lambda)\hat{\mathbf{k}}$ such that $\mathbf{p} = \hbar\mathbf{k}$. Given that photon momentum is proportional to frequency, photons of high frequency have high momenta and exhibit the most particle-like behavior. X rays and gamma rays, for example, have many clearly ballistic properties.

8. *Polarization.* For plane-polarized (also called linearly polarized) photons,[†] the plane within which the electric field vector oscillates can sit at any angle containing the wavevector. By convention, the direction of the electric field vector defines the orientation of the polarization. As shown in Fig. 4, the magnetic field also oscillates in a plane orthogonal to the electric field; however, the "plane of polarization" generally refers to the electric vector. Even for individual photons, a wide variety of other polarization states are also possible: in circular polarizations, the electric field vector sweeps out a helix about the direction of propagation, and the magnetic vector is advanced or retarded from it by $\pi/2$ radians. Elliptical polarization states are of an intermediate nature, between linear and circular. Other, beam-related polarization topics are discussed more fully in the next section.

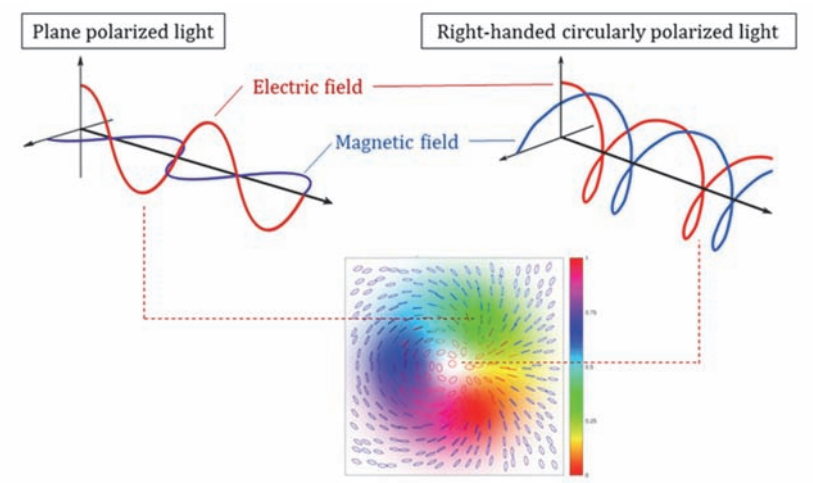

Figure 4 Top left: Plane- (linearly) polarized light, where the electric and magnetic field oscillations are in phase and both are transverse to the direction of propagation. Top right: Right-handed circularly polarized light, in which the field vectors are $\pi/2$ out of phase, and both circulate around the propagation axis. Lower image [courtesy of Enrique Galvez, Colgate University]: False-color representation of a vector polarization beam whose polarization state varies from linear, through elliptical, to circular around the axis. The full-spectrum coloring emphasizes the orientation of the polarization ellipse relative to the radial direction (yellow = radial, blue = azimuthal), and the color intensity denotes the intensity of the beam. The color of the superimposed ellipses represent the handedness of the local polarization state (blue = left, red = right).

[†] The notion that individual photons can *only* exist in states of left or right circular polarization is false. It is true that only photons of those kinds have well-defined integer spin (see item 9 in this subsection) along the propagation axis, but superposition states can exist, too. The concept is not dissimilar to the mixing of $p_{\pm 1}$ as p_x or p_y orbitals.

9. *Spin.* Many of the key properties of photons relate to the fact that they have an intrinsic spin $S = 1$ and so are classified as bosons, i.e., particles with integer spin that display collective behavior properly described by a Bose–Einstein distribution. In simple terms, this means that their oscillating electromagnetic fields keep in step as they propagate. Through this, coherent beams of highly monochromatic and unidirectional light can be produced; this is, of course, the basis for laser action.

10. *Angular momentum.* The intrinsic spin of each photon is associated with angular momentum, a feature that plays an important role in the selection rules in optical spectroscopy. Circularly polarized photons have the special property of quantum angular momentum. The two circular polarization states of opposite handedness, left- and right-handed, respectively carry a +1 or –1 unit of angular momentum $\hbar$. Commonly, plane-polarized light is converted to a circular polarization state by passing it through an optical element known as a *quarter-wave plate*, which differentially retards orthogonal polarization components. A different kind of angular momentum, described as "orbital," can also be generated using more complex optical elements, such as a spatial light modulator,[60] which produce spatially structured beams (see Sections 4.2 and 4.4).

2.2 Properties of Photons in a Beam

To the list in the previous section we can add *beam properties*, i.e., properties that primarily relate to photon relationships within a propagating group. In fact, for any source of light delivering a sufficient output to be recognized as a beam, there are countless additional properties that might be added, such as the moments that represent any form of distribution over optical frequency or temporal profile, or a degree of beam polarization. Nonetheless, there are two key parameters of overriding importance, intensity and phase, whose interplay involves fundamental quantum principles.

11. *Intensity.* The most obvious parameter expressing the intensity of light in photon quantities is a flux, cast as the number of photons per unit time traversing a unit area at normal incidence. Since each photon conveys energy $\hbar\omega$, it is readily shown that $I = (N/V)\hbar c\omega$, where I denotes *irradiance*, and N is the number of photons in a volume V. This expression is especially well-suited to laser light, in which beam divergence is minimal; the term in parentheses can be regarded as an instantaneous "photon density." For applications to emission processes, the term "radiant exitance" is a better descriptor of the same parameter I. Most other traditional radiometric measures of intensity are ill-suited to photon-based descriptions. For example, luminous, or radiant, intensity (power per unit solid angle) is clearly more appropriate for uncollimated optical output.

12. *Coherence and photon statistics.* As mentioned earlier, the boson character of photons enables light to propagate with a degree of coherence between different photons traveling in the same direction. However, at the heart of quantum optics there is a number-phase uncertainty principle that means there is always a degree of trade-off between certainty over the number of photons—which we have seen relates directly to intensity—and certainty over phase. Although Dirac originally suggested a simple uncertainty relation of the familiar form $\Delta N \Delta \phi \geq \frac{1}{2}$ (where ϕ denotes the optical phase), the precise relationship eventually proved resistant to such a simple form of expression.[61,62] Nonetheless, it was correctly established that, for example, radiation with a precisely known intensity cannot display any coherence features.

This last issue also relates to the fact that a beam delivered by any source of light, even the most stable continuous-wave laser, always has intensity fluctuations (due to individual atoms or optical centers[‡] being responsible for each photon emission). Despite its origin in correlated emission events, laser light does not usually exhibit the photon *bunching* (non-uniform flux) that characterizes conventional light sources. As a result of nonlinear optical processes (see Section 5.3), photons may alternatively exhibit *antibunching*, which is a property that exhibits the non-classical, quantum nature of light.[63]

Most forms of optical emission deliver "thermal" light in the sense that their intensity fluctuations follow a Bose–Einstein distribution. Conversely, a Poisson distribution characterizes the most stable forms of laser emission. In the latter case, the photon statistics approximate to a state of optimal trade-off between the stability of intensity and coherence.[64] Section 4.3 describes, in more detail, the quantum basis for the phase and intensity fluctuations; it transpires that a *coherent state* of the radiation is closest to the properties exhibited by the most stable laser sources. In the sphere of nonlinear optics, substantial differences in behavior prove to emerge from issues of photon statistics, as will be shown in Section 5.3.

For laser emission, there are other features relating to coherence that need to be considered. It is apparent that only light with an infinitely narrow linewidth can sustain exact coherence over arbitrarily large distances. More generally, the inverse of the frequency linewidth constrains the local *coherence time*, and the inverse linewidth in wavenumbers correspondingly determines a *coherence length* within whose span, at any point in the beam, coherence is sustained. A more demanding aspect of the same principle arises in the case of pulsed lasers. For the ultrashort (sub-picosecond and femtosecond) pulses that are common today, consideration of the Fourier transform shows that even to produce an idealized

[‡] The term "optical center" is used here as a generic descriptor for localized units that represent the origins for optical response, such as photon absorption or emission. Examples of such centers include atoms, ions, or molecules, either free, in solution, or isolated within an essentially transparent host material. Other examples are quantum dots and nano-emitters.

Gaussian temporal shape, there has to be a corresponding Gaussian distribution of the optical frequencies. However, research on *Kerr frequency combs*—sources of light comprising a regular spread of discrete optical frequencies —has shown that sustained coherence may mitigate the problem and circumvent an instability to which such sources can otherwise be prone.[65]

2.3 Radiation Modes and Polarization

In the formal language of quantum optics, which we shall be pursuing shortly, a photon may be considered a single quantum of a radiation mode; the number of photons in a closed, well-defined region signifies the *occupation number* of that mode. Each mode is defined by a distinct combination of wavevector and polarization, the former being determined by both optical frequency and direction of propagation. The radiation states for modes with a different wavevector are mathematically orthogonal; physically, this signifies that any individual photon, freely propagating in space, cannot spontaneously change its energy or direction. Polarization is a more complex issue, inviting further discussion.

We are all familiar with the phenomenon of crossed polarizers preventing optical transmission; this signifies the orthogonality of the corresponding radiation modes. However, other orientations of one polarizer against the other will permit a degree of throughput. This is because any plane polarization is physically and mathematically equivalent to a combination of two orthogonal polarizations (in the same plane) with suitable weightings. Similar remarks can be made about other polarization states. In general, for light propagating in a particular direction, it suffices to define any two specifically orthogonal polarizations, and then any other polarization state can be expressed in terms of them as a linear combination.[66]

There are two equally valid mathematical representations of this feature, both of which cast the entire realm of polarization states as points on the surface of a sphere. The historically earlier one is called the Poincaré sphere,[67] in honor of Henri Poincaré. The other is the Bloch sphere,[68] named after Felix Bloch. Since both are commonly used, we exhibit both of them in Fig. 5. Crucially, in each representation, any two states represented by opposing points provide a basis in terms of which any other polarization state can be cast. Commonly, these are chosen as *left* and *right circular* polarizations (L and R), or *horizontal* and *vertical* plane polarizations (H and V). By the use of specially tailored optics, it is possible to produce a *vector polarization* beam whose cross-section contains every state of polarization, as illustrated in Fig. 4. Such a beam is often referred to as a *Poincaré beam*.[69]

There are several arguments in favor of the Bloch sphere representation, especially its casting of surface positions in terms of conventional spherical polar coordinates. This representation in fact has its origins in two-state quantum mechanics, which is pertinent to the dynamics of spin-half particles, for example, describing states that are not simply “spin-up” or “spin-down.” A further application is in the physics of qubits, which provides for *quantum superpositions* of the simple binary states “0” and “1.” The latter has particular relevance to

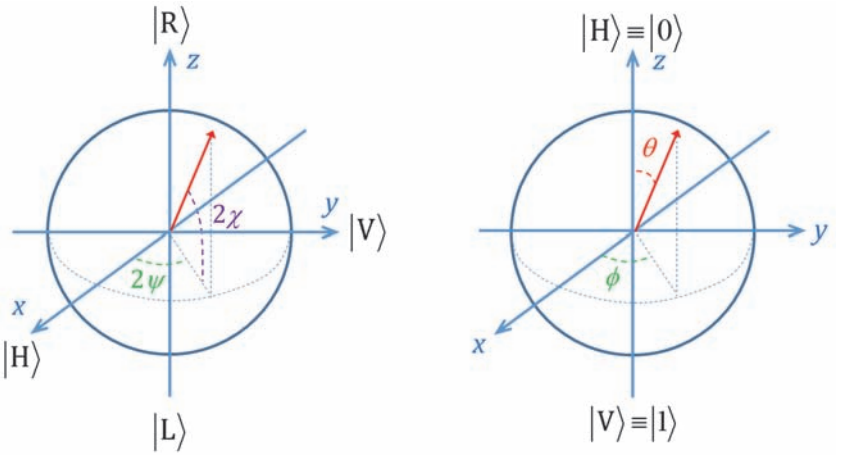

Figure 5 Poincaré sphere (left) and Bloch sphere (right) representations of optical polarization. On the Poincaré sphere, the "poles" are specifically states of circular polarization; on the Bloch sphere, the poles may be either plane polarizations, as described in the text with reference to Eq. (1), or circular polarizations. In the latter case, the basis $\hat{\mathbf{i}}$ and $\hat{\mathbf{j}}$ in that equation are replaced by $\mathbf{e}^{(L)}$ and $\mathbf{e}^{(R)}$.

photons; we return to this in Section 3.4. For the present, we describe the specific application to photon polarization. Based on the Bloch sphere, an arbitrary polarization unit vector $\mathbf{e}$ is generally expressible as follows:

$$\mathbf{e} = \cos(\theta/2)\hat{\mathbf{i}} + e^{i\phi}\sin(\theta/2)\hat{\mathbf{j}}. \tag{1}$$

In this expression, $\hat{\mathbf{i}}$ and $\hat{\mathbf{j}}$ are unit vectors in real, physical space, perpendicular to the unit wavevector $\hat{\mathbf{k}}$; θ and ϕ are spherical polar angular coordinates, for which $0 \le \theta \le \pi$ and $0 \le \phi \le 2\pi$, defining a point on the Bloch unit sphere. For example, two mutually perpendicular plane polarizations, arbitrarily designated H and V, may be rendered by $\theta = 0$ and $\theta = \pi$, respectively, simply delivering $\hat{\mathbf{i}}$ and $\hat{\mathbf{j}}$; equally, the circular polarizations, L and R respectively in the optics convention, are given by $\theta = \pi/2$, $\phi = \pi/2$ and $\theta = \pi/2$, $\phi = 3\pi/2$, such that

$$\mathbf{e}^{(L)} = \frac{1}{\sqrt{2}}\left(\hat{\mathbf{i}} + i\hat{\mathbf{j}}\right); \quad \mathbf{e}^{(R)} = \frac{1}{\sqrt{2}}\left(\hat{\mathbf{i}} - i\hat{\mathbf{j}}\right). \tag{2}$$

Every other pair of values for $\phi \neq (\pi/2, 3\pi/2)$ and $\theta \neq (0, \pi/2, \pi)$ denotes a generic state of elliptical polarization. For some purposes, it is expedient to represent a generic basis pair of orthonormal polarization vectors. Using the identities $e^{i(\phi+\pi)} = -e^{i\phi}$ and $\cos((\pi-\theta)/2) = \sin(\theta/2)$, we can cast the polarization state whose Bloch representation is diametrically opposite the one represented by Eq. (1) as

$$\mathbf{e}' = \sin(\theta/2)\hat{\mathbf{i}} - e^{i\phi}\cos(\theta/2)\hat{\mathbf{j}}. \tag{3}$$

Every pair of polarization states given by Eqs. (1) and (3) satisfies the orthogonality relation $\mathbf{e} \cdot \overline{\mathbf{e}}' = 0$, in which the overbar serves to identify the complex conjugate.

The preceding description, which serves to describe beams of uniform polarization in terms of photon states, is readily linked to macroscopic quantities that are expedient for characterizing beams with a statistical distribution of photon polarizations, physically manifesting as partial polarization. *Stokes parameters* are most widely used in this respect. This is a set of four numbers conventionally labeled S_0, S_1, S_2, S_3. The first of these is simply identified as the intensity I (clearly proportional to the number of photons, for monochromatic light), which serves as a normalizing constant in each of the others. With reference to the Poincaré sphere representation in Fig. 5, we then have $\{S_0,S_1,S_2,S_3\} \equiv \{I,\ Ip\cos 2\psi\cos 2\chi,\ Ip\sin 2\psi\cos 2\chi,\ Ip\sin 2\chi\}$, where p is the degree of polarization. Hence, for example, we represent *unpolarized* light by the Stokes vector (1,0,0,0). Changes in the Stokes vector, on propagation through a potentially absorbing medium, are then generally represented by a transform known as the 4×4 *Mueller matrix*:[70] this formalism is valid provided the material exhibits a linear optical response (i.e., proportional to the input intensity), which is usually true for conventional or continuous-wave laser light. Unpolarized light in fact behaves, in the linear optics regime, as an equal mixture of polarization states corresponding to directly opposite positions on the Poincaré or Bloch sphere, e.g., as an input of $\frac{1}{2}(I_H + I_V)$ or $\frac{1}{2}(I_L + I_R)$. However, this equivalence breaks down when a nonlinear response occurs.[71] We shall explore optical nonlinearity in detail in Section 5.3.

2.4 Photons in Optics

The preceding description of photon modes and polarization features exhibits no obvious departures from conventional, classical optics. This reflects operation of the correspondence principle dictum, which states that classical behavior is exhibited when the quantity of photons is very large.[72] Let us return to the equation that relates the number of photons N in a volume V to irradiance I, rewritten in the following form:

$$N = \frac{IV\lambda}{hc^2}. \tag{4}$$

For most kinds of optics, even at the lowest levels of beam intensity, the volume of any optical element that the beam fills provides a very large number of photons at any instant in time. To take an example, the number of photons in a 50-mm^2 cross-section beam of 5-mW radiation at a wavelength of 500 nm, traversing a lens 5 mm wide, is 200,000. So the classical formulations of optical theory work well even at considerably lower levels of intensity or with smaller volumes. Such a conclusion is valid for most kinds of passive optics, processes in which there is no active change in the optical medium.

However, there is a key corollary: quantum effects will always be significant where processes occur at the atomic or molecular level, e.g., when the light produces optical transitions. Indeed, the mechanism of the photoelectric effect, a key pointer to the quantum nature of light, involves photoionization at the atomic level. As another illustration, if we apply Eq. (4) to the case of sunlight falling onto the leaves in a tree canopy, taking into account the kW m^{-2} order of intensity and the size and typical distribution of chlorophyll molecules within the leaves, we find that a photon reaches one of these molecules only about once a second.[73] So the primary processes of photosynthesis, initiated by light absorption, cannot be reasonably described without using the language of photons. Indeed, this is true for almost all processes that fall within the province of optical spectroscopy, and a broad span of topics in photophysics, photochemistry, and photobiology.

There is another important area in which Eq. (4) indicates the likelihood of departures from classical behavior: when we look at phenomena that are specifically associated with very low intensities, quantum effects can also be expected to be significant. This is precisely where one finds many forefront developments connected to quantum optics and photonics, as will be discussed in the next chapter.

We now provide a brief overview of photon propagation within media; they do not generally exhibit departures from classical behavior, and full descriptions can be found in any book of reference in optics. Topics that are discussed here include the dispersion relations for propagation inside dielectric media, group velocity issues, and the equations that govern surface and interface phenomena.

First, the wavevector and optical frequency for light propagating inside a medium are given by the familiar dispersion relations and involve the refractive index n. This is, of course, a quantity defined with reference to a bulk material; it is generally given by the expression $n = (\varepsilon_r \mu_r)^{1/2}$, where ε_r is the relative electric permittivity (dielectric constant), and μ_r is the relative magnetic permeability. Only in gases, such as air, can the vacuum value $n = 1$ be considered a reasonable approximation. In anisotropic media, such as dichroic crystals, the value may differ according to the direction of propagation. For most natural materials, and indeed most conventional optical materials, the relative magnetic permeability is close to unity,[§] and the relationship simplifies to a form that can be related to the electric susceptibility $\chi^{(1)} = \varepsilon_r - 1$ (where the superscript on the left identifies a linear response) and hence the polarizability α in the case of molecular media. The corresponding formula, based on the Lorentz–Lorenz or Clausius–Mossotti equation, is given by

$$\frac{n^2 - 1}{n^2 + 2} = \tfrac{1}{3}\varepsilon_0^{-1}\rho_N \alpha, \tag{5}$$

[§] The propagation of light in many artificially constructed *metamaterials* does often have significant magnetic attributes.

where ε_0 is the vacuum permittivity, and ρ_N is the number density, which, in the case of molecular materials, is identified as the number of molecules per unit volume. The refractive index is usually regarded as registering a reduction in the speed of light within a medium. In Section 5.2, we shall elucidate the physical mechanism by which light suffers this change, making it clear why the polarizability should be involved. For the present, it is appropriate to simply note that the polarizability itself signifies the extent to which photons of the throughput radiation engage with the electronic properties of the material. The greater the coupling is, the larger the polarizability and hence the higher the value for the refractive index.

For a given material, the refractive index always has a degree of variation with wavelength (equally, with optical frequency) that is known as *dispersion*. Such variations are most prominent in frequency regions close to an optical absorption band, again reflecting the formal dependence on polarizability. (The underlying principle is discussed in Section 5.2). An example is shown in Fig. 6.

One other way that this form of relationship is commonly exhibited is via a plot of optical frequency ω against the magnitude of the wavevector k, known as a *dispersion curve*. If we explicitly represent the optical frequency dependence of the refractive index by n_ω, then since the gradient of this curve is $\omega = (c/n_\omega)k$, the frequency-dependent phase velocity $v_p = \omega/k$ will usually have an upper limit of c for regions in which the refractive index is close to unity, i.e., where there is negligible dispersion. However, across regions of strong dispersion (resonance) associated with optical absorption, the slope decreases; photons are slowed as their energy is progressively engaged with electronic excitation of the medium.

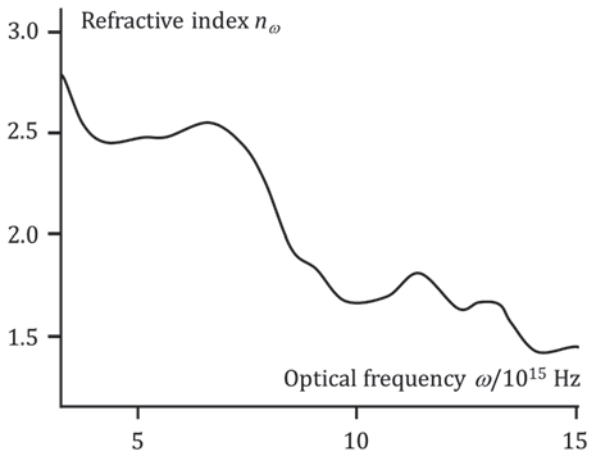

Figure 6 Variation in refractive index of indium nitride with optical frequency ω. Redrawn from data given by Djurišić and Li.[74]

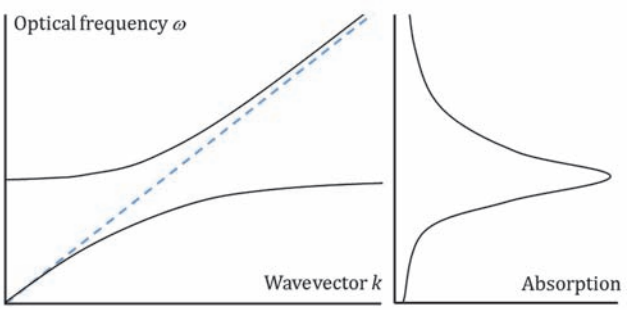

Figure 7 Idealized depiction of optical dispersion: (left) Variation of optical frequency with wavevector (solid black curves) across (right) a region of strong absorption associated with polariton propagation. The blue dashes show a line of slope *c*, the speed of light in vacuum, which everywhere exceeds the group velocity v_g, represented by the gradient of the dispersion curve. Close to the peak absorption, the dramatic reduction of group velocity (flatter sections of the curves) manifests the photon progressively engaged with local electronic structures, exhibiting the character of a polariton.

Under these conditions, where photons display a character essentially "dressed" by the medium,[**] they are best described as *polaritons*.[75] If one considers a sufficiently extensive range of optical frequencies, most materials will display more than one resonance, and, in an ideal case, the corresponding dispersion curve appears in the form shown in Fig. 7. Note that it is possible for two or more optical frequencies to relate to the same wavenumber.

Next we observe that the effective speed of propagation of wavepackets, or pulsed light, is determined by the group velocity v_g, a function of optical frequency ω. Distinct from the phase velocity v_p, this is defined by $d\omega/dk$ and more expediently expressed as

$$v_g = \frac{c}{n_\omega + \omega\left(dn_\omega/d\omega\right)}. \tag{6}$$

The additional (second) term in the denominator, which distinguishes this expression from the phase velocity, may be either positive or negative. Close to sharp resonances, this can lead to unusually slow or fast light; as observed previously, individual photons nonetheless propagate at the phase velocity, obviating any possibility of superluminal conveyance of information.

To continue our survey of photon properties, we now observe the behavior of photons that impinge upon an interface between two media differing in refractive index. As we have seen, the classical refractive index and associated dispersion

[**] Some authors introduce here the concept of photons with an "effective mass," a misnomer because the energy of a free photon has, at least in part, been converted into an electronic excitation of a material.

features provide a key to the effects of a medium on photon propagation. Once again the behavior of photons at an interface, or a region of spatially varying refractive index, in many respects follows the principles of classical optics. In particular, the Fresnel equations continue to hold with an intensity-defined reflectance R and transmittance T, related through $R + T = 1$. However, the corresponding equations are better cast in terms of field amplitudes with complex reflection and transmission coefficients (r and t, respectively) such that $|r|^2 = R$ and $|t|^2 = T$. The two complex coefficients can then be reinterpreted in terms of quantum states, as will be discussed in the next chapter.

For photons traveling in a region of refractive index n_1 impinging upon a region of index n_2 (assuming, for simplicity, a normal angle of incidence), we have

$$r = \frac{n_1 - n_2}{n_1 + n_2}. \tag{7}$$

An important corollary is that when the intercepted region has a comparatively higher refractive index $n_2 > n_1$, the electric field amplitude for the reflected photon (formally the state vector) undergoes a change in sign. This is usually expressed as the reflected light undergoing a π phase shift because $e^{i\pi} = -1$.

In media constructed with internal boundaries between regions of differing refractive index, the interplay of reflection and refraction—especially the condition of *total internal reflection*—enables light to be directed along predetermined paths. This is, of course, the principle behind all kinds of waveguide and fiber optics. Graded-index (GRIN) fibers exploit this feature (see Fig. 8).

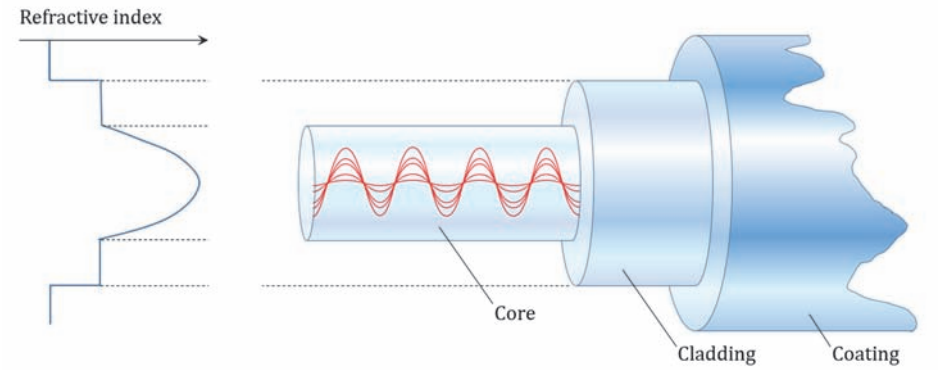

Figure 8 A graded-index fiber. The core fiber has a radially graded index of refraction, ideally with a parabolic dependence on distance from the core axis, as indicated by the middle section of the graph on the left. This guides light along the core with minimal loss. The center of the illustration exhibits photon paths for coherent input. Note that the guided wave has a repeat length on the macroscopic scale, greatly exceeding the optical wavelength.

Here, the inner core has a radially graded refractive index, diminishing outwards from the center. Any marginally off-axis light traveling along the fiber is continually redirected inwards, resulting in a quasi-sinusoidal path.[76,††] However, when periodic internal structures of nanoscale dimension become involved, e.g., in "holey fibers," more complicated effects come into play: this is the province of photonic crystals.

2.5 Photonic Crystals

In their simplest form, photonic crystals are layered structures constructed from repeatedly alternating layers of two materials with differing refractive index.[77–79] The alternating structure may be constructed in one, two, or three dimensions, as illustrated by Fig. 9(a–c). Each pair of adjacent layers has the same combined thickness, producing a regular spatial periodicity; the two components may or may not have the same thickness. Photons propagating through such a structure experience the combined effects of Bragg scattering[80] (whenever the spatial period equals a multiple of half the effective wavelength within the dual material) and repeated interface reflection. The latter condition, which owes its origin to a phase relation, also plays into the standing wave condition for a laser cavity.

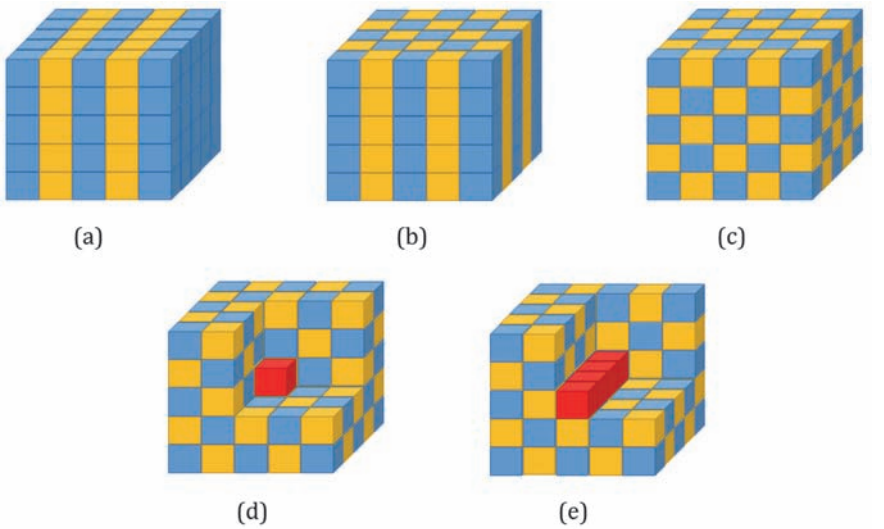

Figure 9 Photonic crystals constructed in (a) one, (b) two, and (c) three dimensions. In these structures, light can be contained within either (d) a point or (e) a linear defect.

†† The guided optical paths within an ideally structured GRIN fiber are solutions of the Helmholtz wave equation.

To understand and quantify these phase relationships, the concept of *optical path length* is often deployed. Recall that each photon experiences a 2π change in phase over the span of a wavelength. On traversing a small distance d within a material of refractive index n, the change in phase is, therefore, determined by the relative magnitude of d and the wavelength λ within the medium, the latter given by $\lambda = \lambda_0/n$, where λ_0 is the vacuum wavelength. Consequently, if light of wavelength λ_0 impinges upon the photonic crystal, the optical path length within any layer i of width d_i and refractive index n_i is $d_i n_i$ (and the associated phase change across it is $2\pi d_i n_i/\lambda_0$). For a two-component photonic crystal with contrasting refractive indices $n_1 >> n_2$, the optical path difference across each repeating unit is $d_1 n_1 + d_2 n_2$. The effective obstruction to forward propagation, when both terms in this expression are similar to $\lambda_0/4$, produces a photonic *bandgap*, examples of which are shown in Fig. 10. This means that the transmission of a range of frequencies, given by $\omega_0 \pm \Delta\omega$, is effectively blocked (where ω_0 is the frequency at the center of the gap). A useful quantifier of the bandgap, which is independent of the crystal dimensions and relates to the reflection coefficient of Eq. (7), is the following ratio:[81]

$$\frac{\Delta\omega}{\omega_0} = \frac{2}{\pi}\sin^{-1}\left(\frac{n_1 - n_2}{n_1 + n_2}\right). \tag{8}$$

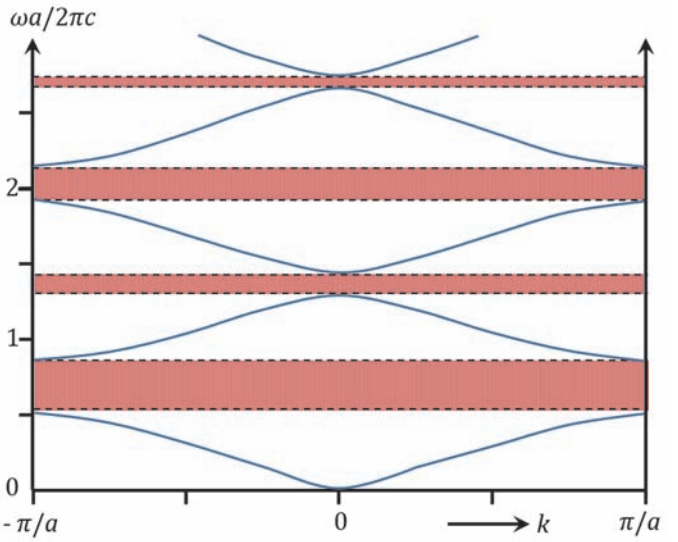

Figure 10 Band structure for a multilayer dielectric comprising alternating layers of equal thickness *a*, with refractive indices 2.9 and 6.7. Shaded regions denote photonic bandgaps; photons whose frequencies fall in this range cannot propagate through the material. For a layer thickness a = 1 μm, for example, the first bandgap spans wavelengths centered on 677 nm. Redrawn from Lipson and Lu.[83]

This is generally reported as a percentage. When photonic crystals contain a point or a linear defect, as depicted by Fig. 9(d–e), light with a frequency within the bandgap will be confined to the defect. As a result, the point defect can trap the light (the character of which is described by cavity QED, a subject that is outlined in Section 5.2), or the linear defect can direct the light, thus acting as a waveguide.[82] The capacity to engineer bandgaps in photonic crystals, fabricated with a judicious choice of materials, now plays a major role in the design of waveguides and fiber optics.[83]

2.6 Surface Plasmons

A highly active area of research is in the emerging field of *surface plasmons*. Analogous to the fact that light is composed of photons, surface plasmons are quanta of charge oscillations (free electrons in a plasma) that can form on the surface of a metal. Of most pertinent interest is the coupling of plasmons with light to form surface plasmon polaritons.[84–88] The strongly enhanced electric fields that surface plasmons produce at boundaries and edges, and their ability to guide light without a need for an optical fiber,[89] lead to a rich variety of applications, including surface-plasmon-based circuits,[90] near-field imaging,[91] photovoltaic devices,[92] nanosensors,[93] micro- and nano-fluidic systems,[94] nanoscale spectroscopy,[95] photodetectors,[96] and nanomedicine.[97] On smooth metals, surface plasmon polaritons share the quantized propagation features of both electrons and photons, and their character is strongly influenced by the specific electronic properties of the metal (at optical frequencies). Under normal circumstances, the surface plasmon of a smooth metal cannot be excited directly with light from vacuum because of a sizeable mismatch between the momentum conveyed by a free-space photon and the momentum of a plasmon at identical frequencies. However, this problem can be overcome by arranging for light to impinge upon a metallic film by internal reflection inside a prism, wherein the photon momentum is larger than its vacuum value.[98]

Chapter 3
Quantum Optics and Informatics

3.1 Interference of a Single Photon

The kinds of study originally conducted by Thomas Young—in particular, the celebrated "double slit" experiment[99] that we briefly examined in Chapter 1 (see Fig. 1)—provide a capacity to reveal far more than the wave nature of light, important as that is. True enough, the observed characteristic fringe pattern, when monochromatic light passes through two closely spaced slits onto a screen, appears to be simply explicable on the basis of waves from each slit undergoing constructive and destructive interference at different positions on the screen. Yet, astonishingly, these patterns of interference are still exhibited when individual photons of a low-intensity input beam reach the screen one at a time, showing that it cannot in fact be a matter of different photons having to interfere with each other. Indeed, Dirac enunciated the general principle[100] that photons can never directly interact with each other.* The double slit and other such experiments indicate that each photon interacts in a delocalized, wave-like manner with both slits *at the same time*. Successive experiments build interference patterns that conform to an exact mathematical distribution formula, but the position at which an individual photon is detected in any particular instance cannot be predicted; this is a quintessential illustration of *quantum uncertainty*.

Using the path integral approach of quantum theory,[101] the phenomenon is more accurately represented by introducing a summation over all possible routes between the source and the screen on which the pattern appears, signifying an entire "lifetime" for each photon involved in the experiment. This relates to the fact that the actual trajectory is unknown without an observation, and thus we only obtain the probabilities of the photon striking the screen at different positions and times; all trajectories (potentialities) must be considered in a superposition. Each route is considered equally probable, and the variation in phase produces *quantum interference*. The differences in phase of each trajectory, at varying positions on the screen, generates the fringe pattern. An intriguing variation on this experiment involves "marking" the photons so that the actual route of each photon to the screen is known. Remarkably, in such a case, the fringe patterns do not appear because quantum interference cannot occur. A consequence of the observation of the photon route is an effect that, in other quantum mechanical connections, is known

* Exceptions can arise in the sphere of high-energy physics.

as a *collapse of the wavefunction*.† However, it is possible for the fringe patterns to reappear when information on the route of the photons is lost; this is known as a *quantum eraser*.[102–106]

The quantum interference of light is most readily appreciated from several conceptually simpler experiments based on *beamsplitters*. However, to describe them properly requires the introduction of an appropriate, formal mathematical representation. In terms of quantum states, for example, the reflective and transmissive behavior of a low number of photons is generally cast in the form of *Dirac brackets* (kets). Thus, each single photon in a mode labeled "1," approaching an interface (see Fig. 11), may emerge in a quantum superposition of paths 2 and 3, with the former designating a throughput mode and the latter a reflected mode. As such, we write

$$|1\rangle_1 \rightarrow t|1\rangle_2|0\rangle_3 + r|0\rangle_2|1\rangle_3 . \tag{9}$$

Here, for example, $|1\rangle_2|0\rangle_3$ denotes one photon in radiation mode 2 and none in mode 3. Equation (9) therefore signifies that the output is divided into the two output channels with probability $|t|^2 = T$ for the single photon being transmitted (no photons in the reflected mode) and $|r|^2 = R$ for reflection (none in the transmitted mode). Thus, for an interface with 50% reflectivity (at a commonly assumed 45° angle of incidence), $|r|^2 = |t|^2 = ½$. Every case must satisfy the normalization condition $|r|^2 + |t|^2 = 1$.

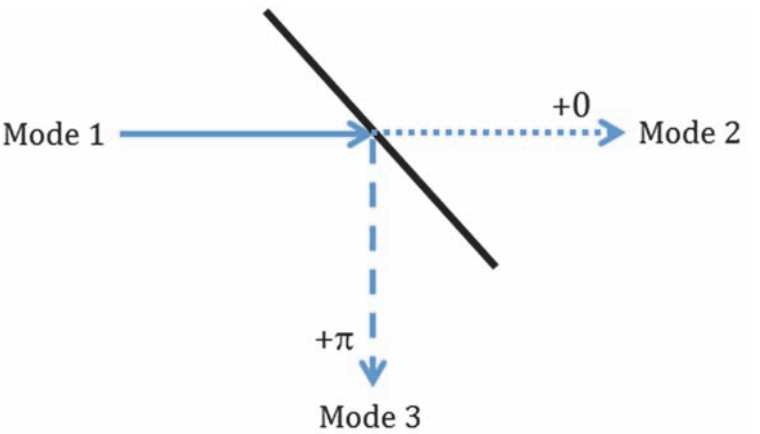

Figure 11 Splitting of an incident photon state (mode 1), at an interface, into a superposition of a transmitted state (mode 2) and a reflected state (mode 3). Here, mode 2 has no phase change, whereas mode 3 has a π phase change.

† Strictly, the term "wavefunction" is not applicable to individual photons (see Section 4.1).

Many of the most rewarding experiments are based on semi-reflective beamsplitters, which are commonly used in optics to separate a ray of incident light into two. This device works on the principle that light can be both reflected and transmitted as it travels through media of differing refractive indices; this concept has been well understood, in terms of the Fresnel equations, since the early 1800s. It follows from Eq. (7) that the coefficient r has a difference in sign according to whether light impinges upon an interface of higher, or lower, refractive index. As the light has a waveform, a change in sign is equivalent to a half-wave (π) phase shift.

Consider a beam of light that encounters a beamsplitter composed of a glass plate, with a reflective dielectric coating on one side (Fig. 12). While the transmitted beam has no change in phase, the reflected beam depends on the direction of incidence: light immediately reflected by the refractive coating has a π phase shift (air-to-reflector), but light that initially passes through the glass has no phase shift (glass-to-reflector). This occurs because the refractive index of the reflector is between that of the air and glass; the π phase shift only occurs when light passes from a low-refractive-index material into a high one.

A Mach–Zehnder interferometer measures the relative phase of the two paths of a split beam.[107,108] As shown in Fig. 13, it comprises two 50:50 beamsplitters (i.e., 50% reflected, 50% transmitted) and two 100% reflectors. Due to the different phase shifts that can occur for light reflection, one detector measures constructive interference between the two pathways, and the other measures destructive interference.[109] Remarkably, due to the superposition, each photon traveling through a Mach–Zehnder interferometer will produce an interference pattern at its detectors.[110]

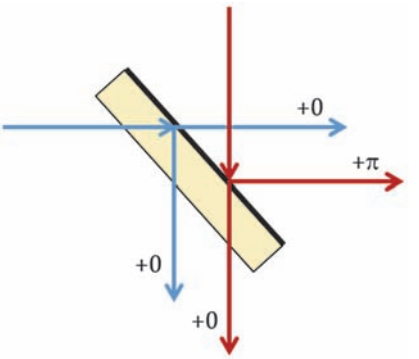

Figure 12 Optical phase changes produced by a semi-reflective beamsplitter composed of a glass plate (yellow) with a reflective dielectric coating on one side (thick black line). When light travels through the glass before reaching the coating (blue arrow from the left), the transmitted and reflected beams suffer no phase change. For light striking the coating without traveling through glass (red arrow from the top), the transmitted beam has no phase change, but the reflected beam has a π phase change.

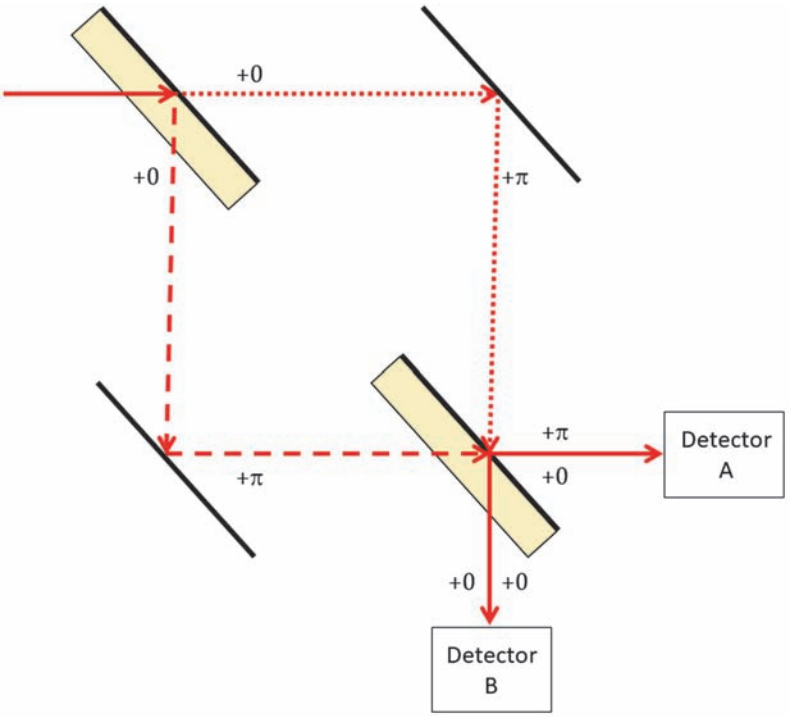

Figure 13 Mach–Zehnder interferometer, where the elements colored yellow are 50:50 beamsplitters, and black lines are 100% reflectors. The incident beam (red arrow, top left) separates into two at the first beamsplitter, i.e., it is both reflected (dashed arrow) and transmitted (dotted arrow), and then recombined at the second beamsplitter. Due to the phase shift (Fig. 11), the upper and lower pathways have 2π and π phase shifts at detector A, respectively; consequently, destructive interference occurs due to the π phase difference between pathways. In contrast, at detector B, both pathways have a π phase shift, and thus constructive interference occurs.

A related experiment, which shows distinct quantum mechanical effects involving *two* photons, is based on a two-sided mirror thin enough to allow exactly 50% transmission; this is known as the *Hong–Ou–Mandel effect*.[111] Identical beams of light, input at the same angle, are directed onto the same point on each side of the mirror, which is flanked by two photodetectors (Fig. 14). Intuition suggests that any photon registered at one of these detectors has a 50% chance of arriving from the partially transmitted beam and 50% from the other input, reflected off the mirror. However, theory and experiment again reveal remarkable quantum effects when the intensity of each input is sufficiently reduced to a level that gives individual photons only sporadically. It transpires that whenever two photons arrive at the mirror together, one from each source, then there is no possibility at all that both detectors can register a photon; this means that it is impossible to have either both photons transmitted or both photons reflected. As a

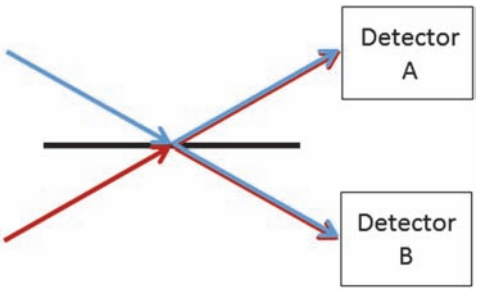

Figure 14 The Hong–Ou–Mandel effect. Two identical beams (input from the left) intercept a thin two-sided mirror (thick black line); the input beams have identical wavelength (different-color lines are for clarity only). When two photons, one from each input, simultaneously arrive at the mirror, it proves impossible for both photons to be transmitted or both photons to be reflected. Consequently, the two detectors are never triggered simultaneously.

result of destructive interference, the only possible outcome is for two photons to emerge in the same direction. The full description of such phenomena requires the development of photon creation operators, which will be examined in Section 4.1.

3.2 Entanglement

Quantum entanglement is a feature of fundamental significance in quantum mechanics. Moreover, it represents a key to the implementation of quantum information and computation technologies. At its heart are operations that are most readily achieved with photons, primarily based on beamsplitters and Mach–Zehnder optics. To achieve advances that can integrate with (and in certain respects supplant) state-of-the-art electronics, operations obviously need to be reduced from the level of an optical bench to the electronic chip, and integrated silicon chip implementations are advancing the forefront of technology.[112] To understand the capacity and power of quantum features to drive this area forward, we have to properly understand the true nature of quantum entanglement.

Until the mid-1960s, there were essentially two distinct perspectives on the observation (technically, the measurement) of a quantum state. The first, often described as the orthodox viewpoint, understood the act of measurement as establishing (in the sense of creating rather than identifying) the physical properties of the system. The counterpart, realist view contended that such attributes are defined *before* any measurement. As a result, a complete description of the physical reality would have to invoke other information, termed *local hidden variables*. The EPR (Einstein, Podolsky, and Rosen) paradox was devised to prove that the latter is the true supposition. The crux of their argument is that "when the momentum of a particle is known, its coordinate has no physical reality."[113] As will be evident, this is essentially adding a level of physical interpretation to a simpler notion enshrined in the uncertainty principle. A description to aid clarification of this position was later offered by David Bohm and Yakir Aharonov;[114] a comparable narrative, in terms of photons, now follows.

Consider a process (for example, parametric down-conversion, whose mechanism is discussed in Section 5.3) in which photons are released in pairs, together satisfying both linear and angular momentum conservation. Emerging from a stationary source, each photon in the pair thus travels outwards in opposite directions, and their polarizations must conform to opposite points on the Poincaré or Bloch sphere (Fig. 5). Such photon pairs are, therefore, said to be in an *entangled* state for the following reason. Suppose we choose to interrogate the light emitted in one direction with a linear polarizer. Before measurement, the state of each photon can be represented as, say, a superposition of horizontal and vertical polarizations, and we cannot know which photon has an H or V polarization without an observation. Suppose the polarization of a photon is measured when the photons are already a large distance apart; instantly, it is determined that the other photon must have the counterpart polarization. Therefore, if one of the photons is observed to have H polarization, it becomes simultaneously evident that the result of any polarization measurement on the other photon must be consistent with V polarization (or vice versa).

To a realist, it may seem that this conclusion offers no surprise: the photons may be considered to have had the observed polarizations when they were created, although not known to any observer. By contrast, the orthodox viewpoint says that the two polarizations are *formed* by the measurement. Einstein strongly disagreed with such reasoning, on the basis that that this "spooky action-at-a-distance" could not be instantaneous because a faster-than-light signal between the particles would violate special relativity. This is the nub of the paradox. The correlation between separate particles is now known as quantum entanglement. There is an important distinction here from the sampling of a classical system known to contain two dissimilar objects. In the quantum case, the *initial* state of the system cannot itself be said (without measurement and, therefore, wavefunction collapse) to comprise two separable entities.

The groundbreaking work of John Bell nonetheless proved that the quantum perspective correctly describes reality, i.e., the existence of any local hidden variables would be incompatible with the predictions of quantum mechanics.[115] Augmenting this view, Bell test experiments prove that such variables are untenable in all circumstances.[116–118] When a system of entangled objects evolves into a state in which the components are separated by great distances, the system still behaves as a single entity. This means that the measurement of any single component has the effect of a measurement on the whole. Exploiting quantum principles such as entanglement, especially relating to two-state systems known as qubits, provides the foundation for a host of novel effects and information-based applications.

3.3 Qubits Based on Light

As specified in Section 2.3, photons that are indistinguishable by their wavevector—meaning that they have the same wavelength and direction of propagation—may still be measurably distinguished if they differ in polarization. In fact, any two polarizations relating to opposite points on the Poincaré or Bloch

sphere are, in principle, completely separable by suitable polarizer optics. This well-known axiom forms the basis for many fundamental effects and applications in the field of quantum optics. It signifies that information can be conveyed in a binary basis, the common choice being the two orthogonal plane polarizations labelled H and V. However, the method by which this scheme works is different from conventional binary arithmetic, where every "bit" of information is absolutely one of the two values, 0 or 1. The difference arises because there is an infinite set of polarization states that is neither exactly H nor V. For example, light with a plane of polarization set at 45°, exactly halfway between the two, can pass through either an H or V polarizer with a 50% probability. At the level of individual photons, each quantum act of measurement thus collapses the probability to either 0% or 100%. The latent information, before such a measurement, is therefore best represented by a qubit, which allows there to be a superposition of the two basis states (i.e., H and V, equally expressible as 0 and 1).

In fact, any two-state quantum system is acceptable as a qubit, provided that the physical properties that represent the 0 or 1 are distinguishable and stable. Other means of implementation include the following:

- The most obvious possibility is for the absence or presence of a photon to be registered as the qubit basis; here, $|0\rangle$ and $|1\rangle$ are number (Fock) states that signify the number of photons.
- Left- or right-handed circularly polarized light. This type of light is in principle more easily defined and implemented for use as a qubit, compared to linearly polarized light, because they do not depend on any specific configuration of axes; both have a cycle-averaged cylindrical symmetry about the propagation axis, as explained in Section 2.1.
- Amplitude- or phase-squeezed light. As we observed in the previous chapter, the number of photons (the amplitude) and the phase of a laser beam cannot both be known exactly. Laser light can be described by a coherent state, in which the amplitude and the phase are equally uncertain. In a *squeezed* coherent state either the amplitude or the phase has enhanced precision, i.e., a reduced uncertainty, which means that its counterpart quantity becomes even less certain.[119] More details are given in Section 4.3.
- Short- or long-path in time-bin encoding. The latter involves sending uncorrelated photons (more precisely a photon wavepacket) through a two-path Mach–Zehnder interferometer with pathways of different lengths. Each photon exits the apparatus in a superposition of an "early time bin" and a "late time bin."[120,121] Reversible conversion of time-bin qubits to those based on polarization has been demonstrated.[122]

In industry, qubit systems based on superconductors are currently of most interest. These schemes usually involve a Josephson junction, i.e., two superconductors

separated by a thin insulating barrier, in which quantum tunneling of Cooper (spin-correlated) electron pairs through the insulator can occur.[123,124]

3.4 Theory of a Qubit

A quantum description of the two-slit experiment requires integration over the infinite number of possible trajectories, as stated in Section 3.1. In contrast, any qubit system will comprise two finite and discrete possibilities; in such cases, a simple summation will suffice. Hereby, the state of a qubit $|\Psi\rangle$, which may be represented by a single photon, can be written in terms of two quantum states in a superposition, i.e.,

$$|\Psi\rangle = \alpha_0 |0\rangle + \alpha_1 |1\rangle, \tag{10}$$

where the probability amplitudes α_0 and α_1 correspond to states $|0\rangle$ and $|1\rangle$, and thus the probability of observing $|0\rangle$ or $|1\rangle$ is $|\alpha_0|^2$ or $|\alpha_1|^2$, respectively. A qubit is sometimes called a quantum coin in the metaphorical sense that only two discrete and measurable possibilities may occur. The probability distribution of a fair quantum coin is 1/2 for $|0\rangle$ and 1/2 for $|1\rangle$, which corresponds to $\alpha_0 = \alpha_1 = 1/\sqrt{2}$ in the simplest case. A loaded quantum coin could have a probability of 1/3 for $|0\rangle$ and 2/3 for $|1\rangle$, meaning that $\alpha_0 = 1/\sqrt{3}$ and $\alpha_1 = \sqrt{2}/\sqrt{3}$ in this instance. When observation of either state is equally possible, another possible value of α_0 and α_1 is the complex number $1/2 + 1/2i$.

Notwithstanding the possibility of using a polarization basis for qubit implementation, it proves useful to adopt some of the formulation of polarization states in other cases. Analogous to the polarization of light, the qubit state can thus, in general, be visualized as a point on the surface of a Bloch sphere (right side of Fig. 5), in which the north pole represents $|0\rangle$ and the south pole is given by $|1\rangle$. All other possibilities, i.e., $|0\rangle$ and $|1\rangle$ in a superposition, corresponding to various values of α_0 and α_1, will reside somewhere on the surface of the sphere. If the qubit state is located on the equator, the probability of observing $|0\rangle$ or $|1\rangle$ is the same; any position on the northern or southern hemisphere respectively signifies that $|0\rangle$ or $|1\rangle$ is the more probable outcome.

At the point of observation, the collapse of the qubit state irreversibly positions the system at the north or south pole of the Bloch sphere. With respect to the Bloch sphere, analogous to Eq. (1), the state of the qubit can be written as

$$|\Psi\rangle = \cos\left(\frac{\theta}{2}\right)|0\rangle + e^{i\phi}\sin\left(\frac{\theta}{2}\right)|1\rangle. \tag{11}$$

Here, when determining the probability of observing $|0\rangle$ or $|1\rangle$, the angle θ is the important quantity because $|\alpha_0|^2 = \cos^2(\theta/2)$ and $|\alpha_1|^2 = \sin^2(\theta/2)$; in this instance, the phase factor $e^{i\phi}$ has no physical meaning since $e^{i\phi}e^{-i\phi} - 1$.

Only the standard basis, i.e., $|0\rangle$ and $|1\rangle$, has been considered thus far. Analogous to polarizations represented on the Poincaré sphere, any two orthogonal states can be chosen as the basis states. In quantum information, a common alternative is the following "sign basis" set that arises from $\theta = \pm\pi/2$, $\phi = 0$:

$$|+\rangle = \frac{1}{\sqrt{2}}\left(|0\rangle + |1\rangle\right),\ |-\rangle = \frac{1}{\sqrt{2}}\left(|0\rangle - |1\rangle\right), \tag{12}$$

which are necessarily normalized and mutually orthogonal. The basis states $|+\rangle$ and $|-\rangle$ are indistinguishable when measured in the standard basis. This occurs because the probability of observing $|0\rangle$ or $|1\rangle$ is 1/2 in both cases; the difference between $|+\rangle$ and $|-\rangle$ is the phase change, i.e., the change in sign on $|1\rangle$, that has no effect on the probability (because $\pm 1^2 = 1$). Hence, to differentiate between $|+\rangle$ and $|-\rangle$ and thereby detect the phase change, a measurement in another basis state is required—the most obvious one is the sign basis itself. An observation in the sign basis results in the qubit state residing at one of two positions on the equator of the Bloch sphere (relating to $|+\rangle$ or $|-\rangle$), rather than the north or south pole in the standard basis. If the qubit state is measured as $|+\rangle$ or $|-\rangle$, we cannot simultaneously know its exact state in terms of either a $|0\rangle$ or a $|1\rangle$ given that these two states are equally uncertain (to the maximum extent) following such an observation.

3.5 Quantum Logic Gates

In general, it has been shown that any logical operation (more precisely, any operation represented by a discrete unitary operator) can be constructed from a series of 2D beamsplitter operations.[125] In the context of information processing, data that is encapsulated in a qubit is physically processed by quantum logic gates. Such gates, in contrast to their classical electronic equivalents, are always reversible because they evolve according to Schrödinger's equation. However, the measurement of a qubit is irreversible; the state of the qubit before the observation is lost and cannot be recovered. Modification of the qubit state, due to the application of a logic gate, can be represented by a change in its position on the surface of the Bloch sphere. The three quantum logic gates that involve a partial rotation around the *x*, *y*, or *z* axes enable access to any point on the surface of the sphere when applied in combination; each one technically signifies a rotation in Hilbert space. As a result, starting from any initial state, all acceptable configurations of the qubit state can be achieved using just these three gates.

Let us assume the simple case of a ($|0\rangle$, $|1\rangle$) basis. It proves helpful to develop a vector representation in which

$$|0\rangle \equiv \begin{pmatrix} 1 \\ 0 \end{pmatrix};\ \ \langle 0| \equiv \begin{pmatrix} 1 & 0 \end{pmatrix},$$
$$|1\rangle \equiv \begin{pmatrix} 0 \\ 1 \end{pmatrix};\ \ \langle 1| \equiv \begin{pmatrix} 0 & 1 \end{pmatrix}. \tag{13}$$

Gates of special interest for quantum computational purposes are known as the bit flip X, phase flip Z, and Hadamard transform H, which may be represented thus:

$$\mathrm{X} = |0\rangle\langle 1| + |1\rangle\langle 0| \equiv \begin{pmatrix} 0 & 1 \\ 1 & 0 \end{pmatrix}, \tag{14}$$

$$\mathrm{Z} = |0\rangle\langle 0| - |1\rangle\langle 1| \equiv \begin{pmatrix} 1 & 0 \\ 0 & -1 \end{pmatrix}, \tag{15}$$

$$\mathrm{H} = \tfrac{1}{\sqrt{2}}\left(|0\rangle\langle 0| + |1\rangle\langle 0| + |0\rangle\langle 1| - |1\rangle\langle 1|\right) \equiv \begin{pmatrix} \frac{1}{\sqrt{2}} & \frac{1}{\sqrt{2}} \\ \frac{1}{\sqrt{2}} & -\frac{1}{\sqrt{2}} \end{pmatrix}, \tag{16}$$

expressed in both the "outer product" and matrix forms. As illustrated in Fig. 15(a–b), applying a bit flip or a phase flip to a qubit results in an interchange of |0⟩ and |1⟩, or a change in sign on |1⟩, respectively. In contrast, as shown in Fig. 15(c), the Hadamard transform involves the conversion of |0⟩ or |1⟩ into a superposition. This results in a transition from the standard basis into the sign basis. Given that all quantum gates are reversible, operating the Hadamard gate on a qubit in the sign basis produces a result in the standard basis.

When two or more qubits are employed, important physics may arise in the form of quantum entanglement. Qubits that are entangled cannot be treated as individual and isolated entities: in the sphere of optics, two-photon states afford the simplest possibility of implementing this principle. In a radiation state where two photons are entangled, neither can be defined without reference to its partner. The most commonly studied case is that of the *Bell states*, one of which is given by

$$\Psi = \frac{1}{\sqrt{2}}|00\rangle + \frac{1}{\sqrt{2}}|11\rangle \equiv \left(\tfrac{1}{\sqrt{2}} \quad 0 \quad 0 \quad \tfrac{1}{\sqrt{2}}\right)^{\mathrm{T}}, \tag{17}$$

where |00⟩ is shorthand for |0⟩|0⟩, etc., in which the first and second digit correspond to the state of the first and second qubit, respectively. In the column vector representation (exhibited in Eq. (17) as the row vector transpose), the basis set is $\{|00\rangle,|01\rangle,|10\rangle,|11\rangle\}$. Observation of the first qubit in the Bell state collapses the state function of both qubits. The state of the first qubit is either |0⟩ or |1⟩ with a probability of ½; when the measurement occurs at the first qubit, the state of the second qubit will simultaneously lose its superposition, emerging as |0⟩ or |1⟩, respectively.

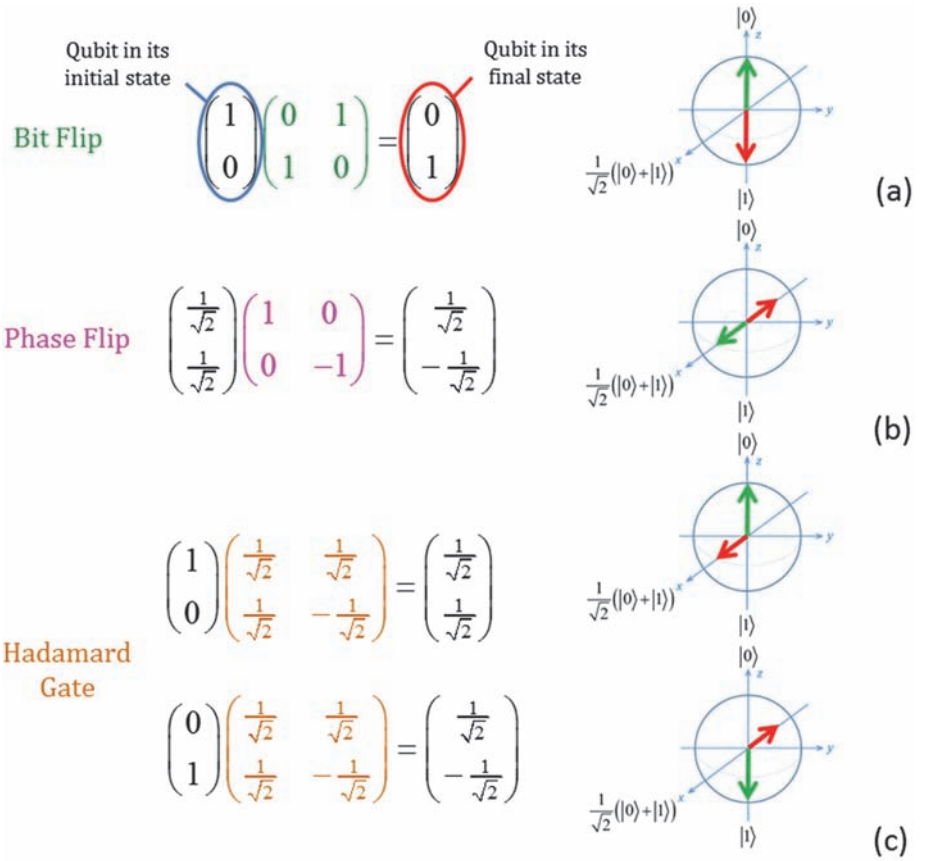

Figure 15 Matrix form of the quantum logic gates: (a) bit flip, (b) phase flip, and (c) Hadamard transform, and their effects on a qubit. Each diagram, based on a Bloch sphere, is used to visualize the state of the qubit before (green arrow) and after (red arrow) the quantum gate is applied.

Quantum circuits are diagrams used to represent the manipulation of multiple qubits by a set of quantum logic gates. In such diagrams, a single horizontal line depicts a qubit, and a double horizontal line symbolizes a classical bit. The latter occurs after measurement of a qubit, itself signified by the icon of a meter. Time flows from left to right, so that the leftmost logic gates are applied to the qubits first. Inputs to the circuit are to the left, and outputs are from the right. The number of inputs equals the number of outputs because quantum circuits are reversible, before qubit measurement. Two-qubit gates often appear in quantum circuits and usually involve entangled qubits.

The entanglement of two qubits, to produce a Bell state, can be achieved with a two-qubit gate known as a controlled-NOT (CNOT) gate. In such a gate, a target qubit interchanges $|0\rangle$ and $|1\rangle$ when the control qubit is set to $|1\rangle$. With inputs $|0\rangle$ and $|1\rangle$, the CNOT gate acts analogously to its classical equivalent. Quantum features occur when one of the inputs is converted into the sign basis via a

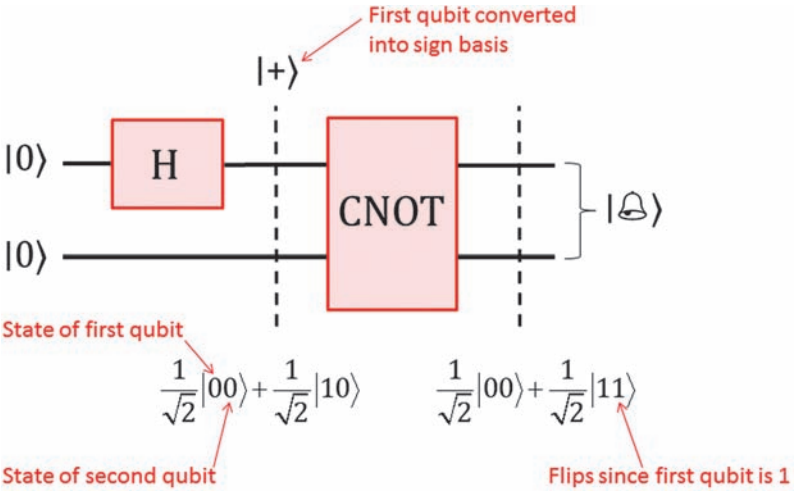

Figure 16 Quantum circuit for the entanglement of two independent qubits |0⟩ into a Bell state |🔔⟩. This involves a Hadamard transform H and a CNOT gate. The value of the two qubits, in shorthand form below the circuit, is provided at certain positions (vertical dashed lines).

Hadamard transform. For example, the Bell state of Eq. (17) is generated by two inputs of |0⟩ into the quantum circuit of Fig. 16. A two-qubit gate is represented by a 4 × 4 matrix rather than a 2 × 2 matrix of single qubit gates. The matrix form of the CNOT gate is written as

$$\mathrm{CNOT}=\begin{pmatrix}1&0&0&0\\0&1&0&0\\0&0&0&1\\0&0&1&0\end{pmatrix}, \tag{18}$$

whereas the two input qubits of Fig. 16 are represented by

$$|00\rangle=\begin{pmatrix}1&0&0&0\end{pmatrix}^{\mathrm{T}}. \tag{19}$$

After one of the inputs passes through a Hadamard transform, the CNOT gate entangles the two qubits into a Bell state, as signified by Fig. 17.

The implementation of logical operations, based on the quantum states of light, thus opens up broad new avenues of application. The attraction is not only a substantial reduction of the losses associated with conventional electronic circuitry, which allows significantly greater energy efficiency, but also the possibility of distinctive advantages in processing efficiency. Through quantum entanglement between qubits, there is a computational principle known as *Shor's algorithm* that can produce a significant speedup in integer factorization. Thus, the

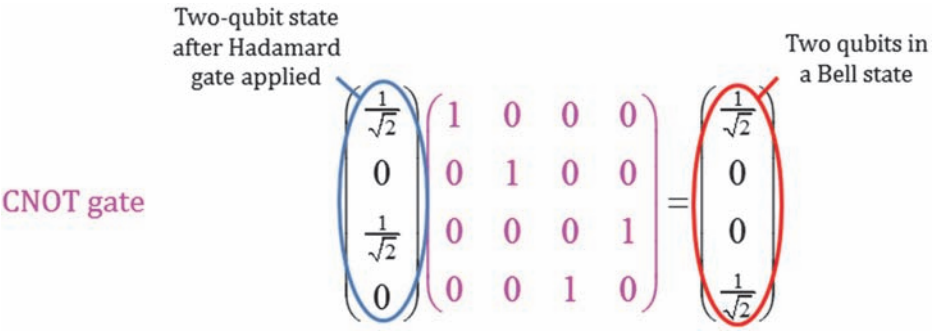

Figure 17 Matrix form of a CNOT gate applied to a two-qubit state, based on the quantum circuit of Fig. 16. The CNOT gate is a two-qubit gate represented by a 4×4 matrix.

breaking of public-key cryptography, previously assumed to be computationally intractable, could be a possibility. At present, by use of this form of quantum algorithm, factorization with up to 15 photonic qubits has been demonstrated.[126,127] Beyond the sphere of cryptography, a principle of much wider applicability is the prospect of using quantum protocols for dramatically faster searching of databases. For a given database with N entries, the extent of reduction in the number of operations has been shown to scale with approximately $\sqrt{N}$.[128]

3.6 Quantum Teleportation

In recent years, the term "teleport," whose origins surprisingly date back to the nineteenth century (though the concept, perhaps, gained more prominence in *Star Trek* and other kinds of science fiction), has, to some extent, been misappropriated to signify something rather different from material transposition. In quantum technologies, it now denotes the conveyance of a quantum state from one location to another, for which the substrates are, in general, materially distinct. However, the transmittance of a quantum state is usually fraught with more complications than simply dispatching conventional information. In particular, the capacity to transmit such information with complete fidelity is frustrated by a principle known as the *no-cloning theorem*, which dictates that a qubit state cannot be copied with 100% success.[129] This necessarily complicates viable quantum procedures for securely delivering encrypted information between physically separated parties. The implementation of strategies to encrypt and decrypt messages, by sharing a random secret key that is known by and accessible to no other party, is termed *quantum key distribution*.[130]

The closest alternative to qubit copying, called *quantum teleportation*,[131] is now explained. In quantum information, it is convention that data sharing involves two persons conventionally named Alice and Bob. Their capacity to exploit quantum communication is based on prior establishment of a shared, entangled state. To begin, Alice has an unknown qubit that she wants to send to Bob; her second qubit is the one that is entangled to a third, held by Bob. On examining the quantum circuit of Fig. 18, a CNOT gate is first applied to Alice's two qubits. Then

(entering Region I of the circuit) Alice measures her entangled qubit and sends the outcome to Bob. If the result is $|0\rangle$, Bob does nothing; otherwise, he applies a bit flip to his qubit. At this point in the circuit, Alice applies a Hadamard gate to the unknown qubit, takes a measurement, and again transmits the result to Bob. Once more (in region II), if the outcome is $|0\rangle$ Bob does nothing, but otherwise he applies a phase flip. The final result is that Bob has recreated the unknown qubit and that Alice has destroyed both of her qubits due to their measurement. The latter means that quantum teleportation is entirely compatible with the no-cloning theorem. The experimental realization of quantum teleportation was first achieved using a set of photonic qubits.[132] Today, teleportation has been accomplished with a myriad of different substances and technologies;[133] alongside quantum key distribution, it is expected to shape the future of the processing and transmitting of data.

Before moving on, it is interesting to note and reflect on the pervasive assumption and application of a binary basis for quantum logic. In each of the different forms of optical implementation (some of which are listed in Section 3.3), a two-fold basis affords the platform for qubit computation. In the realm of atom optics, a two-level atom can represent a similar kind of platform. We are all familiar with the binary arithmetic at the core of classical computing, with origins

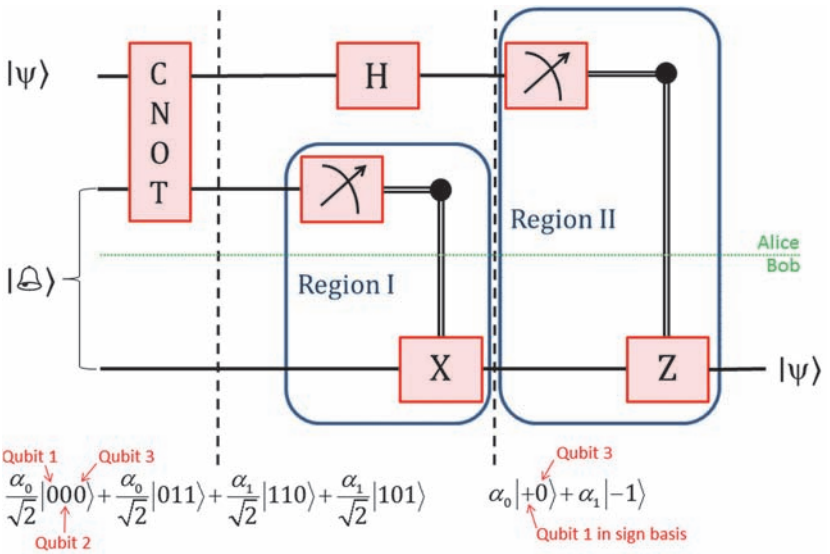

Figure 18 Quantum circuit for quantum teleportation, in which Alice sends an unknown qubit to Bob. To mediate the transfer of this qubit, Alice and Bob each share an entangled qubit in a Bell state. The H, X, and Z gates are the Hadamard transform, bit flip, and phase flip, respectively, and the meter symbol (showing an arrow against a notional dial) denotes an observation. Following the CNOT gate, the state of the three qubits is expressed at the lower left; the status of this entangled state is again given after Region I. The unknown qubit is reproduced by Bob at the end of the circuit.

in the earliest electronic forms of on/off switching component. However, to achieve a greater density of coding information, a base higher than two clearly has attractions. An alternative strategy to multi-photon qubits is to deploy a smaller number of photons in a high-dimensional state. For example, it is possible to engineer two-photon, high-dimensional states by exploiting quantum interference effects.[134,135] Still wider opportunities arise in connection with structured light, as will emerge in Section 4.4.

Chapter 4
Quantum Fields

The starting point for the formal classical description of electromagnetic radiation is usually Maxwell's equations. Originally, there were 20 equations, which essentially summarized earlier works by Karl Gauss, André-Marie Ampère, Michael Faraday, and others. Maxwell added the idea of a "displacement current" to complete his electromagnetic theory.[12] Many years later, the number of Maxwell's equations was lowered to four by Oliver Heaviside.[136] By use of the curl and divergence operators of vector calculus, he was able to produce the form of Maxwell's equations whose vacuum formulation is familiar today (Table 1). Often overlooked and undervalued is the analysis and experimental testing of Maxwell's original equations by Heinrich Hertz, which facilitated their acceptance and advancement.[137]

One of the key results underpinning a quantum formulation of electrodynamics is the following equation, in which a volume integral succinctly expresses the energy of any radiation field H_{rad} in terms of the position **r**-dependent electric and magnetic induction fields **E**(**r**) and **B**(**r**), respectively:

$$H_{\text{rad}} = \frac{\varepsilon_0}{2}\int_V \left(\left|\mathbf{E}(\mathbf{r})\right|^2 + c^2 \left|\mathbf{B}(\mathbf{r})\right|^2 \right) d^3 r. \tag{20}$$

Here, the constant ε_0 is the permittivity of free space.

Table 1 Maxwell's equations in terms of differentials (spatial derivatives), where **E** and **B** are the electric and magnetic induction fields, respectively. Here, the symbol ρ is the electric charge density, ε_0 is the permittivity of free space, μ_0 is the permeability of free space, and t is time. **J** denotes the displacement current.

Name	Equation	Note
Gauss' law	$\nabla \cdot \mathbf{E} = \frac{\rho}{\varepsilon_0}$	Spatial variations in the electric field are associated with charges
Gauss' law for magnetism	$\nabla \cdot \mathbf{B} = 0$	There are no magnetic monopoles
Faraday's law	$\nabla \times \mathbf{E} = -\frac{\partial \mathbf{B}}{\partial t}$	A spatially circulating electric field drives a time-varying magnetic field
Ampère's law	$\nabla \times \mathbf{B} = \mu_0 \left(\mathbf{J} + \varepsilon_0 \frac{\partial \mathbf{E}}{\partial t} \right)$	A current and a time-varying electric field generate a spatially circulating magnetic field

4.1 Operator Formulation

In the quantum formulation, the electric **E** and magnetic **B** fields are promoted from the vector status of classical theory into operators. These quantum expressions comprise lowering a and raising $a^\dagger$ ladder operators, which individually relate to processes that terminate or produce a photon, respectively. Each involves an upward or downward movement on the "ladder rungs" of discrete energy levels, as shown in Fig. 19. Formally, these ladder operators act on a number (Fock) state $|N\rangle$ so that

$$a|N\rangle = N^{1/2}|N-1\rangle \tag{21}$$

represents an annihilation of a photon, and

$$a^\dagger|N\rangle = (N+1)^{1/2}|N+1\rangle \tag{22}$$

signifies photon creation; N is any positive integer that denotes the number of photons.*

In its simplest form, for a plane-polarized input laser (or other well-collimated) beam with a negligible-frequency linewidth, a single radiation mode has a quantum form expressible in terms of number states $|N\rangle$ that satisfy a *completeness relation*

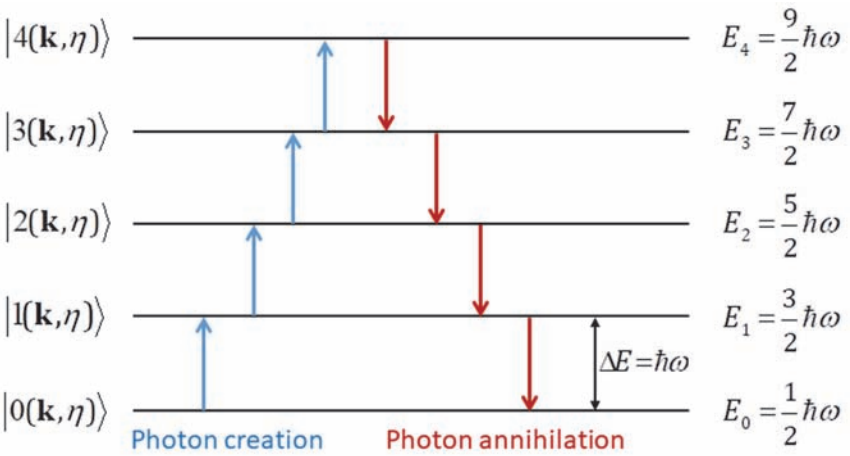

Figure 19 Operation of the photon creation and annihilation ladder operators.

* Fock states are specially constructed to embody the symmetrization that is necessary for a system of identical particles. Their usage allows the states of any specific radiation mode to be expressed in simple terms of the occupation number of that mode, identified as the number of photons it contains.

$$\sum_{N=0}^{\infty} |N\rangle\langle N| = 1, \tag{23}$$

and the associated electric field can be expressed in operator form as

$$\mathbf{E} = \left(\frac{\hbar ck}{2\varepsilon_0 V}\right)^{\frac{1}{2}} \left(a - a^{\dagger}\right)\mathbf{e}. \tag{24}$$

Here, **e** is the electric polarization vector introduced in Eq. (1), k is the magnitude of a specific photon wavevector **k** (ck equals ω), and V now defines an arbitrary volume that allows for quantization of the system. The latter parameter may be taken as the volume of any region that includes the entirety of the matter–radiation interaction at photon level; since it is arbitrary, V will always disappear in any final result. Equation (24) clearly exhibits a connection with the quantum mechanics of simple harmonic motion,[138] including a non-zero ground state energy, as we shall see later. It is also significant that the following operator commutation relation

$$\left[a, a^{\dagger}\right] \equiv aa^{\dagger} - a^{\dagger}a = 1 \tag{25}$$

is consistent with an integer spin of a photon (as explained earlier, the photon is indeed such a particle, i.e., a *boson*).

Equation (24) provides an effective representation of the electric field when only one radiation mode is employed. More generally, Eq. (24) will involve a summation over both **k** and polarization η. With this in mind, the full expression for the electric and magnetic field of a photon are cast as follows, in which the polarization unit vector is now explicitly represented as $\mathbf{e}^{(\eta)}(\mathbf{k})$:

$$\mathbf{E}(\mathbf{r}) = i\sum_{\mathbf{k},\eta}\left(\frac{\hbar ck}{2\varepsilon_0 V}\right)^{\frac{1}{2}} \left\{\mathbf{e}^{(\eta)}(\mathbf{k})a^{(\eta)}(\mathbf{k})e^{i\mathbf{k}\cdot\mathbf{r}} - \overline{\mathbf{e}}^{(\eta)}(\mathbf{k})a^{\dagger(\eta)}(\mathbf{k})e^{-i\mathbf{k}\cdot\mathbf{r}}\right\}, \tag{26}$$

$$\mathbf{B}(\mathbf{r}) = i\sum_{\mathbf{k},\eta}\left(\frac{\hbar k}{2\varepsilon_0 cV}\right)^{\frac{1}{2}} \left\{\mathbf{b}^{(\eta)}(\mathbf{k})a^{(\eta)}(\mathbf{k})e^{i\mathbf{k}\cdot\mathbf{r}} - \overline{\mathbf{b}}^{(\eta)}(\mathbf{k})a^{\dagger(\eta)}(\mathbf{k})e^{-i\mathbf{k}\cdot\mathbf{r}}\right\}. \tag{27}$$

In Eq. (27), the magnetic polarization vector of each photon is denoted by $\mathbf{b}^{(\eta)}(\mathbf{k}) = \mathbf{e}^{(\eta)}(\mathbf{k}) \times \hat{\mathbf{k}}$ (overbars signify complex conjugates), which depends upon the photon mode (**k**, η), and the phase factors are $e^{\pm i\mathbf{k}\cdot\mathbf{r}}$. It may be noted that, in the preceding mode representations, electric and magnetic polarization vectors are invariably orthogonal to their corresponding wavevectors, signifying *plane wave* expansion; in other words, the *wavefronts* (surfaces of constant phase) are parallel

planes, consistent with a notional infinitely remote source. In the Schrödinger picture assumed here, $\mathbf{E}(\mathbf{r})$ and $\mathbf{B}(\mathbf{r})$ are explicitly time-independent because a dependence on this quantity is held within the state vector. It is worth noting that the entirety of the second term in each of the preceding expressions is the Hermitian conjugate of the first (where variables are complex conjugated and operators become their Hermitian conjugates) so that in each expression the braces can be closed after $e^{i\mathbf{k}.\mathbf{r}}$ and "+ *h.c.*" is added. This mathematical device is followed in Section 4.4.

In one-center processes, such as single-photon absorption, the site of interaction can be chosen as the origin for the spatial coordinates without any loss of generality. In addition, considerably more elaborate constructs for the electric and magnetic field operators that explicitly account for refractive and dissipative corrections have been derived by Gediminas Juzeliūnas.[139] However, in practice, the free-field (vacuum) form given by Eqs. (26) and (27) are most commonly used.

In quantum theory, the energy of the radiation field is also defined by an operator. An expression for which can be found by inserting Eqs. (26) and (27) into Eq. (20) so that the following is determined:

$$H_{\text{rad}} = \sum_{\mathbf{k},\eta} \left(N^{(\eta)}(\mathbf{k}) + \frac{1}{2} \right) \hbar\omega, \tag{28}$$

where the dependence of ω on $\mathbf{k}$ is left implicit; and $N^{(\eta)}(\mathbf{k}) = a^{\dagger(\eta)}(\mathbf{k})a^{(\eta)}(\mathbf{k})$ is the *number operator*, which returns the number of photons N when applied to a Fock state. Moreover, for the ground state of the radiation, $\frac{1}{2}\hbar\omega$ represents the zero-point energy, associated with *vacuum fluctuations* that are present even in the absence of radiation (see Section 4.5). On inspection of Eq. (28), the energy of a single photon is appropriately determined as $\hbar\omega$ because $N^{(\eta)}(\mathbf{k})\,|1\rangle = 1|1\rangle$.

In general, it is important not to interpret the eigenstates of H_{rad} as "photon wavefunctions." There is one exception: the distinction is less significant (other than for precision of terminology) for modes that contain a single photon. For this reason, a blurring of definitions is sometimes allowed in accounts of quantum optical systems, where the behavior of individual photons is of primary interest. However, in general, it can be asserted that there is no such thing as a *photon wavefunction*. Consider any specific radiation mode $(\mathbf{k},\eta)$: there is no way to represent the wavefunction for the two-photon state $|2(\mathbf{k},\eta)\rangle$ as any kind of combination or product of one-photon $|1(\mathbf{k},\eta)\rangle$ state wavefunctions. This is not really surprising; in the same way, it is not possible to represent the wavefunction for a 2*s* electron in hydrogen in simple terms of 1*s* wavefunctions. In the radiation case, to do so would also misrepresent the vacuum energy, which does not scale with N but is exactly $\frac{1}{2}\hbar\omega$ for both the $|1(\mathbf{k},\eta)\rangle$ and $|2(\mathbf{k},\eta)\rangle$ states.[140]

The most obvious feature of Eq. (28), other than its non-zero ground state energy, is its equally spaced set of energy levels. In a certain sense, it seems obvious that a state with N photons should have N times as much energy (measured from the ground state) as one photon—in other words, we can anticipate an equally

spaced set of energy levels, extending upwards to infinite extent. However, it is a logical corollary of this expectation that the underlying quantum theory has to be of simple harmonic oscillator form.[141,†]

4.2 Linear and Angular Momentum

As outlined in Section 2.1, photons can have both a linear and an angular momentum. The total linear momentum of the quantized electromagnetic radiation $\mathbf{P}_{\text{rad}}$, which comprises all populated photon modes, is expressed as

$$\mathbf{P}_{\text{rad}} = \sum_{\mathbf{k},\eta} N^{(\eta)}(\mathbf{k})\hbar\mathbf{k}, \tag{29}$$

in which the zero-point momentum for each mode $\frac{1}{2}\hbar\mathbf{k}$ vanishes due to each $\mathbf{k}$ in the summation having a matching $-\mathbf{k}$ (c.f., the zero-point energy, which persists because energy is a positive quantity only). From this expression, the linear momentum of each photon is $\hbar\mathbf{k}$.

The total *angular* momentum of the quantized electromagnetic radiation $\mathbf{J}_{\text{rad}}$ can be rewritten in terms of spin and orbital, so that $\mathbf{J}_{\text{rad}} = \mathbf{S}_{\text{rad}} + \mathbf{L}_{\text{rad}}$. This separation is achievable by assuming that the light has paraxial form, i.e., subject to the same conditions as apply for the small-angle approximation in Gaussian optics. Non-paraxial light is not considered in this book; such analyses are found elsewhere.[142–145] Radiation states of circular polarization are eigenstates of the operator for quantum spin $\mathbf{S}_{\text{rad}}$. This is consistent with an angular momentum of $\pm\hbar$ per photon with the sign determined by handedness; the vector quantity directed along $\mathbf{k}$ is thus expressible as $\pm\hbar\hat{\mathbf{k}}$. This spin feature is conveyed with

$$\mathbf{S}_{\text{rad}} = \sum_{\mathbf{k}} \left\{ N^{(\text{L})}(\mathbf{k}) - N^{(\text{R})}(\mathbf{k}) \right\} \hbar\hat{\mathbf{k}}, \tag{30}$$

where the mode summation is specifically cast in terms of circular polarizations, either left- or right-handed light, as denoted by the superscript L and R. This expression indicates that the spin-angular momentum $\mathbf{S}_{\text{rad}}$ depends solely on the disparity of left- and right-handed photon populations.[146,147]

The basis set for the mode expansion in Eqs. (26) and (27) comprise plane waves. Such modes have no orbital angular momentum (OAM), and therefore a different form of basis is required to express the properties of beams with non-zero OAM. It emerges that the corresponding operator $\mathbf{L}_{\text{rad}}$ is most expediently expressed in terms of a modal basis associated with a helical wavefront. (This will be more readily understood when we consider the detailed form of vortex modes in Section 4.4: their optical phase depends on both axial position and angular

† Any infinite set of equally spaced discrete energy levels necessarily owes its origins to a Hamiltonian that accommodates terms quadratic in a pair of dynamical variables corresponding to non-commuting quantum operators.

disposition so that any surface of constant phase can no longer be simply transverse to the beam.) Typically, the chosen basis are Laguerre–Gaussian (LG) modes[148]

$$\mathbf{L}_{\mathrm{rad}} = \sum_{k,\eta,l,p} N_{lp}^{(\eta)}(\mathbf{k})\, l\hbar\hat{\mathbf{k}}, \tag{31}$$

in which the four degrees of freedom are the magnitude of a wavevector k, polarization η, and the indices l and p as integers that, in the case of LG modes, designate the order and degree of the corresponding Laguerre polynomial, respectively. The former index is often known as the *topological charge*; the latter is the *radial index* that represents the number of radial nodes $p + 1$ within the transverse field distribution of the beam. In passing, it is useful to note that by casting the sum over η explicitly in terms of a basis comprising left- and right-handed circular polarizations, we arrive at[149]

$$\mathbf{L}_{\mathrm{rad}} = \sum_{k,l,p} \left\{ N_{lp}^{(L)}(\mathbf{k}) + N_{lp}^{(R)}(\mathbf{k}) \right\} l\hbar\hat{\mathbf{k}}, \tag{32}$$

which forms a neat counterpart to the spin angular momentum given by Eq. (30). The previous expressions indicate that the OAM has no connection with any spin helicity associated with polarization.[150] Furthermore, a photon endowed with topological charge is found to have an OAM of magnitude $l\hbar$. Some of the associated features are considered in greater detail in Section 4.4.

4.3 Photon Statistics and Quantum States

So far in this chapter, only Fock states have been considered; they are eigenstates of the radiation Hamiltonian, which correspond to a precise energy and are therefore associated with a definite number of photons. Essentially, such states describe beams of light in which the intensity is unequivocally constant. However, no light source can truly be described in this way. The discrete, statistical nature of the radiative transitions that produce light in any real source precludes an exactly fixed intensity of emission, and indeed the form of the fluctuations proves to be a characteristic feature of each source. For example, the intensity fluctuations delivered by a thermal source are typically of Bose–Einstein form, whereas those of the most stable laser sources are closer in form to a Poisson distribution (see Fig. 20). The interpretation of any such fluctuations in terms of photon statistics introduces a need for other forms of quantum state representation. In view of the special role that laser light has in the study of quantum features, it is this case that we now examine in more detail.

The number states form a complete basis set for any radiation mode, and hence any quantum state representation of a given mode can be expressed in terms of them. The state representation that gives rise to Poisson statistics is specifically the

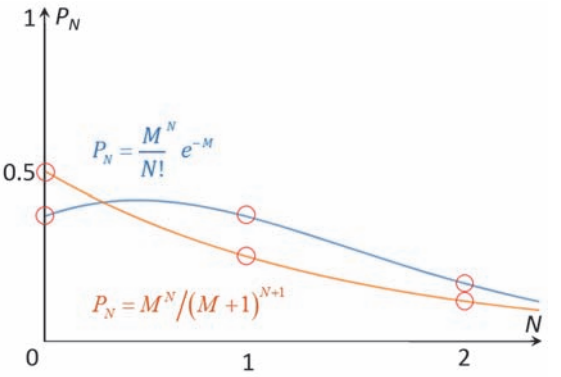

Figure 20 Comparison of Bose–Einstein (orange curve) and Poisson (blue curve) photon statistics for the same mean number of photons M in a small volume. For the Bose–Einstein case, the instantaneous probability P_N of finding N photons is always greatest for $N = 0$, though outweighed by the summed probabilities for $N \geq 1$. Note that the curves are only meaningful for integer values of N, as indicated (red circles). For $M = 1$, the probability of zero photons is 0.5 for Bose–Einstein statistics, whereas for the Poisson case the probabilities of zero or one photon are equal.

coherent state. Assuming reference to just one specific mode, and therefore dropping the associated labels $(\mathbf{k}, \eta)$ for clarity, the coherent state $|\alpha\rangle$ is expressible as follows:

$$|\alpha\rangle = e^{-\frac{1}{2}|\alpha|^2} \sum_{N=0}^{\infty} \frac{\alpha^N}{(N!)^{\frac{1}{2}}} |N\rangle, \tag{33}$$

where α is a complex number with indeterminate phase. Strictly, Eq. (33) represents one member of an *overcomplete basis* given that the counterpart to the completeness relation of Eq. (23) is now

$$\int |\alpha\rangle\langle\alpha| d^2\alpha = 1, \tag{34}$$

where there is double integration over both the real and imaginary parts of α.

There are several notable properties of a coherent state. First, it is readily proven to be an eigenstate of the annihilation operator, i.e.,

$$a|\alpha\rangle = \alpha|\alpha\rangle. \tag{35}$$

The physical significance for the modulus of α then emerges: its square $|\alpha|^2$ represents the mean number of photons M in a Poisson distribution cast as

$$P_N = \frac{M}{N!}^N e^{-M}. \tag{36}$$

The electric (and magnetic) field properties of coherent states exhibit a variety of other interesting and useful features. First, the larger the value of $|\alpha|$ is, the more closely the electromagnetic fields approximate to the propagating characteristics of a classical (sine) wave, with proportionately less quantum noise. This is of particular significance to optics; notably, the output of a well-behaved continuous-wave laser approximates, more closely than any other source, to a classical wave. Furthermore, the interplay of intensity and phase is a manifestation of a fundamental quantum uncertainty principle, whose origin lies in the following operator commutation relation:[55]

$$\left[N^{(\eta)}(\mathbf{k}), \exp\left(i\theta^{(\eta)}(\mathbf{k}) \right) \right] = -\exp\left(i\theta^{(\eta)}(\mathbf{k}) \right), \tag{37}$$

where $N^{(\eta)}(\mathbf{k})$ is the number operator introduced previously, and $\theta^{(\eta)}(\mathbf{k})$ represents a phase operator. This relation applies individually to each mode of any complete, orthogonal set of states for a specific optical mode. The quantum optical phase, whose operator appears here, does not signify a relative phase between individual photons; it denotes a relative phase between the radiation state vectors for states with, for example, one photon and with two (identical) photons.‡ A historic compendium of the various attempts to tackle the issue is to be found in a volume edited by Stephen Barnett and John Vaccaro.[151]

The coherent state is a minimum uncertainty state in which neither the number of photons nor the phase is precisely defined. In contrast, the non-zero right-hand side of Eq. (37) indicates a physical result that if the number of photons is well-defined—as it is for the number states $|N\rangle$, discussed previously—then the optical phase is completely undeterminable. Figure 21 illustrates the interplay of photon number and phase for a coherent state; reading downwards, the three panels show the increasing conformity to a classical wave as the mean number of photons is increased. As stated earlier, in a squeezed coherent state either the number of photons or the phase has enhanced precision, i.e., a reduced uncertainty, which means that its counterpart quantity becomes comparatively less certain. In the former case, the photon number distribution is denoted as sub-Poissonian, indicating that it is narrower than the corresponding coherent state.[152]

4.4 Structured Light

To exhibit OAM, light has to have a special kind of beam structure whose quantized form is designated by eigenstates and eigenvalues of the operator $\mathbf{L}_{\text{rad}}$.

‡ The quantum phase operator is ill-defined, being associated with problems due to its cyclic domain.

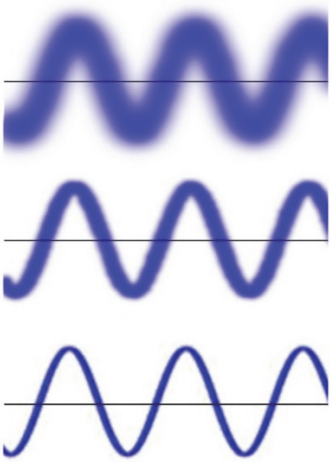

Figure 21 Schematic illustration (top to bottom) of the progressive reduction in phase uncertainty with an increase in the mean number of photons, for the same optical mode.

Commonly, any such radiation state is known as an *optical vortex*, alternatively called *twisted light*. Achieving this type of structure places constraints upon the form of the transverse field distribution, specific forms of which are considered later. However, in each case, the key attribute is a phase factor that varies around the beam.

This is readily understood as follows: the standard form of a quantum angular momentum operator, expressed in terms of the angular position about the appropriate rotational axis, is $-i\hbar\partial/\partial\phi$. Thus, a beam with a phase factor of the form $e^{il\phi}$, where ϕ is the azimuthal angle around the beam axis, will convey a corresponding orbital angular momentum $l\hbar$: for continuity in the fields, l has to assume a positive or a negative integer value. The incorporation of such a phase factor in the electromagnetic field expansions immediately signifies that there has to be a singularity along the beam axis, where ϕ is undefined. (If all phases were present, destructive interference would be observed.) For this reason, twisted light is intimately connected with the field of *singular optics*. Other forms of structured light may not necessarily convey OAM, e.g., *Airy* beams (so-called *self-accelerating* or *non-diffracting* beams) in which regions of positive and negative OAM balance each other out.[153]

In the most common forms of twisted light, the value of l determines the number of distinct helical surfaces formed by the optical wavefront, as they wind around a common propagation axis within the span of a wavelength, and with either a positive or a negative sense of twist. For this reason, l is often called the *winding number* or, more formally, *topological charge*. The electric and magnetic fields both exhibit this feature, illustrated in Fig. 22. Light with this kind of wavefront structure includes Laguerre–Gaussian modes and all but the simplest

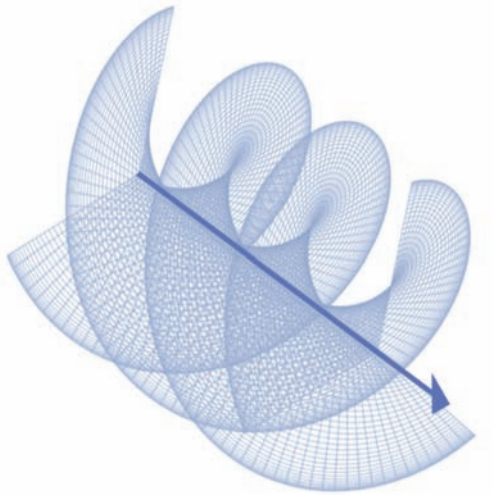

Figure 22 Wavefront surface for an optical vortex with a topological charge of three, over the span of three wavelengths (three intertwined helical surfaces).

forms of Bessel and Mathieu beams.[154–156] Experimental methods for bestowing a conventional Gaussian beam with OAM commonly involve passage of the beam through spatial light modulators (SLMs),[157,158,60] pitch-fork holograms,[159–161] spiral phase-plates,[162] paired cylindrical lenses,[163] *q*-plates,[164] or with the use of hyperbolic metamaterials.[165] Moreover, a theoretical method has been proposed for the direct generation of light endowed with OAM, based on light emission from an array of nanoparticles.[166–168]

The theoretical basis for the concept of a vortex beam was established in a series of works.[154,169,170] For Laguerre–Gaussian modes,[§] the explicit formulations for the electric and magnetic field expansions (previously defined in Eqs. (26) and (27) for plane-wave light) are now written as follows, with the position vector **r** having reference to cylindrical coordinates (z, r, ϕ):[171]

$$\mathbf{E}(\mathbf{r}) = i \sum_{k,\eta,l,p} \left(\frac{\hbar c k}{2\varepsilon_0 V} \right)^{\frac{1}{2}} f_{l,p}(r) \left\{ \mathbf{e}_{l,p}^{(\eta)}(\mathbf{k}) a_{l,p}^{(\eta)}(\mathbf{k}) e^{i(\mathbf{k}\cdot\mathbf{r}+l\phi)} \right\} + h.c., \tag{38}$$

$$\mathbf{B}(\mathbf{r}) = i \sum_{k,\eta,l,p} \left(\frac{\hbar k}{2\varepsilon_0 c V} \right)^{\frac{1}{2}} f_{l,p}(r) \left\{ \mathbf{b}_{l,p}^{(\eta)}(\mathbf{k}) a_{l,p}^{(\eta)}(\mathbf{k}) e^{i(\mathbf{k}\cdot\mathbf{r}+l\phi)} \right\} + h.c., \tag{39}$$

where z is the axial position, r denotes the off-axial radial distance, and $f_{l,p}(r)$ is a normalized radial function whose form depends on l only through its modulus.

[§] The field equations for Laguerre–Gaussian beams can be derived as paraxial solutions in cylindrical coordinates to the scalar Helmholtz equation.

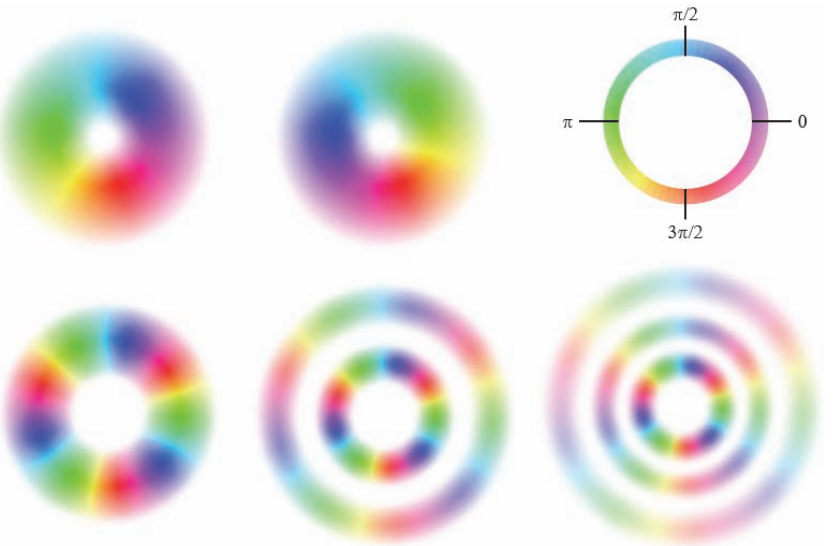

Figure 23 Transverse field distributions for five Laguerre–Gaussian modes, with their associated intensity and phase structure. Top: l = 1 (left) and l = –1 (right), with p = 0; bottom: l = 3, with p = 0, 1, 2 (left, center, right). The depth of color denotes the radially varying intensity. White areas represent where this is negligible; the hues denote phase, running through the spectrum over continuous multiples of 2π (key top right).

Consequently, all information on wavefront handedness is found within the phase factors, in which a positive or negative sign for l represents a helical wavefront structure of left- or right-handed helicity, respectively. Typical examples of transverse field distributions for Laguerre–Gaussian modes are presented in Fig. 23, which depicts the associated intensity and phase structure; note that the phase singularity leads to a zero intensity along the axis for all cases $l > 0$. Laguerre–Gaussian beams with $l > 1$, $p > 0$ are, in a sense, similar in nature to higher-order Bessel beams; the latter has non-diffracting and self-healing properties.[172–175] The electric and magnetic field expansions for the Bessel beam are identical to Eqs. (38) and (39), except that $f_{l,p}(r)$ is substituted with an l^{th}-order Bessel function. Mathieu beams are essentially Bessel beams with elliptical (rather than circular) rings, with field expressions correspondingly similar in form.[176,177]

Many of the prospective applications for structured light lie in the realm of quantum informatics. This is due to the additional information offered by each photon of the complex beam (beyond that afforded by a simple binary basis of polarization, for example). Indeed, it proves possible to sort photons according to their topological charge l[178] or differences in radial distribution associated with index p.[179] Owing to the fact that the former is an essentially unbounded parameter, it can constitute a multi-dimensional basis for the high-density conveyance of information. The attractive prospects of using structured light for communication are enhanced by the possibility of multi-dimension entanglement,[180] affording new opportunities to achieve secure, free-space communication links.[181]

4.5 Vacuum Radiation

There is one seemingly innocuous feature of Eq. (28) that has not received our full attention; it is the ground state energy of $\frac{1}{2}\hbar\omega$ associated with each radiation mode $(\mathbf{k},\eta)$. In free space, there is no restriction on the possible orientations or magnitudes of the wavevector **k**; light of any wavelength can travel in any direction. In consequence, the radiation Hamiltonian contains in its sum an infinite energy. This alarming prospect is not an insignificant problem, though we shall see that it can be circumvented. However, it transpires that this difficulty is not just an awkward artifact to be explained away; it has physically meaningful connotations.

First, let us see where this infinite energy originates. We may recall that the ground state of a simple harmonic oscillator is non-zero, essentially because its kinetic and potential energies (which involve a quadratic dependence on momentum and position coordinate, respectively) can never both be zero. Otherwise, the oscillation would cease at a definite momentum p and position q (both being precisely zero along some common axis), which would contravene Heisenberg's uncertainty principle $\Delta p \Delta q \geq \hbar/2$. It turns out that the same principle applies to the two parts of the expression for energy, given in Eq. (20), that is quadratic in the electromagnetic fields **E** and **B**; they can never both be zero. (The **E** and **B** fields also have a non-zero commutator, e.g., p. 64 in Craig and Thirunamachandran[182]) This tallies with the fact that each field has an essentially sinusoidal wave-like nature that necessarily averages to zero over the duration of an optical cycle, whereas the average of $\sin^2$ is non-zero.

The notion of infinitely many oscillations with an associated infinite energy is often described in terms of vacuum fluctuations (vacuum fields).[183] Here, the descriptor "vacuum" signifies that the associated fields and energy are present even in regions devoid of any matter or light. However, it should not be understood as relating only to such regions; these effects are present throughout our physical universe, permeating space itself.

There is an entirely pragmatic way to avoid the problem of having an infinite background energy, which is to recognize that it remains unchanged in the course of any normal optical interaction. Any arbitrary amount of energy can equally be added to the initial and final state energies, and the dynamics will observably be the same—the infinite value is just an unusually perverse case. In this sense, the lack of direct observability might suggest that the zero-point energy is not worthy of serious attention. However, there are particular aspects that do have significant physical consequences,[183] an illustration of which is outlined in the next section.

4.6 Casimir Effect

As stated previously, the essential reason why vacuum fields relate to an infinite energy is that there is a continuum of possible wavevector magnitudes and directions. However, any presence of matter may modify this condition in certain circumstances; the simplest to envisage is the space between two parallel, perfectly conducting plates. Based on standard wave theory, it would be argued that only

plane waves with nodes at each surface could be supported. (At the microscopic level, much the same principle applies to the theory of photonic crystals presented in Section 2.5.)

It follows that because the cavity can only support modes whose half-wavelength can fit an integer number of times inside it, the longest supportable wavelength is half the plate separation, with higher-order harmonics for all other allowed modes—the detailed calculation must also account for the transverse mode structure.[184,185] Thus, the net zero-point energy between the plates is countably modified compared to the free space. This energy shift is interpreted as a progressive lowering in potential energy as the plates are moved towards each other from infinite separation. Moreover, because this energy is quantitatively different according to the plate spacing, there has to be an associated force. Performing the intricate calculations for this effect reveals an attractive force between the plates that scales almost linearly with the plate area. The upshot is a force per unit area—an inward pressure P—of magnitude:

$$P = \frac{\pi^2 \hbar c}{240 a^4}, \tag{40}$$

where a is the separation between the plates. This result for the Casimir effect is astonishing in several respects. It is a rare example of an equation that has an identical form in any major system of units; moreover, this result contains no electrical constants of either fundamental or material form. However, the main reason for drawing attention to this feature, of clearly quantum optical origin, is that it proves not only measurable but significant at the nanoscale level. Indeed, it proves necessary to account for this effect when considering the design and operating characteristics of nanoelectromechanical systems (NEMS).[186,187] It is remarkable that, even when no light is present, the absence of any photons can still generate a substantial effect.

Chapter 5
Light–Matter Interactions

5.1 Foundations

Up until now, we have only considered light propagating essentially in vacuum; this has been used as the basis to describe the effects of reflection, refraction, and transmission in a medium. These essentially passive phenomena, alone, serve as a reminder that nothing is achieved with light, or learned about it, without material interaction. However, a more extensive realm of science centers upon light actively coupling with matter—and many of the systems, in which the photonic aspects of light are most clearly manifest, concern matter in the form of atoms, molecules, or nanoparticles.

A quantum analysis of light–matter interactions typically begins with the system Hamiltonian H, the energy operator of the system. In basic quantum mechanics, the "system" simply comprises matter, and the state wavefunctions are secured as eigenstates of the corresponding Hamiltonian H_{mat}. A quantum formulation of the radiation requires the additional inclusion of a radiation Hamiltonian H_{rad}. Here, it becomes appropriate to use the representation of quantum electrodynamics (QED): however, because the charges that comprise matter move at significantly sub-luminal speeds in almost all optics and photonics applications, the full relativistic form of QED is unnecessary. To complete the full Hamiltonian for systems in which light and matter are *not* isolated from each other, an interaction Hamiltonian H_{int} is also required. The system Hamiltonian can thus be decomposed into three parts:

$$H = H_{\text{mat}} + H_{\text{rad}} + H_{\text{int}}. \tag{41}$$

In most circumstances, even for light interacting with an extremely small, free-moving particle, such as an electron,[188] the energies associated with the operator H_{int} are much smaller than those represented by H_{mat} and H_{rad}; hence, light–matter interactions only perturb the system represented by $H_0 = H_{\text{mat}} + H_{\text{rad}}$.* Based on this perturbation, the following general expression for the *matrix element*† M_{FI}—for progression from an initial system state $|I\rangle$ to a final state $|F\rangle$—is developed:

* Light–matter interactions are strong at ultra-high laser intensities (above ~10^{21} W cm^{-2}); in such conditions, non-perturbative methods should be employed.

† The term "matrix element," which is standard terminology, arises from some formulations in which there is a matrix of components that describes all of the couplings between a full set of initial and final states.

$$M_{FI} = \sum_{q=0}^{\infty} \langle F | H_{\text{int}} (T_0 H_{\text{int}})^q | I \rangle, \tag{42}$$

where T_0, known as a *resolvent operator*, is denoted by $T_0 \approx (E_I - H_0)^{-1}$, in which E_I is the energy of the initial system state. Using the completeness relation of quantum mechanics, i.e., Eq. (23), the previous expression can be recast as the following infinite series:

$$\begin{aligned} M_{FI} = & \langle F | H_{\text{int}} | I \rangle + \sum_R \frac{\langle F | H_{\text{int}} | R \rangle \langle R | H_{\text{int}} | I \rangle}{(E_I - E_R)} \\ & + \sum_{R,S} \frac{\langle F | H_{\text{int}} | S \rangle \langle S | H_{\text{int}} | R \rangle \langle R | H_{\text{int}} | I \rangle}{(E_I - E_R)(E_I - E_S)} \\ & + \sum_{R,S,T} \frac{\langle F | H_{\text{int}} | T \rangle \langle T | H_{\text{int}} | S \rangle \langle S | H_{\text{int}} | R \rangle \langle R | H_{\text{int}} | I \rangle}{(E_I - E_R)(E_I - E_S)(E_I - E_T)} + \ldots, \end{aligned} \tag{43}$$

where $|R\rangle$, $|S\rangle$, and $|T\rangle$ are virtual intermediate states, and E_R, E_S, and E_T are the energies of these states.

To proceed further, linking the previous expression to photon interactions, we now need to identify the form of the Hamiltonian term H_{int}. Although there is an alternative "minimal coupling" formulation that can lead to the same results,[189] almost all of the common forms of optics express this interaction in terms of an electric dipolar coupling with the electric field of the radiation, i.e.,

$$H_{\text{int}} = -\boldsymbol{\mu} \cdot \mathbf{E}(\mathbf{r}). \tag{44}$$

Here, both $\boldsymbol{\mu}$ and $\mathbf{E}(\mathbf{r})$ are operators, where the former acts on matter states, and the latter acts on radiation states. With the electric field explicitly cast in terms of photon creation and annihilation operators according to Eq. (26), the first term in that equation relates to photon annihilation, and the second term relates to creation. Consequently, each action of H_{int} must either create or destroy a photon. For this reason, the first term in Eq. (43) is the key term to describe conventional (single-photon) absorption or emission. Successive terms in that equation relate to processes of progressively higher photon order; a term with an integer q interactions in its numerator will represent a q-photon process. However, the photon order concerns a sum of all input and output photons. For example, the second term in Eq. (43) describes not only two-photon absorption but also the much more familiar process of light scattering, which involves an input photon and an output photon. Both will be examined in detail in the next section.

The determination of an experimentally quantifiable variable from Eq. (43) usually involves finding the modulus squared of the matrix element M_{FI}.

Commonly, results are expressible in terms of a rate Γ, through use of the Fermi rule:

$$\Gamma = \frac{2\pi}{\hbar}\left|M_{FI}\right|^2 \rho. \tag{45}$$

Here, ρ represents the density of states, signifying the number of quantum states per unit energy interval. In general, this physically represents the fact that even the highest-resolution experiments will always register signals across a finite bandwidth; the precise interpretation will depend on the specific details of the process to which the Fermi rule is applied.

5.2 Absorption, Scattering, and Emission

This section concisely describes the three processes that account for the most prominent effects in our everyday visual world. As will become evident, absorption, stimulated emission, and scattering are linear optical processes, i.e., their rates of occurrence depend linearly on the intensity of the input light. For spontaneous emission processes, such as fluorescence and phosphorescence, there is, of course, no input. We begin by focusing on the processes of photon absorption and emission; as mentioned previously, they are both described by the leading term in Eq. (43), and the associated rates emerge from the Fermi rule.

First, consider an absorption process in a resonant-frequency beam providing N photons per volume V that promotes a molecule (arbitrarily positioned at the origin) from its ground state $|0\rangle$ to a bound excited state $|f\rangle$. Here and henceforth, we use lowercase symbols to identify electronic excited states. The one-photon absorption mechanism is illustrated by Fig. 24. At this juncture, explicit representation of the system basis in terms of both radiation and material states is required. This is conventionally achieved by writing their product in the form $|I\rangle \equiv |0{:}N\rangle$, which signifies that in the initial system state the molecule is in its ground electronic level, and there are N photons of the resonant radiation mode. Drawing on Eqs. (21) and (24), and finding that only the annihilation operator is required, the following is obtained:

Figure 24 Scheme depicting one-photon absorption: a quantum released from the radiation state excites the molecule (or atom).

$$M_{FI}^{\text{abs}} = \left\langle F \left| H_{\text{int}} \right| I \right\rangle = \left\langle f : (N-1) \left| -\boldsymbol{\mu} \cdot \mathbf{E} \right| 0 : N \right\rangle = -\left\langle f \left| \boldsymbol{\mu} \right| 0 \right\rangle \cdot \left\langle (N-1) \left| \mathbf{E} \right| N \right\rangle$$
$$= -i\boldsymbol{\mu}^{f0} \cdot \mathbf{e} \left(\frac{N\hbar ck}{2\varepsilon_0 V} \right)^{\frac{1}{2}}. \tag{46}$$

Here, $\hbar ck = \hbar\omega = h\nu$ is the photon energy, equal to the energy required for the transition $|f\rangle \leftarrow |0\rangle$ (conventionally written in this way, i.e., backwards), and $\boldsymbol{\mu}^{f0}$ signifies the associated *transition electric dipole moment*. After substituting the previous M_{FI}^{abs} into the Fermi rule of Eq. (45), assuming monochromatic, plane-polarized radiation, and associating the density of states with the excited level, we find

$$\Gamma = \frac{\pi ck \rho_f}{\varepsilon_0} \left(\frac{N}{V} \right) \left| \boldsymbol{\mu}^{f0} \right|^2 \cos^2 \theta, \tag{47}$$

where θ is the angle between the transition dipole and the electric polarization vector of the incident light; and ρ_f is a density of states ascribed to the excited state. Finally, we can use the connection between the "photon density" N/V and the irradiance, given in Section 2.2 as $I = (N/V)\hbar c\omega$, to secure the final result:

$$\Gamma = \frac{\pi \rho_f}{\hbar c \varepsilon_0} I \left| \boldsymbol{\mu}^{f0} \right|^2 \cos^2 \theta. \tag{48}$$

In a fluid medium, a 3D orientational average of the $\cos^2\theta$ factor simply reduces to 1/3. Equation (48) explicitly exhibits the linear dependence on input intensity, which is readily shown to lead to the familiar Beer's law decay associated with the passage of light through an absorbing medium.‡ Moreover, the square of the transition dipole moment is the fundamental quantity that determines the photometric *oscillator strength* (e.g., see p. 432 in Atkins and Friedman[190]).

Before leaving absorption, it is worth noting that other phenomena, such as the photoelectric effect (which occurs not in atomic or molecular media but on solid metal surfaces), involve a fundamentally similar mechanism, except in two respects: one is that the transition dipole is associated with a delocalized excitation, and the other is that there is excitation into a continuum with a broad density of states, rather than a bound excited state. The continuum is associated with the unconstrained kinetic energies of detached electrons. Consequently, there is a spectrum of optical wavelengths that can be absorbed, with a familiar threshold corresponding in energy to a "work function."

‡ This follows from the fact that the rate of intensity reduction per unit distance $-dI/dx$ is proportional to $-dI/dt$ and hence also to Γ, which is itself proportional to I. Hence, there is an exponential decay with distance.

Moving to the case of emission, it might be supposed in many respects that the theory would be similar because emission is essentially the time-inverse of absorption. For *stimulated* emission, this is indeed true. If there is an initial radiation state containing N photons resonant with the decay transition $|0\rangle \leftarrow |f\rangle$, and the emission increases their number by one, then the matrix element for the emission of another photon into the same throughput mode is given by

$$M_{FI}^{\text{stim}} = \left\langle F \left| H_{\text{int}} \right| I \right\rangle = \left\langle 0 : (N+1) \left| -\boldsymbol{\mu} \cdot \mathbf{E} \right| f : N \right\rangle = i\boldsymbol{\mu}^{0f} \cdot \mathbf{e} \left(\frac{(N+1)\hbar ck}{2\varepsilon_0 V} \right)^{\frac{1}{2}}, \tag{49}$$

using source Eqs. (22) and (24). On the assumption of a sufficient flux of photons to approximate $(N + 1)/V \approx N/V$, the rate of stimulated emission then emerges as

$$\Gamma = \frac{\pi \rho_f}{\hbar c \varepsilon_0} I \left| \boldsymbol{\mu}^{0f} \right|^2 \cos^2 \theta. \tag{50}$$

The apparently minor difference in the results for absorption, i.e., Eq. (48), and stimulated emission, Eq. (50), is in fact insignificant; the modulus square of the transition moments for excitation and decay are easily shown to be identical. The exact equivalence of the two expressions (cast in a slightly different guise, in terms of "B coefficients") is a feature first identified by Albert Einstein.[191,§] Of course, in two-level systems, the relative number of molecules in the two different initial states, i.e., $|0\rangle$ or $|f\rangle$, has also to be taken into account; because the Boltzmann distribution applies to systems under thermal equilibrium, the number of molecules in the initial excited state is much less than the number in the ground state, which means that absorption will dominate anywhere outside the radio-frequency range. *Population inversion*, i.e., when the number of molecules in the excited state outweighs those in the ground state, is necessary for laser action; this requires three- or four-level systems.

The large-flux assumption made previously, which is perfectly reasonable for systems such as lasers where stimulated emission is prevalent, obviously fails when there is no light initially present, i.e., $N = 0$. Then, with the $(N+1)$ of Eq. (49) effectively replaced by unity, the result delivers a rate of spontaneous emission. Some further intricacies are necessary to secure a result accounting for the possibility of emission over 4π steradians; it suffices to say that the result is non-zero and relates, in a similar way, to Einstein's "A coefficient." Here, a strikingly different outcome arises when the radiation field is treated classically. Performing the same calculation, correctly dealing with matter using quantum mechanics but with an electric field simply represented as the wave $E(t) = E_0 \cos \omega t$, gives a zero

§ Einstein's formulation, from pre-laser days, was cast in a form to accommodate radiation with a substantial frequency bandwidth.

result because the interaction Hamiltonian (Eq. (44)) vanishes. In this connection, "semiclassical" theory (i.e., treating matter quantum mechanically but radiation fields classically) proves remarkably in error. It suggests that an isolated atom or molecule in an excited state could never radiatively decay: fluorescence and phosphorescence, as we know them, would not exist. The failure, acutely observed in the textbook by Gilbert Grynberg et al.,[6] is one of the *cause célèbres* vindicating the use of a fully quantized, photon-based description as presented earlier.

It is interesting to observe that the dissymmetry of absorption and emission processes, associated with thermal equilibrium and a density of states for the material excited state, can effectively disappear under specially contrived conditions. Here, photons are trapped inside a suitably reflective microscopic cavity, one that contains an atom with a transition resonant in frequency with the light. Isolated atoms have characteristically discrete and well-separated energy levels; in the standard representation of such a situation, the upper and lower levels of the transition, usually the ground state $|g\rangle$ and excited level $|e\rangle$, are considered to be the only relevant features of the atom, which is therefore described as a "two-level" atom. Accordingly, there is an exact resonance between two system states $|g{:}N\rangle$ and $|e{:}(N{-}1)\rangle$. This condition leads to *Rabi oscillations*: the populations of the two atomic levels sinusoidally oscillate, with a frequency determined by the strength of the atom–photon coupling. The system thus exhibits features known as *cavity QED*.[192] Systems of this kind are of considerable interest for quantum optics, with potential computing applications.

Now, before leaving the field of linear optics, we turn to the scattering of light by molecules, focusing on *Rayleigh scattering* for simplicity and commonplace application. As we saw in earlier chapters, photons are distinguished according to the radiation mode whose occupancy they represent. Therefore, in any form of deflective (non-forward) scattering, it is not strictly meaningful to countenance photons elastically "bouncing off" atoms or molecules. An individual scattering event takes an input photon and produces a distinctly different (even though the same energy) photon. Fundamentally, therefore, light scattering is a two-photon process, as indicated in Fig. 25. However, this is not a two-step process: there is no single, physically measurable intermediate state, and the photon input and output events do not occur at discernibly different times. Indeed, since energy is not conserved until the process is complete, the fleeting departure from

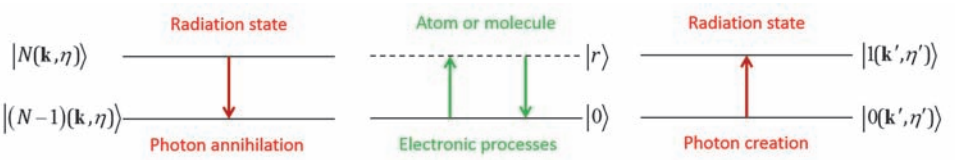

Figure 25 Radiation and matter state transitions in non-forward Rayleigh scattering. The higher level shown for the electronic processes, represented by the dashed line, denotes a virtual level—it is not a real electronic excited state.

conservation can be sustained only within the constraints of the time–energy uncertainty principle.

Here, the molecule returns to its ground state via what has to be represented as a superposition of intermediate states $|r\rangle$, whereas the radiation undergoes an overall transition $|(N-1)\rangle_1|1\rangle_2 \leftarrow |N\rangle_1|0\rangle_2$, i.e., it loses a photon from the input mode and generates one in an output mode. Accordingly, the rate of scattering is described by the second term in the perturbation series, Eq. (43). The result for the matrix element emerges in the following form:[182]

$$\begin{aligned} M_{FI}^{\text{scat}} &= \left(\frac{\hbar\omega}{2\varepsilon_0 V}\right)\sum_r\left[\frac{\left(\mu_i^{0r}e_i'\right)\left(\mu_j^{r0}e_j\right)}{E_0-E_r+\hbar\omega}+\frac{\left(\mu_j^{0r}e_j\right)\left(\mu_i^{r0}e_i'\right)}{E_0-E_r+\hbar\omega}\right] \\ &= -\left(\frac{\hbar\omega}{2\varepsilon_0 V}\right)\alpha_{ij}(\omega)\vec{e}_i'e_j, \end{aligned} \tag{51}$$

where E_0 is the molecular ground state energy, and E_r is the energy of an arbitrary state $|r\rangle$; $\mathbf{e}$ is the polarization vector for the input, and $\mathbf{e}'$ denotes the output (whose complex conjugate appears here because this photon is emitted). Also, for convenience, we now express scalar products through reference to their Cartesian components, e.g., $(\mathbf{a}\cdot\mathbf{b}) = a_i b_i$, in which the subscript i stands for x, y, or z. This means of expression also adopts the Einstein *implied summation convention* for summing, over all three directions, any or all repeated Cartesian indices, facilitating the concise expression on the right of Eq. (51). The rate of non-forward Rayleigh scattering is again determined from the Fermi rule of Eq. (45).

Equation (51) entails the i, j components of the *molecular polarizability* $\boldsymbol{\alpha}(\omega)$, an optical frequency-dependent tensor. (Each index i and j can take each of three directions, so the result is in principle expressible as a 3×3 matrix.) Classically, the polarizability is conceived as quantifying the propensity of a molecule to exhibit a dipolar (essentially, 1D charge-shifting) response to an applied electric field, one with oscillatory character in this case. The polarizability is most succinctly expressed as

$$\alpha_{ij}(\omega) = \frac{2}{\hbar}\sum_r\left(\frac{\omega_{r0}}{\omega_{r0}^2-\omega^2}\right)\mu_i^{0r}\mu_j^{r0}, \tag{52}$$

where ω_{r0} signifies the gap in circular frequency terms between the ground state and state $|r\rangle$. When single, scalar values α are reported for polarizability, the meaning is $\frac{1}{3}Tr\{\alpha\}$.

From the form of Eq. (52), it is evident that the polarizability will have values that most strongly vary with optical frequency (a feature known as optical dispersion; see Section 2.4) in regions of absorption. Nonetheless, it is necessary to tailor the previous expression to correctly represent the associated lineshape,

and to circumvent a divergence that would otherwise arise with optical frequencies ω approaching any frequency gap ω_{r0}, for states r connected to the ground state by an electric-dipole allowed transition. Close to resonance, a variety of physically distinct features and processes come into play, including the finite lifetime of electronic excited states, the manifold of vibrational states typically associated with each of those states, and a finite radiation linewidth. Accordingly, a phenomenological expedient is commonly introduced;[6] the necessary procedure and the detailed formula that emerges for a complex polarizability with a Lorentzian lineshape are explicitly given by Andrews and Ford.[193] The result is a form of expression in which an imaginary component of the polarizability emerges, consistent with a classical interpretation of resonance absorption.

From the preceding derivation, it is instructive to observe how the two terms, within the square brackets in Eq. (51), arise. The apparent upward and downward electronic transitions in Fig. 25 cannot be considered precisely simultaneous because this would be inconsistent with the time–energy uncertainty principle, although there is indeed no discernible time lag in the overall scattering process. In fact, theory requires two possibilities to be accounted for, wherein the emergent photon is created either imperceptibly after or before the incoming photon is annihilated. The need to accommodate both possibilities exhibits a calculational principle at the heart of quantum theory, the path integral ("sum-over-paths") method discussed in Section 3.1, largely developed by Richard Feynman.[194] It also reflects that an interaction Hamiltonian, such as the electric dipole form represented by Eq. (44), which contains an electric field operator that comprises photon creation and annihilation operators (as in Eq. (26)), only allows one kind of action (i.e., the termination or production of a photon) to occur in each operation. When multiple possibilities exist for the quantum sequence of events involved in multiphoton processes, *state-sequence diagrams*[195–197] can present a helpful means of concisely exhibiting the possibilities—and they also play a part in the associated calculations.[**] The state-sequence diagram for non-forward Rayleigh scattering is shown in Fig. 26.

The theory of *forward* Rayleigh scattering proceeds along similar lines to that given earlier—the key difference being that the input and output modes are the same: thus it becomes clear why polarizability is the molecular property that modifies the rectilinear propagation of light through a material medium, principally in slowing it down. This property is also involved in determining surface reflectivity.[198] Both effects are, of course, registered on the macroscopic scale in terms of refractive index. Establishing this link elucidates, at the photon level, the physical mechanism responsible for the Lorentz–Lorenz connection

[**] State-sequence diagrams represent an alternative to traditional Feynman (time-ordered) diagrams. The advantage of the former is that for any specific optical process, the information content of all relevant Feynman diagrams (running into the hundreds in some applications) is subsumed within a single state-sequence diagram that depicts the entirety of quantum paths from the initial to the final state.

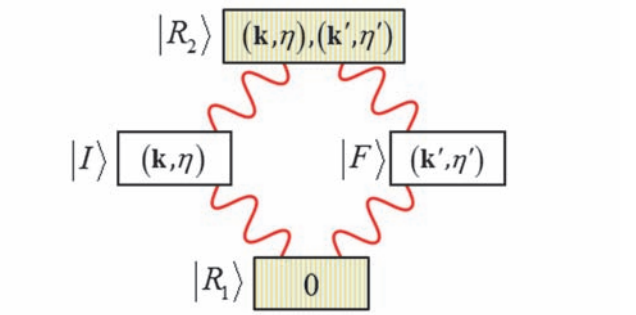

Figure 26 Simplified state-sequence diagram for non-forward Rayleigh scattering, indicating the states of the radiation field (alone) from an initial state $|I\rangle$ through to a final state $|F\rangle$ via one of two virtual "intermediate" state $|R_1\rangle$ and $|R_2\rangle$ paths, using terminology consistent with Eq. (43). In the lower route $|I\rangle \rightarrow |R_1\rangle \rightarrow |F\rangle$, the annihilation of input photon $(\mathbf{k},\eta)$ precedes the creation of output photon $(\mathbf{k}',\eta')$; in the upper route $|I\rangle \rightarrow |R_2\rangle \rightarrow |F\rangle$, the converse applies. The former generates the first term in square brackets in Eq. (51), and the latter produces the second term.

between refractive index and polarizability, observed in Eq. (5). For more general applicability to the bulk condensed phase, the corresponding form of the response is often quantified by another scalar quantity known as the *linear susceptibility*, connected to the polarizability (now understood as a quantity relating to any representative local response) through correction by local field factors, giving

$$\chi^{(1)} = \frac{N'\varepsilon_0^{-1}\alpha}{1-\frac{1}{3}N'\varepsilon_0^{-1}\alpha}, \tag{53}$$

where N' is the number density of the units represented by the polarizability α.

5.3 Nonlinear Optics

Across the broad realm of optics, the theory of most phenomena is well served by a classical description of light. As observed in Section 2.4, the representation of how passive optical elements operate (i.e., putting aside active processes such as the photoelectric effect) generally justifies a tacit assumption that the sheer number of photons involved is sufficient for the "large quantum number" correspondence principle to ensure essentially classical behavior. For this reason, the operation of lenses, mirrors, gratings, etc., is more than adequately described by classical wave or ray optics. One might suppose that the same logic applies when sufficiently high intensities lead to a departure from a linear dependence on input. To some extent, this is true, though for processes that generate a weak signal, quantum effects can come into prominence. However, a range of distinctively different kinds of process come into play at high intensities, and their typically nonlinear dependence on intensity is now reflected in the generic term "nonlinear optics."

The field of nonlinear optics is one of the most striking developments to emerge from the development of the laser more than fifty years ago. Optical frequency doubling (second harmonic generation, SHG), for instance, which produces collimated emission in non-centrosymmetric crystals, has proven to be the preeminent means of converting laser output to a shorter wavelength. The basic principles of SHG, and other such nonlinear phenomena, were rapidly established and consolidated, notably in a treatise by Nicolaas Bloembergen (published in 1965).[199] Since then, a swift growth of diverse applications, including spectroscopic sensing, optical communications, and signal processing, have established and underscored the technical significance of nonlinear optical response. Most applications are based on *parametric* processes, those in which both matter and the radiation field separately conserve energy and linear momentum. There are several modern introductions to the subject, including texts by Sudhanshu Jha,[200] Elmar Sauter,[201] Guangsheng He and Song Liu,[202] Yuen-Ron Shen,[203] Richard Sutherland,[204] Partha Banerjee,[205] Lukas Novotny and Bert Hecht,[206] and Robert Boyd.[207]

Following Bloembergen's lead, nonlinear optics is commonly regarded and described as an extension of conventional, linear optics. The subject is typically introduced with reference to a classical oscillatory electric polarization, accommodating correction terms that become significant at high intensities. The material parameters that quantify the extent of the nonlinear response are cast as coefficients in a power series—nonlinear optical susceptibilities signifying a propensity to generate optical harmonics, for example. At a deeper, photonic level, a more in-depth knowledge of the structure and properties of each nonlinear susceptibility tensor is required. The form of a specific nonlinear susceptibility tensor depends on the process that it represents. Typically, the derivations of these tensors involve a development based on time-dependent perturbation theory, i.e., Eqs. (42) and (43).

Before we pursue a photon-based description, we outline the common semiclassical approach to exhibit both its insights and its shortcomings. This representation commonly depicts the linear response to an applied electric field, considered responsible for the induction of a dipole moment, as only an approximation to the true response of many materials. When such a field is oscillatory, as in the optical case, it is reasoned that the correction terms associated with nonlinear response are responsible for the generation of optical harmonics, i.e.,[199]

$$P_i = \varepsilon_0 \left\{ \sum_j \chi_{ij}^{(1)} E_j + \sum_{j,k} \chi_{ijk}^{(2)} E_j E_k + \sum_{j,k,l} \chi_{ijkl}^{(3)} E_j E_k E_l + \ldots \right\}, \tag{54}$$

which represents component i of a vector "electric polarization" $\mathbf{P}$ for the material, $\mathbf{E}$ is the applied electric field, and $\boldsymbol{\chi}^{(q)}$ is the q^{th}-order electric susceptibility with the status of a tensor of rank $(q + 1)$, as denoted by the number of indices. This expression again adopts the convention of implied summation over repeated

indices. By representing the electromagnetic radiation as a classical wave that varies sinusoidally with time t, namely,

$$E(t) = E_0 \cos \omega t, \tag{55}$$

and then inserting this expression into Eq. (54), the following result emerges:

$$\begin{aligned} P_i(t) = {} & \chi_{ij}^{(1)} E_{0j} \cos \omega t + \tfrac{1}{2} \chi_{ijk}^{(2)} E_{0j} E_{0k} (1 + \cos 2\omega t) \\ & + \tfrac{1}{4} \chi_{ijkl}^{(3)} E_{0j} E_{0k} E_{0l} (3 \cos \omega t + \cos 3\omega t) + ... \end{aligned} \tag{56}$$

The first correction term to the linear response, that is, the second term of Eq. (56), is thus considered the source of an optical second harmonic 2ω; the next correction is deemed the origin of a third harmonic; and so on. From any such representation, it is simple enough to verify that the even harmonics are forbidden in centrosymmetric media (given that the polarization must change sign under the symmetry operation of space inversion, whereas the responsible term in Eq. (56) does not). However, to derive the detailed structure of the linear and nonlinear susceptibilities, one usually has recourse to essentially prescriptive methods, first proposed by John Ward, based on time-orderings.[208]

There are many reasons, as delineated elsewhere,[209,210] why the preceding description is unsatisfactory. For example, Eq. (56) logically implies that a medium with a non-vanishing $\boldsymbol{\chi}^{(2)}$ will always generate some amount of second harmonic, even at intensity levels that would correspond to only one photon of input, whereas, of course, two input photons are required for every second harmonic photon that is produced. The mistake owes its origin to the misrepresentation of the optical field by a classical wave—a description that makes no provision for accommodating quantized energy levels. It is, in fact, simple and instructive to show that the statistical probability of two photons arriving together leads to the observed quadratic dependence on intensity.[211] Other commonly overlooked problems with the semiclassical approach involve the discarding of terms, such as the unity in the second "SHG" term, which signify an entirely different process, in this instance, a linear electro-optic effect[212] that is completely unrelated to SHG. Moreover, the fact that the modulus square of the polarization is deemed to represent an observable signal becomes problematic because the resulting cross-terms have no physical significance.

A photon-based foundation for describing nonlinear optical phenomena presents none of these difficulties. For example, no cross-terms of the kind discussed earlier arise because different processes are associated with different radiation state transitions. In Section 5.2, we saw how the linear response associated with the polarizability derives from the second term in Eq. (43) because scattering is a two-photon process. Similarly, the third term describes the three-photon process of SHG (two in and one out per conversion event), which involves

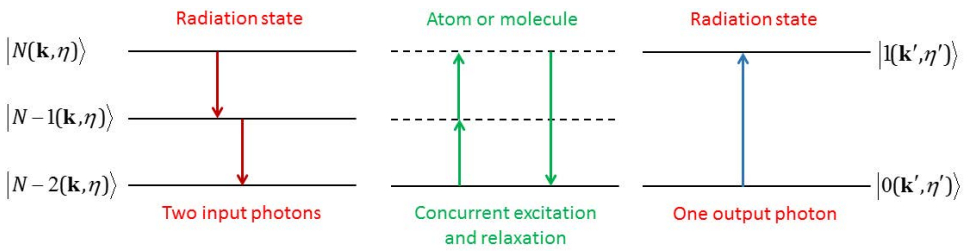

Figure 27 Radiation and matter state transitions in second harmonic generation. Two photons of frequency ω from the input mode $(\mathbf{k},\eta)$ are converted into one of frequency ω' with output mode $(\mathbf{k}',\eta')$. Again, dashes denote virtual levels.

the radiation field undergoing a transition represented by $|(N-2)\rangle_1|1\rangle_2 \leftarrow |N\rangle_1|0\rangle_2$ (as illustrated in Fig. 27). Here, the forward-directed output mode, labeled by the subscript 2, has twice the optical frequency of the input mode, labeled 1.

Working through the detailed analysis delivers a matrix element cast in terms of a third-rank *hyperpolarizability* tensor, with components $\beta_{ijk}(\omega)$:[209]

$$M_{FI}^{\mathrm{SHG}} = -i\left(\frac{\hbar\omega}{2\varepsilon_0 V}\right)^{3/2} \beta_{ijk}(\omega)\vec{e}_i e_j e_k, \tag{57}$$

where

$$\begin{aligned}\beta_{ijk}(\omega) = \sum_{r,s}\Bigg[&\frac{\mu_i^{0s}\mu_j^{sr}\mu_k^{r0}}{(E_0 - E_s + 2\hbar\omega)(E_0 - E_r + \hbar\omega)} \\ &+ \frac{\mu_j^{0s}\mu_i^{sr}\mu_k^{r0}}{(E_0 - E_s - \hbar\omega)(E_0 - E_r + \hbar\omega)} \\ &+ \frac{\mu_j^{0s}\mu_k^{sr}\mu_i^{r0}}{(E_0 - E_s - \hbar\omega)(E_0 - E_r - 2\hbar\omega)}\Bigg].\end{aligned} \tag{58}$$

As is evident from the preceding equation, the structure of the hyperpolarizability accommodates three distinct pathways between the initial and final radiation states, as illustrated in Fig. 28. Once again, phenomenological damping has to be introduced to correctly represent dispersion lineshapes, resulting in a tensor whose components have an imaginary part, which becomes significant within the region of any absorption band.[213]

Turning from the molecular level to the bulk, the incorporation of appropriate Lorentz field factors enables the local response to be related to a bulk nonlinear susceptibility labeled $\boldsymbol{\chi}^{(2)}$, the superscript designating a quadratic response to the

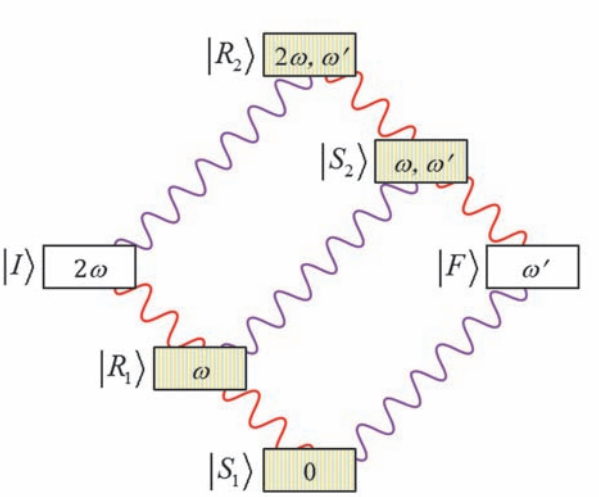

Figure 28 Simplified state-sequence diagram for second harmonic generation, indicating states of the radiation field. Two photons of frequency ω, in the initial state $|I\rangle$, are converted into one photon of frequency ω' in the final state $|F\rangle$. The conversion process proceeds through a quantum superposition of three paths, traversing virtual intermediate states depicted by shaded boxes. Consistent with Eq. (43) are three routes, consecutively corresponding to the three terms in Eq. (58): (*a*) $|I\rangle \rightarrow |R_1\rangle \rightarrow |S_1\rangle \rightarrow |F\rangle$; (*b*) $|I\rangle \rightarrow |R_1\rangle \rightarrow |S_2\rangle \rightarrow |F\rangle$, and (*c*) $|I\rangle \rightarrow |R_2\rangle \rightarrow |S_2\rangle \rightarrow |F\rangle$. Each annihilation of an input photon ω is represented by a downward red wave; the creation of a frequency-doubled photon ω' is denoted by an upward purple wave. In each path, transient positive (upward) or negative (downward) departures from exact energy conservation, permitted within the constraints of time–energy uncertainty, are rectified in the final state (which has an energy equal to $|I\rangle$).

input fields. Since other three-photon processes, such as sum-frequency generation (SFG), also engage nonlinear susceptibilities of the same rank, it is often more helpful to explicitly label each χ tensor with its optical frequency parameters, with the output preceding the input. Thus, for SHG we have $\chi^{(2)}(-2\omega;\omega,\omega)$, and for SFG, $\chi^{(2)}(-\omega';\omega_1,\omega_2)$, where $\omega' = \omega_1 + \omega_2$. For the former, the relation to the local hyperpolarizability, conventionally expressed in terms of scalar quantities, is given by[214]

$$\chi^{(2)}\left(-2\omega;\omega,\omega\right) = N'\varepsilon_0^{-1}\beta\left(1-\tfrac{1}{3}N'\varepsilon_0^{-1}\alpha\left(2\omega\right)\right)^{-1}\left(1-\tfrac{1}{3}N'\varepsilon_0^{-1}\alpha\left(\omega\right)\right)^{-2}. \qquad (59)$$

It may be observed that the semiclassical rationale for the emergence of a second harmonic, Eq. (56), is based on the assumption of quadratic response and use of the simple trigonometric identity $(\cos\omega t)^2 = \frac{1}{2}(1 + \cos 2\omega t)$. A similar logic applies for SFG, which commonly involves a strong throughput beam of frequency ω_1, acting as a pump, coupling with an "idler" beam of frequency ω_2 to generate the

required $\omega_1 + \omega_2$ output.[215] In fact, a wide range of frequency-conversion schemes are based on SFG for up-conversion, or a counterpart difference-frequency generation (DFG) process to produce output of a down-converted frequency $\omega_1 - \omega_2$. Representations of SHG, SFG, and DFG are given in Fig. 29(a–c). For all of these parametric processes, the material response tensors can be evaluated using methods based on time-ordered[208] or state-sequence[216] diagrams. More recently, these approaches have been supplemented by coupled-cluster calculations.[217]

A case of special interest for its quantum optical relevance is spontaneous parametric down-conversion (SPDC), in which single input photons generate output in the form of correlated photon pairs.[218] In an obvious sense, the case of degenerate down-conversion (DDC), where both output photons have the same frequency, might be construed as a time-inverse of SHG (compare Figs. 29(a) and 29(d)). Semiclassical descriptions encounter another stumbling block here: if there is no idler beam present, then there seems to be no basis for any sub-frequency (i.e., less than ω) to emerge from the throughput beam. As we observed for spontaneous emission, QED again produces results without any such difficulty. Namely, in the photon picture, the radiation field simply undergoes the energy-conserving transition $\hbar\omega \rightarrow \hbar(\frac{1}{2}\omega) + \hbar(\frac{1}{2}\omega)$. The property of quantum entanglement (see Section 3.2) naturally arises here, based on path separation of correlated photon pairs, thus signifying that when one of the photons is detected, wavefunction collapse occurs for the pair.[219–221] The extent of entanglement may even extend to polarization.[222,223] More broadly, the detection of one such photon can be configured to "herald" the imminent arrival of its partner at a separate location; this is a concept of considerable significance for many quantum-information applications connected to single-photon technology.[224]

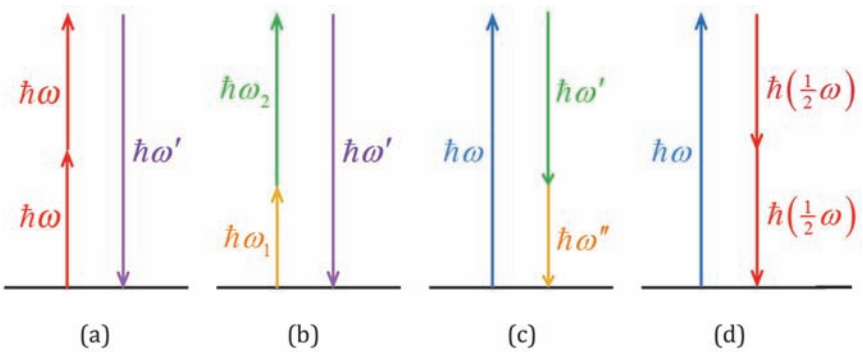

Figure 29 Radiation state transitions for (a) SHG, (b) SFG, (c) DFG, and (d) DDC; see text for details. Upward arrows denote photons from the input radiation, and the downward arrows generally depict output photons, although in (c) one of the output modes may be pre-populated by an "idler" input. In such representations, no significance can be attached to the apparent sequence of three-photon events; theory requires all distinct orderings to be accounted for, in accordance with Eq. (43).

Before leaving the sphere of nonlinear optics, it is worth noting that the manifestations of quantum phase and photon statistics noticeably come into play here. At simplest, a process whose fundamental mechanism entails the absorption of M photons ($M = 2$ for both two-photon absorption and SHG, for example) produces a rate that depends on the following intensity factor:

$$\left\langle I^M \right\rangle = g^{(M)} \left\langle \bar{I} \right\rangle^M, \tag{60}$$

where $\bar{I}$ is the mean (time-averaged) irradiance, and $g^{(M)}$ is the degree of M^{th}-order coherence.[††] For single-mode radiation, the coherence factor is expressible in operator form as follows, in which angular brackets denote an expectation value:

$$g^{(M)} = \frac{\left\langle a^{\dagger M} a^M \right\rangle}{\left\langle a^\dagger a \right\rangle^M}, \tag{61}$$

whose numerical value can produce widely diverse results for different kinds of photon statistics. For example, $g^{(M)}$ has the value of unity for all orders M in an ideal coherent state, whereas the much more chaotic fluctuations of thermal light correspond to $g^{(M)} = M!$.[225] Therefore, multiphoton absorption and harmonic generation processes can exhibit a striking dependence on the extent of intensity fluctuations, whereas no such dependence is observed across the board in linear optics ($M = 1$).

5.4 Near- and Far-Field Optics

The depiction of light as a traveling wave is a major pillar of classical optics and electromagnetism. As we have seen, the fact that such a representation does not account for quantum phenomena demands attention. In other respects, however, interesting links can be established between the classical and quantum formulation, and the latter can afford fresh insights. One particular example is the difference in the behavior of light according to its distance of travel from an emissive source (the progressively diminishing intensity notwithstanding). Putting aside surface effects,[226] the character of light with wavelength λ in the *near-field* (or near-zone) region, defined as a distance regime $(0, \lambda/2\pi)$ is known to be very different to the form of light that propagates onwards, beyond the locality of the emitter in the *far field* (or wave zone).[‡‡]

Most optical observations involve radiation propagating in the far-field, where

[††] For simplicity, we present the definition for degrees of coherence that relate to a single point in space and time.

[‡‡] Here, the evanescent fields that may arise at interfaces are not considered: they do not propagate energy, and their description in terms of photons is unhelpful.

the distances from the source are significantly larger than the wavelength. However, it has emerged that near-field radiation represents an extremely useful means of conveying excitation energy over small distances, in a variety of connections. The levels of intensity required to produce a meaningful signal are much lower than conventionally propagating light, and, in addition, significantly sub-wavelength resolution can be achieved. In the visible wavelength range, for example, it has long been anticipated that such features might be exploited to achieve enhanced-resolution imaging;[227] the vision came to fruition with the development of near-field microscopy,[228,229] a technique extensively used in biological applications.[230,231] In the same context, many other recent advances are associated with the local influence of surface plasmons,[232] where enhanced forms of near-field light are generated in the vicinity of nanostructured metal surfaces. Moreover, several other technologies exploit near-field couplings at much longer wavelengths, namely in the radio-frequency region. While traditional radio communication is commonly conducted in the far field, near-field communication (NFC) is increasingly used for ticketing or contactless payment devices, particularly through integration with mobile phones.[233]

We now focus on light emitted via an electric dipole transition, identifying its different character in the near and far fields.[§§] Over the space of several wavelengths, the functional forms of the phase and amplitude exhibit a significant change in character due to the onset of retardation (a manifestation of the finite speed of light as a constraint on the speed of information transfer).[58,234] To begin, we note that the detection of any radiation requires a photodetector, whose operation almost invariably involves absorption. The entirety of the process begins with photon emission and ends with photon absorption, and thus it represents a quantum system that is closed in the absence of dissipation and decoherence processes.

In the QED framework represented by Eq. (41), there is clearly no term directly connecting the source and detector; the only way that energy can transfer from one position to the other is through coupling with the radiation field—which is cast as an operator H_{rad} and is therefore always present. Moreover, the electromagnetic field operators entail summations over radiation modes of arbitrary photon energy, not being restricted to the precise energy delivered to the detector by the source. Technically, therefore, the mediation of this process has to occur by borrowing energy from the vacuum fluctuations and then restoring it; this entails the creation and subsequent annihilation of a *virtual photon*. When calculations on this basis are performed, the result emerges as a field that irradiates from a source with distinct near-field and far-field character. In detail, once again written in terms of an Einstein summation, the electric field registered by a detector at a displacement **R** from the source has the form

[§§] Although light emission from a magnetic dipole moment is possible, it is usually disregarded in most subjects in optics. However, magnetic dipoles can have vital importance when considering chirality and surface plasmons.

$$E_j(\mathbf{R}) = -\frac{\mu_i e^{ikR}}{4\pi\varepsilon_0 R^3}\left\{\left(\delta_{ij} - 3\hat{R}_i\hat{R}_j\right) - (ikR)\left(\delta_{ij} - 3\hat{R}_i\hat{R}_j\right) - (kR)^2\left(\delta_{ij} - \hat{R}_i\hat{R}_j\right)\right\}, \quad (62)$$

where it is clear that the first and third terms dominate in the near field ($kR \ll 1$) and far field ($kR \gg 1$), respectively.*** This expression can also be rewritten in an equivalent form, which appears in classical retardation electrodynamics, i.e.,[235]

$$\begin{aligned}\mathbf{E}(\mathbf{R}) &= k^2\left(\hat{\mathbf{R}}\cdot\boldsymbol{\mu}\right)\cdot\hat{\mathbf{R}}\frac{e^{ikR}}{4\pi\varepsilon_0 R} \\ &\quad + \left[3\hat{\mathbf{R}}\left(\hat{\mathbf{R}}\cdot\boldsymbol{\mu}\right) - \boldsymbol{\mu}\right]\left(\frac{1}{4\pi\varepsilon_0 R^3} - \frac{ik}{4\pi\varepsilon_0 R^2}\right)e^{ikR}.\end{aligned} \quad (63)$$

In either representation, the form of result indicates that, while the electric field of far-field radiation is disposed at right angles to the **R**, and therefore known as transverse, it also features a longitudinal component in the near field. This feature signifies an important distinction from the plane-wave representations introduced in Eqs. (26) and (27). In fact, the electric field may be split into longitudinal and transverse components (with respect to **R**), so that $E_{\|j} = (E_i\hat{R}_i)\hat{R}_j$ and $E_{\perp j} = E_j - E_{\|j}$ represent the longitudinal and transverse components, respectively. Therefore, the explicit forms of the longitudinal and transverse components of the electric field are written as[234]

$$E_{\|j} = \frac{e^{ikR}}{4\pi\varepsilon_0 R^3}\left[2\left(\boldsymbol{\mu}\cdot\hat{\mathbf{R}}\right)(1-ikR)\hat{R}_j\right], \quad (64)$$

$$E_{\perp j} = \frac{e^{ikR}}{4\pi\varepsilon_0 R^3}\left(\left(\boldsymbol{\mu}\cdot\hat{\mathbf{R}}\right)\hat{R}_j - \mu_j\right)\left(1 - ikR - k^2R^2\right), \quad (65)$$

The distinct forms of near- and far-field behavior arising from these results are evident from the $kR \ll 1$ and $kR \gg 1$ limits, respectively. In the former near-field case, terms in the above equations that are linear, or have a higher-order dependence on kR, become negligible and both longitudinal and transverse fields exhibit a clear $1/R^3$ dependence on distance. Conversely, in the far field, the transverse field acquires a $1/R$ dependence that substantially dominates a comparatively negligible longitudinal field.

It is interesting to observe, here, a neat encapsulation of principles drawn from

*** Technically, evaluation of the matrix element for the source-emission and radiation-detection (energy transfer) process, based on the second term in the perturbation series (Eq. (43)), leads to a result in which the detected field **E** features as $M_{FI}^{\text{trans}} = -E_j\mu_j^B$, where μ_j^B is a component of the excitation transition moment for the detection event.

both relativity theory and quantum mechanics—as might be expected from the QED approach. While the change in inverse power dependence with distance is commonly recognized as a relativistic retardation effect, it also signifies a change from largely "virtual" to "real" photon behavior. This is readily observed: $\hbar kR$ is a product of a real photon momentum and its distance of travel, so unless the condition $kR >> 1$ is satisfied, one can expect virtual photons with essentially unlimited momentum to mediate the delivered electric field—and that is exactly what the detailed theory implies.[58,236] Virtual photons, in fact, feature in a surprisingly wide range of nanoscale photonic interactions.[237]

The significance of all these features becomes apparent in a variety of contexts. For example, *near-field scanning optical microscopy* (NSOM or SNOM) represents one of several key methods used to achieve enhanced resolution below the Abbe limit.[228] Another important application is fluorescence *resonance energy transfer* (FRET or RET) between molecules or chromophores; here, a photon-based description of theory has proven the traditionally termed "radiationless" and "radiative" energy transfer[238,239] processes to be simply the near-field and far-field asymptotes of a unified coupling mechanism.[236,240–242] RET has important functions in the operation of organic light-emitting diodes (OLEDs) and luminescence detectors,[243–248] and in laser-frequency conversion in crystalline solids and glasses doped with lanthanide metal ions,[249–254] where sequential energy-transfer processes, mediated by near-field coupling, expedite tailored up-conversion. Other notable uses arise in optical communications, switching, and logic gate devices.[255–259]

5.5 Force and Torque Photonics

The original concept of manipulating matter with light in the form of *optical tweezers*, first demonstrated in the 1980s, was based on a mechanism that had already been identified in work by James Clerk Maxwell,[12] a full century earlier. From our modern perspective, the possibility of photons exerting a force seems an obvious consequence of their conveying momentum, and the earliest studies[260] were indeed based on such linear momentum transfer, traditionally termed *radiation pressure*. However, it is not the only means by which optical forces and torques can operate. Most optical tweezing is in fact based on a *gradient force*,[261,262] which can arise in any beam with a spatially non-uniform intensity profile. When attention turns to optically induced torques, it transpires that an even wider range of optical mechanisms can operate. These may involve the transfer of either spin or orbital angular momentum, depending on the character of the light, or an alignment effect that can act on any non-spherical particle, again due to a gradient force.

First, consider the optical force exerted on a completely light-absorbing surface. For applications on the macroscopic scale, the original Maxwell–Bartoli formulation of theory applies. Given that an optical force can be described by both

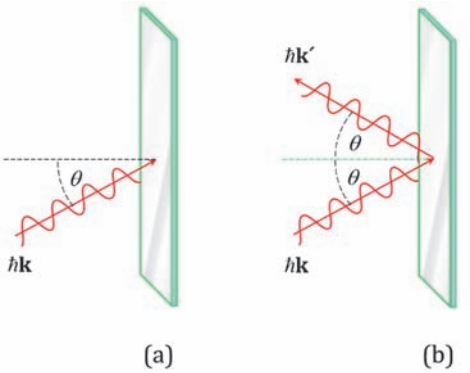

Figure 30 Transfer of momentum to a surface via (a) absorption or (b) reflection.

energy per unit distance and momentum per unit time (from Newton's second law of motion), it follows that optical momentum conveyed by photons can be defined as energy divided by the speed of light. The radiation pressure P, normal to the surface, is the rate of change of momentum divided by the irradiated area so that $P = I\cos^2\theta/c$, where I is the irradiance, and θ is the angle between the surface normal and the incident radiation, as illustrated in Fig. 30(a).[†††]

If the surface were perfectly reflective, then as momentum is imparted on it by both the incident and reflected light, as shown by Fig. 30(b), a factor of two would be included on the right side of the expression. Most surfaces are neither fully absorptive nor reflective; for the case of a reflectivity R, therefore, we find a force $\mathbf{F}$, normal to the surface, given by

$$\mathbf{F} = \frac{1+R}{c}\int I(\mathbf{r})\cos^2\theta d^2\mathbf{r}, \tag{66}$$

where the integral is taken over the irradiated surface. The absorption of light by macroscopic bodies will commonly be followed by essentially stochastic, isotropically distributed processes of internal energy dissipation, producing no ancillary force. One novel application arises for microstructured particles in a liquid suspension, where an *optical wing* effect can be produced.[263]

To address any force-related phenomenon at the photon level, it is appropriate, as always, to start from the matrix element;[264] a flow chart to pursue theory from this perspective is shown in Fig. 31. We can begin with the simple case of photon absorption, for which we use the matrix element expression given in Eq. (46). Figure 31 shows that, in this case, it is the ensuing rate that provides the basis for

[†††] The quadratic dependence on the cosine arises thus: the normal force associated with photon momentum components perpendicular to the surface carries a $\cos\theta$, and while pressure has an inverse dependence on area, the irradiated area is itself inversely proportional to $\cos\theta$. The resultant expression for pressure is a scalar.

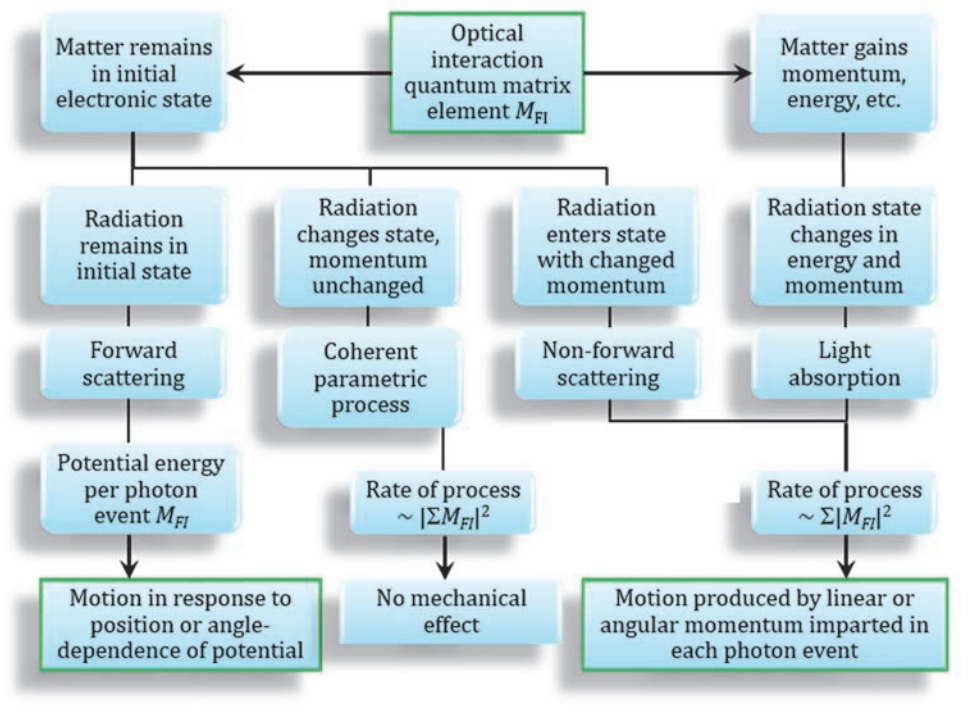

Figure 31 Scheme to determine the optical force from the quantum matrix element. According to the nature of any change in the quantum state of the matter and radiation, different modes of calculation are required. The Σ in the penultimate row signifies summation over all relevant particles.

calculation. The radiation force when N photons are absorbed by one or more particles is determined by multiplying the absorption rate Γ from Eq. (47) by the net linear momentum of the absorbed photons $N\hbar\mathbf{k}$. Assuming $\mathbf{e}\|\boldsymbol{\mu}^{f0}$, with a density of states written as $\rho = I_\omega V/2\pi c\hbar^2\omega$,[182] the radiation force associated with absorption is determined as

$$\mathbf{F} = \frac{I_\omega \mathbf{k}}{2c\varepsilon_0\hbar}\left|\boldsymbol{\mu}^{f0}\right|^2, \tag{67}$$

where I_ω is the irradiance per unit frequency. However, when we consider microscopic or nanoscale particles, often in a system where they are more mobile than in a solid body, we have to consider three possible outcomes. The absorbed photons could have their energy dissipated internally, in which case the previous expression correctly reflects the overall result, but in other situations, absorption may be followed by re-emission. Reflection may also occur, which requires separate consideration because it is essentially non-forward scattering (see Section 4.2) and therefore a concerted two-photon process.

The case of absorption and re-emission is especially significant in connection with "laser cooling," a term that refers to various methods in which laser light is used to systematically cool atoms or small molecules (usually in the form of a low-pressure gas) to lower temperatures. The essence of the technique is resonance absorption, at these optical centers, of a uniformly directed beam, and subsequent processes of electronic state decay produce statistically isotropic, spontaneous emission. As a result, over many cycles of absorption and re-emission, individual particles acquire a net momentum; suitable tuning can ensure that those directed into the incoming beam are most affected (through a Doppler shift), so they are slowed down.[265,266]

In cases where the incident photons are transmitted, rather than absorbed, the treatment of theory is a little more intricate and involves the production of intensity-dependent, internal energy-level shifts, associated with the *dynamic Stark effect*. In such a case, since the level shifts depend on the intensity of the light, an effective potential energy surface is introduced whose magnitude varies with particle position, usually within the cross-section of the trapping beam, and is therefore related to the transverse field distribution. The gradient force is determined from the spatial derivative of the potential energy; consequently, the particle is attracted to the high-intensity part of the trapping beam.

In terms of classical electrodynamics, the gradient force is conventionally defined in terms of the Lorentz force on a point dipole, which, after introducing its constant of proportionality α (the scalar polarizability—see Eq. (52) and the lines following it) is expressed as

$$\left\langle \mathbf{F}(\mathbf{r}) \right\rangle = \frac{\alpha}{2} \nabla \left\langle E(\mathbf{r})^2 \right\rangle. \tag{68}$$

Here, the electric field is involved in a quadratic response, and the gradient force is therefore sustained in an oscillating field. Using second-order perturbation theory, i.e., the $q = 1$ term in Eq. (42), the following matrix element signifies the evaluation of the expectation value as a potential energy ΔU:

$$\Delta U = \mathrm{Re}\, M_{II} = \mathrm{Re}\left\{ \sum_R \frac{\langle I | H_{\mathrm{int}} | R \rangle \langle R | H_{\mathrm{int}} | I \rangle}{E_I - E_R} \right\}, \tag{69}$$

where Re denotes the real part of the expression that follows it. Note that because the initial and final states are the same in this instance, the matrix element is written as M_{II}. In terms of the beam irradiance $I(\mathbf{r})$, the gradient force is thus determined as

$$\mathbf{F}(\mathbf{r}) = \left(\frac{\nabla I(\mathbf{r})}{2\varepsilon_0 c} \right) \alpha_{ij}(\omega) \bar{e}_i e_j. \tag{70}$$

In the structure of the preceding expression, the term $\alpha_{ij}(\omega)\bar{e}_i e_j$ involves the polarizability $\alpha_{ij}(\omega)$: the two polarization vector components relate to the same radiation mode, signifying that the origin of the effect is forward Rayleigh scattering. The previous result shows that the gradient force is directed towards the beam axis, for a regular beam with an intensity maximum at its core (since, at that position, the potential energy is a minimum).

A gradient force of a very different kind arises for larger (micron or larger) particles, usually suspended in a liquid suspension to offset the effects of gravity. Here, a difference in the relative photon flux impinging on the surface of the particle closest to, and furthest from, the axis of a throughput laser beam produces correspondingly different rates of deflection. This also produces attraction to the high-intensity part of the beam as momentum is transferred from the light to the particle.

Torques may result from the application of a light beam through three distinct mechanisms.[264] First, optical torque arises from the spin angular momentum associated with circularly polarized light. This type of torque has been shown to produce an extremely quick particle-rotation rate; in fact, the world's fastest spinning synthetic object has been generated by such a torque.[267] An optical torque $\boldsymbol{\tau}$ of this form is associated with the radiation force, as spin angular momentum is transferred from the light beam to the particle for each absorbed photon. The net result is

$$\boldsymbol{\tau} = \frac{I_\omega \hat{\mathbf{k}}}{2c\varepsilon_0 \hbar} \left| \boldsymbol{\mu}^{f0} \right|^2 . \tag{71}$$

Secondly, suitably structured vortex light can also produce a torque due to orbital angular momentum. In this mechanism, the initial and final system states are *not* identical: the created and annihilated photons (with identical energy) travel in different directions. As a result, in terms of quantum theory, a second radiation mode is assigned to the system states, meaning that the initial and final states differ: $|I\rangle = |N,0;0\rangle$ and $|F\rangle = (N-1), 1;0\rangle$. Here, the first and second elements in each state vector denote radiation modes relating to the annihilation and creation events, respectively, and the third element represents the molecular state. The torque is determined by multiplying the scattering rate (from the Fermi rule) by the radius of the beam ring r_b and the orbital angular momentum per photon $l\hbar\hat{\mathbf{k}}$. Following a rotational average, assuming plane-polarized input and summing over all possible polarizations for the scattered light, the following expression is determined for the observed torque:

$$\boldsymbol{\tau} = \frac{Ik^3 l r_b \hat{\mathbf{k}}}{40\pi\varepsilon_0^2 c} \left(\alpha_{ii}\alpha_{jj} + 7\alpha_{ij}\alpha_{ij} \right). \tag{72}$$

Larger dielectric particles may be treated with electronic properties closer to those of a bulk material; in such cases, it is appropriate to cast the result in terms of the linear optical susceptibility instead of the polarizability. The applications of such torques have become known as *optical spanners* or *optical wrenches*.[268]

Finally, there are orientational effects, which cannot, of course, be exhibited in spherical particles. The simplest cases arise for particles of cylindrical symmetry, in which the polarizability has one value $\alpha_{\parallel}$ for the axial z direction, and another $\alpha_{\perp}$ for each of the other two perpendicular axes. An expression for the associated torque is given by

$$\boldsymbol{\tau} = \frac{2I\omega}{c\varepsilon_0}\left(\alpha_{\perp} - \alpha_{\parallel}\right)\left(e_y \mathbf{i} - e_x \mathbf{j}\right)e_z , \tag{73}$$

where e_x, e_y, and e_z are the Cartesian components of the electric field unit vector directed in the internal x, y, and z directions; **i** and **j** respectively signify the corresponding x and y unit vectors. Such effects are also significant in connection with *optical binding*,[269–271] in which virtual photons play a crucial role in the induction of nanoscale forces leading to light-induced self-assembly.[272]

Afterword

We live in a time of unprecedented activity in the science and technology of light, so much so that the nomination "Century of the Photon" is already heard.* Moreover, technological advances are increasingly focused on quantum physics, to the extent that quantum technology is being regarded as a new discipline. The quantized form of light, the photon, will of course have a prominent role in such developments. Photonics is at the core of recent technological advances in light, and much of it concerns topics that are truly dependent on the quantum-based fundamentals introduced in this book. Furthermore, specifically quantum forms of light are required for a myriad of optical interactions, most of which feature in extensive applications.

The photon is primarily a conveyer of energy. Just as sunlight provides the basis for life (with photosynthesis at the bottom of nearly every food chain)† and vision—both processes associated with photon absorption—so too do we find that many areas of photonic technology are also associated with energy and illumination, primarily in connection with solar energy harvesting[273,274] and solid-state lighting.[275] Of course, the link between photon energy and frequency also provides the basis for a rich diversity of spectroscopic and imaging applications, which in the photonic era have become increasingly pervasive across wide areas of quality control and analysis in the food, health, and safety sectors, as well as in medical and environmental diagnostics.

From another perspective the photon, when regarded as a conveyer of information, is a concept that, beyond simple causality, represents a powerful corollary of modern relativity and cosmology theory. Once again, we may observe how the familiar process of vision, by which we naturally gain most of our information about the outside world, is continually being expanded. Modern society is already heavily dependent on radio and microwave wavelengths for wifi and Bluetooth, now extending to autonomous vehicle sensors operating in the infrared. Moreover, the development of optical fiber coupling, enabling low-loss information processing and communication with single-photon detectors[56,224] (and the prospect of exploiting quantum attributes of light) opens up further channels for the photonic age.

---

* It is fascinating to consider that for the photon—indeed, any particle traveling at the speed of light—relativity theory shows that time has no meaning.

† In this sense, given that almost all life on Earth, since its dawn countless millennia ago, has been sustained only by an endless flux of photons from our Sun, the term "Century of the Photon" might seem naively patronizing.

Yet the lowly photon at the heart of all these developments retains an element of mystery. The second page of the third edition of Rodney Loudon's classic book on quantum optics observed "it is no longer so straightforward to explain what is meant by a 'photon.'"[55] Far from becoming increasingly well understood, the photon appears harder to understand than ever, despite a simplicity that the original concept suggested. Much of the knowledge that has been described in this book would have been unrecognizable to the originators of photon science, some of it unfamiliar to optical scientists even one generation ago. With conservative extrapolation, it seems likely that other surprises may soon be within our grasp.

Photon

Pure energy am I, no other entity existing
Particulate of aspect, though of zero mass consisting.
Contemporaneous are my fields electric and magnetic,
Entwined and co-dependent undulations sympathetic.

I spin with restless energy, yet spend no time in turning,
Imparting it where I should land, selection rules discerning.
You measure me: I cease to be, I cannot live inactive:
I give my energy, my whole, no fractional subtractive.

With simultaneous start and end, in galaxies uncharted,
I vouch for conservation of life-energy imparted.
My destiny uncertain, from some origin once shining,
I travel with celerity defying and defining.

No birth or death for me, nor even tense discrimination,
My grammar elementary: participle conflation.
With start and end contiguous, though space no real constriction,
I find no time to read or rhyme – time is for me a fiction.

Let others count the years, time is inscrutably material:
I nothing know the nature of 'diurnal' or 'sidereal' –
Nor purpose: certainty renounced, unsure of where I'm bound,
Whilst distance is no object, there's no home I've ever found.

Call me entangled, virtual, real, snake-like or sheer ballistic;
Such adjectives serve only to confuse a life simplistic.
What care have I if written off as nothing but a phantom
Or conundrum! I shall ever be your quintessential quantum.

David L. Andrews (reproduced with permission)[276]

References

1. Süptitz, W. and Heimes, S., *Photonics: Technical Applications of Light*, Spectaris GmbH, Berlin (2016).
2. Sänger, E., "Problems of astronautical research," *J. Br. Interplanet. Soc.* **45**, 57–60 (1952).
3. Saleh, B. E. A. and Teich, M. C., *Fundamentals of Photonics*, Wiley, New York (1991).
4. Meyrueis, P., Sakoda, K. and Van de Voorde, M., *Micro- and Nanophotonic Technologies*, Wiley-VCH, Weinheim, Germany (2017).
5. Lewis, G. N., "The conservation of photons," *Nature* **118**, 874–875 (1926).
6. Grynberg, G., Aspect, A. and Fabre, C., *Introduction to Quantum Optics: From the Semi-Classical Approach to Quantized Light*, Cambridge University Press, Cambridge (2010).
7. Bertolotti, M., *The History of the Laser*, CRC Press, Boca Raton, FL (2004).
8. Oon, P. T. and Subramaniam, R., "The nature of light: I. A historical survey up to the pre-Planck era and implications for teaching," *Phys. Educ.* **44**, 384–391 (2009).
9. Lindberg, D. C., "Alhazen's theory of vision and its reception in the West," *Isis* **58**, 321–341 (1967).
10. Sabra, A. I., *Theories of Light: From Descartes to Newton*, Cambridge University Press, Cambridge (1981).
11. Kipnis, N. S., *History of the Principle of Interference of Light*, Birkhäuser Verlag, Basel (1991).
12. Maxwell, J. C., "A dynamical theory of the electromagnetic field," *Philo. Trans. Royal Soc. London* **155**, 459–512 (1865).
13. Kirchhoff, G., "Ueber die Fraunhofer'schen Linien," *Ann. Phys.* (Berlin) **185**, 148–150 (1860).
14. Kirchhoff, G., "Ueber das Verhältniss zwischen dem Emissionsvermögen und dem Absorptionsvermögen der Körper für Wärme und Licht," *Ann. Phys.* (Berlin) **185**, 275–301 (1860).

15. Oon, P. T. and Subramaniam, R., "The nature of light: II. A historical survey from the Planck era and implications for budding physicists," *Phys. Educ.* **44**, 392–397 (2009).

16. Planck, M., "Ueber das Gesetz der Energieverteilung im Normalspectrum," *Ann. Phys.* (Berlin) **309**, 553–563 (1901).

17. Einstein, A., "Über einen die Erzeugung und Verwandlung des Lichtes betreffenden heuristischen Gesichtspunkt," *Ann. Phys.* (Berlin) **17**, 132–148 (1905).

18. Compton, A. H., "A quantum theory of the scattering of x-rays by light elements," *Phys. Rev.* **21**, 483–502 (1923).

19. Kragh, H., "The names of physics: plasma, fission, photon," *Eur. Phys. J. H* **39**, 263–281 (2014).

20. Bartoli, A., "Il calorico raggiante e il secondo principio di termodinamica," *Il Nuovo Cimento* **15**, 193–202 (1884).

21. Maxwell, J. C., *A Treatise on Electricity and Magnetism*, Volume 2, Dover Publications, New York (1954).

22. Lebedev, P. N., "Experimental examination of light pressure," *Ann. Phys.* (Berlin) **6**, 433 (1901).

23. Nichols, E. F. and Hull, G. F., "A preliminary communication on the pressure of heat and light radiation," *Phys. Rev.* **13**, 307–320 (1901).

24. de Broglie, L.-V., "On the theory of quanta," *Ann. Phys.* (Paris) **3**, 22–128 (1925).

25. Raman, C. W. and Bhagavantam, S., "Experimental proof of the spin of the photon," *Ind. Jour. Phy.* **6**, 353-366 (1931).

26. Raman, C. W. and Bhagavantam, S., "Experimental proof of the spin of the photon," *Nature* **129**, 22–23 (1932).

27. Beth, R. A., "Mechanical detection and measurement of the angular momentum of light," *Phys. Rev.* **50**, 115–125 (1936).

28. Andrews, D. L. and Babiker, M., *The Angular Momentum of Light*, Cambridge University Press, Cambridge, UK (2013).

29. Roychoudhuri, C., Kracklauer, A. F. and Creath, K., *The Nature of Light: What is a Photon?*, CRC Press, Boca Raton, FL (2008).

30. Bennett, R., Barlow, T. M. and Beige, A., "A physically motivated quantization of the electromagnetic field," *Eur. J. Phys.* **37**, 014001 (2015).

31. Dirac, P. A. M., "The quantum theory of the emission and absorption of radiation," *Proc. R. Soc. A* **114**, 243–265 (1927).

32. Dirac, P. A. M., *The Principles of Quantum Mechanics*, 4th Ed., Clarendon Press, Oxford (1981).

33. Tomonaga, S., "On a relativistically invariant formulation of the quantum theory of wave fields," *Prog. Theoret. Phys.* **1**, 27–42 (1946).

34. Tomonaga, S., "Development of quantum electrodynamics," *Science* **154**, 864–868 (1966).

35. Schwinger, J., "On quantum-electrodynamics and the magnetic moment of the electron," *Phys. Rev.* **73**, 416–417 (1948).

36. Schwinger, J., "Quantum electrodynamics. I. A covariant formulation," *Phys. Rev.* **74**, 1439–1461 (1948).

37. Feynman, R. P., "Space-time approach to quantum electrodynamics," *Phys. Rev.* **76**, 769–789 (1949).

38. Feynman, R. P., "Mathematical formulation of the quantum theory of electromagnetic interaction," *Phys. Rev.* **80**, 440–457 (1950).

39. Dyson, F. J., "The radiation theories of Tomonaga, Schwinger, and Feynman," *Phys. Rev.* **75**, 486–502 (1949).

40. Power, E. A. and Zienau, S., "Coulomb gauge in non-relativistic quantum electrodynamics and the shape of spectral lines," *Philos. Trans. R. Soc. A* **251**, 427–454 (1959).

41. Power, E. A. and Thirunamachandran, T., "Quantum electrodynamics with nonrelativistic sources. I. Transformation to the multipolar formalism for second-quantized electron and Maxwell interacting fields," *Phys. Rev. A* **28**, 2649–2662 (1983).

42. Power, E. A. and Thirunamachandran, T., "Quantum electrodynamics with nonrelativistic sources. II. Maxwell fields in the vicinity of a molecule," *Phys. Rev. A* **28**, 2663–2670 (1983).

43. Power, E. A. and Thirunamachandran, T., "Quantum electrodynamics with nonrelativistic sources. III. Intermolecular interactions," *Phys. Rev. A* **28**, 2671–2675 (1983).

44. Power, E. A. and Thirunamachandran, T., "Quantum electrodynamics with nonrelativistic sources. IV. Poynting vector, energy densities, and other quadratic operators of the electromagnetic field," *Phys. Rev. A* **45**, 54–63 (1992).

45. Power, E. A. and Thirunamachandran, T., "Quantum electrodynamics with nonrelativistic sources. V. Electromagnetic field correlations and intermolecular interactions between molecules in either ground or excited states," *Phys. Rev. A* **47**, 2539–2551 (1993).

46. Maiman, T., "Stimulated optical radiation in ruby masers," *Nature* **187**, 493–494 (1960).

47. Hanbury Brown, R. and Twiss, R. Q., "A test of a new type of stellar interferometer on Sirius," *Nature* **178**, 1046–1048 (1956).

48. Kimble, H. J., Dagenais, M. and Mandel, L., "Photon antibunching in resonance fluorescence," *Phys. Rev. Lett.* **39**, 691–695 (1977).

49. Mandel, L. and Wolf, E., "Coherence properties of optical fields," *Rev. Mod. Phys.* **37**, 231–287 (1965).

50. Glauber, R. J., "Coherent and incoherent states of the radiation field," *Phys. Rev.* **131**, 2766–2788 (1963).

51. Walls, D. F., "Squeezed states of light," *Nature* **306**, 141–146 (1983).

52. Slusher, R. E., Hollberg, L. W., Yurke, B., Mertz, J. C. and Valley, J. F., "Observation of squeezed states generated by four-wave mixing in an optical cavity," *Phys. Rev. Lett.* **55**, 2409–2412 (1985).

53. Aspect, A., Grangier, P. and Roger, G., "Experimental Tests of Realistic Local Theories via Bell's Theorem," *Phys. Rev. Lett.* **47**, 460–463 (1981).

54. Mandel, L. and Wolf, E., *Optical Coherence and Quantum Optics*, Cambridge University Press, Cambridge, New York (1995).

55. Loudon, R., *The Quantum Theory of Light*, Oxford University Press, Oxford (2000).

56. Prochazka, I., Hamal, K. and Sopko, B., "Recent achievements in single photon detectors and their applications," *J. Mod. Opt.* **51**, 1289–1313 (2004).

57. Andrews, D. L., "A Photon in Perspective," pp. 1–25 in *Photonics Volume 1: Fundamentals of Photonics and Physics*, D. L. Andrews, ed., Wiley, New York (2015).

58. Andrews, D. L. and Bradshaw, D. S., "Virtual photons, dipole fields and energy transfer: a quantum electrodynamical approach," *Eur. J. Phys.* **25**, 845–858 (2004).

59. Boyd, R. W. and Shi, Z., "Slow and Fast Light," pp. 363–386 in *Photonics Volume 1: Fundamentals of Photonics and Physics*, D. L. Andrews, ed., Wiley, New York (2015).

60. Forbes, A., Dudley, A. and McLaren, M., "Creation and detection of optical modes with spatial light modulators," *Adv. Opt. Photon.* **8**, 200–227 (2016).

61. Bialynicki-Birula, I., Freyberger, M. and Schleich, W., "Various measures of quantum phase uncertainty: a comparative study," *Phys. Scr.* **1993**, 113–118 (1993).

62. Opatrny, T., "Number-phase uncertainty relations," *J. Phys. A: Math. Gen.* **28**, 6961–6975 (1995).

63. Loudon, R., "Photon bunching and antibunching," *Phys. Bull.* **27**, 21–23 (1976).

64. Louisell, W. H., *Quantum Statistical Properties of Radiation*, Wiley, New York (1973).

65. Erkintalo, M. and Coen, S., "Coherence properties of Kerr frequency combs," *Opt. Lett.* **39**, 283–286 (2014).

66. Collett, E., *Field Guide to Polarization*, SPIE Press, Bellingham, WA (2005).

67. Zangwill, A., *Modern Electrodynamics*, Cambridge University Press, Cambridge (2013).

68. Barnett, S., *Quantum Information*, Oxford University Press, Oxford (2009).

69. Khajavi, B. and Galvez, E., "High-order disclinations in space-variant polarization," *J. Opt.* **18**, 084003 (2016).

70. Hecht, E., *Optics*, Pearson, Hoboken, NJ (2016).

71. Andrews, D. L. and Thirunamachandran, T., "Polarization effects in nonlinear scattering," *Opt. Commun.* **22**, 312–314 (1977).

72. Makowski, A. J., "A brief survey of various formulations of the correspondence principle," *Eur. J. Phys.* **27**, 1133–1139 (2006).

73. Blankenship, R. E., *Molecular Mechanisms of Photosynthesis*, Blackwell, Oxford (2002).

74. Djurišić, A. B. and Li, E. H., "Modeling the optical constants of hexagonal GaN, InN, and AlN," *J. Appl. Phys.* **85**, 2848–2853 (1999).

75. Ohtsu, M., Kobayashi, K., Kawazoe, T., Yatsui, T. and Naruse, M., *Principles of Nanophotonics*, CRC Press, Boca Raton, FL (2008).

76. Feit, M. and Fleck, J., "Light propagation in graded-index optical fibers," *Appl. Opt.* **17**, 3990–3998 (1978).

77. John, S., "Strong localization of photons in certain disordered dielectric superlattices," *Phys. Rev. Lett.* **58**, 2486–2489 (1987).

78. Yablonovitch, E., "Inhibited spontaneous emission in solid-state physics and electronics," *Phys. Rev. Lett.* **58**, 2059–2062 (1987).

79. Yablonovitch, E., "Photonic band-gap structures," *J. Opt. Soc. Am. B* **10**, 283–295 (1993).

80. Bragg, W. H. and Bragg, W. L., "The reflection of X-rays by crystals," *Proc. Royal Soc. London A* **88**, 428–438 (1913).

81. Lekner, J., "Omnidirectional reflection by multilayer dielectric mirrors," J. *Opt. A: Pure Appl. Opt.* **2**, 349 (2000).

82. Joannopoulos, J. D., Johnson, S. G., Winn, J. N. and Meade, R. D., *Photonic Crystals: Molding the Flow of Light*, 2nd Ed., Princeton University Press, Princeton (2011).

83. Lipson, R. H. and Lu, C., "Photonic crystals: a unique partnership between light and matter," *Eur. J. Phys.* **30**, S33–S48 (2009).

84. Zayats, A. V., Smolyaninov, I. I. and Maradudin, A. A., "Nano-optics of surface plasmon polaritons," *Phys. Rep.* **408**, 131–314 (2005).

85. Pitarke, J. M., Silkin, V. M., Chulkov, E. V. and Echenique, P. M., "Theory of surface plasmons and surface-plasmon polaritons," *Rep. Prog. Phys.* **70**, 1–87 (2007).

86. Zhang, J., Zhang, L. and Xu, W., "Surface plasmon polaritons: physics and applications," *J. Phys. D: Appl. Phys.* **45**, 113001 (2012).

87. Törmä, P. and Barnes, W. L., "Strong coupling between surface plasmon polaritons and emitters: a review," *Rep. Prog. Phys.* **78**, 013901 (2015).

88. Low, T. et al., "Polaritons in layered two-dimensional materials," *Nat. Mater*. **16**, 182–194 (2016).

89. Han, Z. and Bozhevolnyi, S. I., "Radiation guiding with surface plasmon polaritons," *Rep. Prog. Phys.* **76**, 016402 (2013).

90. Ozbay, E., "Plasmonics: Merging photonics and electronics at nanoscale dimensions," *Science* **311**, 189–193 (2006).

91. Kawata, S., Inouye, Y. and Verma, P., "Plasmonics for near-field nano-imaging and superlensing," *Nat. Photonics* **3**, 388–394 (2009).

92. Atwater, H. A. and Polman, A., "Plasmonics for improved photovoltaic devices," *Nat. Mater*. **9**, 205–213 (2010).

93. Anker, J. N., Hall, W. P., Lyandres, O., Shah, N. C., Zhao, J. and Van Duyne, R. P., "Biosensing with plasmonic nanosensors," *Nat. Mater*. **7**, 442–453 (2008).

94. Kim, J., "Joining plasmonics with microfluidics: from convenience to inevitability," *Lab Chip* **12**, 3611–3623 (2012).

95. Sonntag, M. D., Klingsporn, J. M., Zrimsek, A. B., Sharma, B., Ruvuna, L. K. and Van Duyne, R. P., "Molecular plasmonics for nanoscale spectroscopy," *Chem. Soc. Rev.* **43**, 1230–1247 (2014).

96. Schuller, J. A., Barnard, E. S., Cai, W., Jun, Y. C., White, J. S. and Brongersma, M. L., "Plasmonics for extreme light concentration and manipulation," *Nat. Mater.* **9**, 193–204 (2010).

97. Zheng, Y. B., Kiraly, B., Weiss, P. S. and Huang, T. J., "Molecular plasmonics for biology and nanomedicine," *Nanomedicine* **7**, 751–770 (2012).

98. Otto, A., "Excitation of nonradiative surface plasma waves in silver by the method of frustrated total reflection," *Z. Phys. A: Hadrons Nucl.* **216**, 398–410 (1968).

99. Feynman, R. P., Leighton, R. B. and Sands, M. L., *The Feynman Lectures on Physics, Volume III: The New Millennium Edition*, Sections 1.1–1.8, Basic Books, New York (2011).

100. Dirac, P. A. M., *The Principles of Quantum Mechanics*, Clarendon Press, Oxford (1947).

101. Feynman, R. P., "Space-time approach to non-relativistic quantum mechanics," *Rev. Mod. Phys.* **20**, 367–387 (1948).

102. Scully, M. O. and Drühl, K., "Quantum eraser: A proposed photon correlation experiment concerning observation and "delayed choice" in quantum mechanics," *Phys. Rev. A* **25**, 2208–2213 (1982).

103. Kim, Y.-H., Yu, R., Kulik, S. P., Shih, Y. and Scully, M. O., "Delayed "choice" quantum eraser," *Phys. Rev. Lett.* **84**, 1–5 (2000).

104. Aharonov, Y. and Zubairy , M. S., "Time and the quantum: erasing the past and impacting the future," *Science* **307**, 875–879 (2005).

105. Kocsis, S., Braverman, B., Ravets, S., Stevens, M. J., Mirin, R. P., Shalm, L. K. and Steinberg, A. M., "Observing the average trajectories of single photons in a two-slit interferometer," *Science* **332**, 1170–1173 (2011).

106. Nape, I., Ndagano, B. and Forbes, A., "Erasing the orbital angular momentum information of a photon," *Phys. Rev. A* **95**, 053859 (2017).

107. Zehnder, L., "Ein neuer Interferenzrefraktor," *Z. Instrumentenkunde* **11**, 275–285 (1891).

108. Mach, L., "Uber einen Interferenzrefraktor," *Z. Instrumentenkunde* **12**, 89–93 (1892).

109. Zetie, K. P., Adams, S. F. and Tocknell, R. M., "How does a Mach-Zehnder interferometer work?," *Phys. Educ.* **35**, 46–48 (2000).

110. Townsend, P. D., Rarity, J. G. and Tapster, P. R., "Single photon interference in 10 km long optical fibre interferometer," *Electron. Lett.* **29**, 634–635 (1993).

111. Hong, C. K., Ou, Z. Y. and Mandel, L., "Measurement of subpicosecond time intervals between two photons by interference," *Phys. Rev. Lett.* **59**, 2044–2046 (1987).

112. Silverstone, J. W., Bonneau, D., O'Brien, J. L. and Thompson, M. G., "Silicon Quantum Photonics," *IEEE J. Sel. Top. Quant. Electron.* **22**, 390–402 (2016).

113. Einstein, A., Podolsky, B. and Rosen, N., "Can quantum-mechanical description of physical reality be considered complete?," *Phys. Rev.* **47**, 777–780 (1935).

114. Bohm, D. and Aharonov, Y., "Discussion of experimental proof for the paradox of Einstein, Rosen, and Podolsky," *Phys. Rev.* **108**, 1070–1076 (1957).

115. Bell, J. S., "On the Einstein-Podolsky-Rosen paradox," *Physics* **1**, 195–200 (1964).

116. Giustina, M. et al., "Significant-loophole-free test of Bell's theorem with entangled photons," *Phys. Rev. Lett.* **115**, 250401 (2015).

117. Hensen, B. et al., "Loophole-free Bell inequality violation using electron spins separated by 1.3 kilometres," *Nature* **526**, 682–686 (2015).

118. Shalm, L. K. et al., "Strong loophole-free test of local realism," *Phys. Rev. Lett.* **115**, 250402 (2015).

119. Lvovsky, A. I., "Squeezed Light," in Fundamentals of Photonics and Physics., D. L. Andrews, ed. (Wiley, Hoboken, N.J., 2015), pp. 121-203.

120. Donohue, J. M., Agnew, M., Lavoie, J. and Resch, K. J., "Coherent ultrafast measurement of time-bin encoded photons," *Phys. Rev. Lett.* **111**, 153602 (2013).

121. Humphreys, P. C., Metcalf, B. J., Spring, J. B., Moore, M., Jin, X.-M., Barbieri, M., Kolthammer, W. S. and Walmsley, I. A., "Linear optical quantum computing in a single spatial mode," *Phys. Rev. Lett.* **111**, 150501 (2013).

122. Kupchak, C., Bustard, P. J., Heshami, K., Erskine, J., Spanner, M., England, D. G. and Sussman, B. J., "Time-bin-to-polarization conversion of ultrafast photonic qubits," *Phys. Rev. A* **96**, 053812 (2017).

123. Barends, R. et al., "Coherent Josephson qubit suitable for scalable quantum integrated circuits," *Phys. Rev. Lett.* **111**, 080502 (2013).

124. Devoret, M. H. and Schoelkopf, R. J., "Superconducting circuits for quantum information: An outlook," *Science* **339**, 1169–1174 (2013).

125. Reck, M., Zeilinger, A., Bernstein, H. J. and Bertani, P., "Experimental realization of any discrete unitary operator," *Phys. Rev. Lett.* **73**, 58–61 (1994).

126. Lu, C.-Y., Browne, D. E., Yang, T. and Pan, J.-W., "Demonstration of a compiled version of Shor's quantum factoring algorithm using photonic qubits," *Phys. Rev. Lett.* **99**, 250504 (2007).

127. Lanyon, B. P. et al., "Experimental demonstration of a compiled version of Shor's algorithm with quantum entanglement," *Phys. Rev. Lett.* **99**, 250505 (2007).

128. Grover, L. K., "Quantum mechanics helps in searching for a needle in a haystack," *Phys. Rev. Lett.* **79**, 325 (1997).

129. Wootters, W. K. and Zurek, W. H., "A single quantum cannot be cloned," *Nature* **299**, 802–803 (1982).

130. Gisin, N., Ribordy, G., Tittel, W. and Zbinden, H., "Quantum cryptography," *Rev. Mod. Phys.* **74**, 145–195 (2002).

131. Bennett, C. H., Brassard, G., Crépeau, C., Jozsa, R., Peres, A. and Wootters, W. K., "Teleporting an unknown quantum state via dual classical and Einstein-Podolsky-Rosen channels," *Phys. Rev. Lett.* **70**, 1895–1899 (1993).

132. Bouwmeester, D., Pan, J.-W., Mattle, K., Eibl, M., Weinfurter, H. and Zeilinger, A., "Experimental quantum teleportation," *Nature* **390**, 575–579 (1997).

133. Pirandola, S., Eisert, J., Weedbrook, C., Furusawa, A. and Braunstein, S. L., "Advances in quantum teleportation," *Nat. Photonics* **9**, 641 (2015).

134. Zhang, Y., Roux, F. S., Konrad, T., Agnew, M., Leach, J. and Forbes, A., "Engineering two-photon high-dimensional states through quantum interference," *Science Advances* **2**, e1501165 (2016).

135. Malik, M., Erhard, M., Huber, M., Krenn, M., Fickler, R. and Zeilinger, A., "Multi-photon entanglement in high dimensions," *Nat. Photonics* **10**, 248 (2016).

136. Hunt, B. J., *The Maxwellians*, pp. 108–128, Cornell University Press, Ithaca, NY (2005).

137. Sengupta, D. L. and Sarkar, T. K., "Maxwell, Hertz, the Maxwellians, and the early history of electromagnetic waves," *IEEE Trans. Antennas Propag.* **45**, 13–19 (2003).

138. Sakurai, J. J. and Napolitano, J., *Modern Quantum Mechanics*, pp. 89–97, Cambridge University Press, Cambridge (2017).

139. Juzeliūnas., G., "Microscopic theory of quantization of radiation in molecular dielectrics. II. Analysis of microscopic field operators," *Phys. Rev. A* **55**, 929–934 (1997).

140. Andrews, D. L., "The irreducible photon," *Proc. SPIE* **7421**, 742109 (2009).

141. Andrews, D. L. and Dávila Romero, L. C., "A back-to-front derivation: the equal spacing of quantum levels is a proof of simple harmonic oscillator physics," *Eur. J. Phys.* **30**, 1371–1380 (2009).

142. Barnett, S. M. and Allen, L., "Orbital angular momentum and nonparaxial light beams," *Opt. Commun.* **110**, 670–678 (1994).

143. van Enk, S. J. and Nienhuis, G., "Spin and orbital angular momentum of photons," *Europhys. Lett.* **25**, 497–501 (1994).

144. Santamato, E., "Photon orbital angular momentum: problems and perspectives," *Fortschritte der Physik* **52**, 1141–1153 (2004).

145. Bliokh, K. Y., Alonso, M. A., Ostrovskaya, E. A. and Aiello, A., "Angular momenta and spin-orbit interaction of nonparaxial light in free space," *Phys. Rev. A* **82**, 063825 (2010).

146. Andrews, D. L. and Coles, M. M., "Measures of chirality and angular momentum in the electromagnetic field," *Opt. Lett.* **37**, 3009–3011 (2012).

147. Coles, M. M. and Andrews, D. L., "Chirality and angular momentum in optical radiation," *Phys. Rev. A* **85**, 063810 (2012).

148. Andrews, D. L. and Babiker, M., "Quantum Electrodynamics, Angular Momentum and Chirality," in *The Angular Momentum of Light*, D. L. Andrews and M. Babiker, eds., Cambridge University Press, Cambridge (2013).

149. Coles, M. M. and Andrews, D. L., "Photonic measures of helicity: optical vortices and circularly polarized reflection," *Opt. Lett.* **38**, 869–871 (2013).

150. Andrews, D. L., Dávila Romero, L. C. and Babiker, M., "On optical vortex interactions with chiral matter," *Opt. Commun.* **237**, 133–139 (2004).

151. Barnett, S. M. and Vaccaro, J. A., *The Quantum Phase Operator: A Review*, Taylor & Francis, New York (2007).

152. Machida, S., Yamamoto, Y. and Itaya, Y., "Observation of amplitude squeezing in a constant-current–driven semiconductor laser," *Phys. Rev. Lett.* **58**, 1000–1003 (1987).

153. Sztul, H. I. and Alfano, R. R., "The Poynting vector and angular momentum of Airy beams," *Opt. Express* **16**, 9411–9416 (2008).

154. Allen, L., Beijersbergen, M. W., Spreeuw, R. J. C. and Woerdman, J. P., "Orbital angular momentum of light and the transformation of Laguerre-Gaussian laser modes," *Phys. Rev. A* **45**, 8185–8189 (1992).

155. Chávez-Cerda, S., Padgett, M. J., Allison, I., New, G. H. C., Gutiérrez-Vega, J. C., O'Neil, A. T., MacVicar, I. and Courtial, J., "Holographic generation and orbital angular momentum of high-order Mathieu beams," *J. Opt. B: Quantum Semiclass. Opt.* **4**, S52–S57 (2002).

156. Volke-Sepulveda, K., Garcés-Chávez, V., Chávez-Cerda, S., Arlt, J. and Dholakia, K., "Orbital angular momentum of a high-order Bessel light beam," *J. Opt. B: Quantum Semiclass. Opt.* **4**, S82–S89 (2002).

157. Heckenberg, N. R., McDuff, R., Smith, C. P. and White, A. G., "Generation of optical-phase singularities by computer-generated holograms," *Opt. Lett.* **17**, 221–223 (1992).

158. Ostrovsky, A. S., Rickenstorff-Parrao, C. and Arrizón, V., "Generation of the 'perfect' optical vortex using a liquid-crystal spatial light modulator," *Opt. Lett.* **38**, 534–536 (2013).

159. Bazhenov, V. Y., Vasnetsov, M. and Soskin, M., "Laser beams with screw dislocations in their wavefronts," *JETP Lett.* **52**, 429–431 (1990).

160. Bazhenov, V. Y., Soskin, M. and Vasnetsov, M., "Screw dislocations in light wavefronts," *J. Mod. Opt.* **39**, 985–990 (1992).

161. Mirhosseini, M., Magana-Loaiza, O. S., Chen, C., Rodenburg, B., Malik, M. and Boyd, R. W., "Rapid generation of light beams carrying orbital angular momentum," *Opt. Express* **21**, 30196–30203 (2013).

162. Beijersbergen, M. W., Coerwinkel, R. P. C., Kristensen, M. and Woerdman, J. P., "Helical-wave-front laser-beams produced with a spiral phase plate," *Opt. Commun.* **112**, 321–327 (1994).

163. Beijersbergen, M. W., Allen, L., Vanderveen, H. E. L. O. and Woerdman, J. P., "Astigmatic laser mode converters and transfer of orbital angular-momentum," *Opt. Commun.* **96**, 123–132 (1993).

164. Marrucci, L., Manzo, C. and Paparo, D., "Optical spin-to-orbital angular momentum conversion in inhomogeneous anisotropic media," *Phys. Rev. Lett.* **96**, 163905 (2006).

165. Sun, J., Zeng, J. and Litchinitser, N. M., "Twisting light with hyperbolic metamaterials," *Opt. Express* **21**, 14975–14981 (2013).

166. Coles, M. M., Williams, M. D., Saadi, K., Bradshaw, D. S. and Andrews, D. L., "Chiral nanoemitter array: A launchpad for optical vortices," *Laser Photon. Rev.* **7**, 1088–1092 (2013).

167. Williams, M. D., Coles, M. M., Saadi, K., Bradshaw, D. S. and Andrews, D. L., "Optical vortex generation from molecular chromophore arrays," *Phys. Rev. Lett.* **111**, 153603 (2013).

168. Williams, M. D., Coles, M. M., Bradshaw, D. S. and Andrews, D. L., "Direct generation of optical vortices," *Phys. Rev. A* **89**, 033837 (2014).

169. Nye, J. F. and Berry, M. V., "Dislocations in wave trains," *Proc. R. Soc. A* **336**, 165–190 (1974).

170. Coullet, P., Gil, L. and Rocca, F., "Optical vortices," *Opt. Commun.* **73**, 403–408 (1989).

171. Dávila Romero, L. C., Andrews, D. L. and Babiker, M., "A quantum electrodynamics framework for the nonlinear optics of twisted beams," *J. Opt. B: Quantum Semiclass. Opt.* **4**, S66–S72 (2002).

172. Bouchal, Z. and Olivík, M., "Non-diffractive vector Bessel beams," *J. Mod. Opt.* **42**, 1555–1566 (1995).

173. McGloin, D. and Dholakia, K., "Bessel beams: Diffraction in a new light," *Contemporary Physics* **46**, 15–28 (2005).

174. Mazilu, M., Stevenson, D. J., Gunn-Moore, F. and Dholakia, K., "Light beats the spread: "non-diffracting" beams," *Laser Photon. Rev.* **4**, 529–547 (2010).

175. Aiello, A. and Agarwal, G. S., "Wave-optics description of self-healing mechanism in Bessel beams," *Opt. Lett.* **39**, 6819–6822 (2014).

176. López-Mariscal, C., Gutiérrez-Vega, J. C., Milne, G. and Dholakia, K., "Orbital angular momentum transfer in helical Mathieu beams," *Opt. Express* **14**, 4182–4187 (2006).

177. Alpmann, C., Bowman, R., Woerdemann, M., Padgett, M. and Denz, C., "Mathieu beams as versatile light moulds for 3D micro particle assemblies," *Opt. Express* **18**, 26084–26091 (2010).

178. Berkhout, G. C. G., Lavery, M. P. J., Courtial, J., Beijersbergen, M. W. and Padgett, M. J., "Efficient sorting of orbital angular momentum states of light," *Phys. Rev. Lett.* **105**, 153601 (2010).

179. Zhou, Y., Mirhosseini, M., Fu, D., Zhao, J., Hashemi Rafsanjani, S. M., Willner, A. E. and Boyd, R. W., "Sorting photons by radial quantum number," *Phys. Rev. Lett.* **119**, 263602 (2017).

180. Malik, M., Mirhosseini, M., Lavery, M. P., Leach, J., Padgett, M. J. and Boyd, R. W., "Direct measurement of a 27-dimensional orbital-angular-momentum state vector," *Nat. Commun.* **5**, 3115 (2014).

181. Xie, G. et al., "Performance metrics and design considerations for a free-space optical orbital-angular-momentum-multiplexed communication link," *Optica* **2**, 357–365 (2015).

182. Craig, D. P. and Thirunamachandran, T., *Molecular Quantum Electrodynamics: An Introduction to Radiation-Molecule Interactions*, Dover Publications, Mineola, NY (1998).

183. Milonni, P. W., *The Quantum Vacuum: An Introduction to Quantum Electrodynamics*, Academic Press, San Diego (1993).

184. Casimir, H. B. G., "On the attraction between two perfectly conducting plates," *Proc. K. Ned. Akad. Wet.* **51**, 793–795 (1948).

185. Milonni, P. W. and Shih, M.-L., "Casimir forces," *Contemporary Physics* **33**, 313–322 (1992).

186. Lin, W. H. and Zhao, Y. P., "Casimir effect on the pull-in parameters of nanometer switches," *Microsystem Technologies* **11**, 80–85 (2005).

187. Ma, J. B., Jiang, L. and Asokanthan, S. F., "Influence of surface effects on the pull-in instability of NEMS electrostatic switches," *Nanotechnology* **21**, 505708 (2010).

188. Klein, O. and Nishina, Y., "Über die Streuung von Strahlung durch freie Elektronen nach der neuen relativistischen Quantendynamik von Dirac," *Zeitschrift für Physik* **52**, 853–868 (1929).

189. Woolley, R., "The electrodynamics of atoms and molecules," *Adv. Chem. Phys.* **33**, 153–233 (1975).

190. Atkins, P. W. and Friedman, R. S., *Molecular Quantum Mechanics*, Oxford University Press, Oxford (2011).

191. Einstein, A., "Zur Quantentheorie der Strahlung," *Phys. Zeit.* **18**, 121–128 (1916).

192. Miller, R., Northup, T., Birnbaum, K., Boca, A., Boozer, A. and Kimble, H., "Trapped atoms in cavity QED: coupling quantized light and matter," *J. Phys. B: At. Mol. Opt. Phys.* **38**, S551–S565 (2005).

193. Andrews, D. L. and Ford, J. S., "Resonance energy transfer: Influence of neighboring matter absorbing in the wavelength region of the acceptor," *J. Chem. Phys.* **139**, 014107 (2013).

194. Feynman, R. P., Hibbs, A. R. and Styer, D. F., *Quantum Mechanics and Path Integrals*, Dover, New York (2010).

195. Andrews, D. L. and Allcock, P., "A quantum electrodynamical foundation for molecular photonics," *Adv. Chem. Phys.* **119**, 603–675 (2001).

196. Jenkins, R. D., Andrews, D. L. and Dávila Romero, L. C., "A new diagrammatic methodology for non-relativistic quantum electrodynamics," *J. Phys. B: At. Mol. Opt. Phys.* **35**, 445–468 (2002).

197. Bradshaw, D. S. and Andrews, D. L., "Quantum channels in nonlinear optical processes," *J. Nonl. Opt. Phys. Mat.* **18**, 285–299 (2009).

198. Philpott, M. R., "Reflection of light by a semi-infinite dielectric," *J. Chem. Phys.* **60**, 1410–1419 (1974).

199. Bloembergen, N., *Nonlinear Optics*, 4th Ed., World Scientific, Singapore (1996).

200. Jha, S. S., *Perspectives in Optoelectronics*, World Scientific, Singapore (1995).

201. Sauter, E. G., *Nonlinear Optics*, Wiley, New York (1996).

202. He, G. and Liu, S. H., *Physics of Nonlinear Optics*, World Scientific, Singapore (2000).

203. Shen, Y. R., *The Principles of Nonlinear Optics*, Wiley, New York (2002).

204. Sutherland, R. L., *Handbook of Nonlinear Optics*, 2nd Ed., Dekker, New York (2003).

205. Banerjee, P. P., *Nonlinear Optics: Theory, Numerical Modeling, and Applications*, Dekker, New York (2003).

206. Novotny, L. and Hecht, B., *Principles of Nano-Optics*, Cambridge University Press, Cambridge (2006).

207. Boyd, R. W., *Nonlinear Optics*, 3rd Ed., Academic Press, New York (2008).

208. Ward, J. F., "Calculation of nonlinear optical susceptibilities using diagrammatic perturbation theory," *Rev. Mod. Phys.* **37**, 1–18 (1965).

209. Andrews, D. L., "Molecular Theory of Harmonic Generation," pp. 545–606 in *Modern Nonlinear Optics*, Part 2., M. W. Evans and S. Kielich, eds., Wiley, New York (1993).

210. Andrews, D. L. and Allcock, P., "A Quantum Electrodynamical Foundation for Molecular Photonics," pp. 603–675 in *Modern Nonlinear Optics*, Part 1, M. W. Evans, ed., Wiley, New York (2001).

211. Andrews, D. L., "A simple statistical treatment of multiphoton absorption," *Am. J. Phys.* **53**, 1001–1002 (1985).

212. Dávila Romero, L. C., Naguleswaran, S., Stedman, G. E. and Andrews, D. L., "Electro-optic response in isotropic media," *Nonlinear Optics* **23**, 191–201 (2000).

213. Berkovic, G., Meshulam, G. and Kotler, Z., "Measurement and analysis of molecular hyperpolarizability in the two-photon resonance regime," *J. Chem. Phys.* **112**, 3997–4003 (2000).

214. Singer, K. D., Kuzyk, M. G. and Sohn, J. E., "Second-order nonlinear-optical processes in orientationally ordered materials: relationship between molecular and macroscopic properties," *J. Optics B: Quantum and Semiclassical Optics* **4**, 968–976 (1987).

215. Walls, D., "Quantum theory of nonlinear optical phenomena," *J. Phys. A: Math. Gen.* **4**, 813–826 (1971).

216. Andrews, D. L. and Bradshaw, D. S., "A photonic basis for deriving nonlinear optical response," *Eur. J. Phys.* **30**, 239–251 (2009).

217. Beaujean, P. and Champagne, B., "Coupled cluster evaluation of the second and third harmonic scattering responses of small molecules," *Theor. Chem. Acc.* **137**, 50 (2018).

218. Kwiat, P. G., Mattle, K., Weinfurter, H., Zeilinger, A., Sergienko, A. V. and Shih, Y., "New high-intensity source of polarization-entangled photon pairs," *Phys. Rev. Lett.* **75**, 4337 (1995).

219. Horodecki, R., Horodecki, P., Horodecki, M. and Horodecki, K., "Quantum entanglement," *Rev. Mod. Phys.* **81**, 865–942 (2009).

220. Walborn, S. P., Monken, C., Pádua, S. and Ribeiro, P. S., "Spatial correlations in parametric down-conversion," *Phys. Rep.* **495**, 87–139 (2010).

221. Müller, M., Bounouar, S., Jöns, K. D., Glässl, M. and Michler, P., "On-demand generation of indistinguishable polarization-entangled photon pairs," *Nat. Photonics* **8**, 224–228 (2014).

222. Barreiro, J. T., Langford, N. K., Peters, N. A. and Kwiat, P. G., "Generation of hyperentangled photon pairs," *Phys. Rev. Lett.* **95**, 260501 (2005).

223. Barreiro, J. T., Wei, T.-C. and Kwiat, P. G., "Remote preparation of single-photon 'hybrid' entangled and vector-polarization states," *Phys. Rev. Lett.* **105**, 030407 (2010).

224. Eisaman, M. D., Fan, J., Migdall, A. and Polyakov, S. V., "Single-photon sources and detectors," *Rev. Sci. Instrum.* **82**, 071101 (2011).

225. Marcuse, D., *Engineering Quantum Electrodynamics*, Harcourt, Brace & World, San Diego (1970).

226. Milosevic, M., *Internal Reflection and ATR Spectroscopy*, John Wiley & Sons, Hoboken, NJ (2012).

227. Synge, E. H., "A suggested method for extending microscopic resolution into the ultra-microscopic region," *Phil. Mag*. **6**, 356–362 (1928).

228. Betzig, E. and Trautman, J. K., "Near-field optics: Microscopy, spectroscopy, and surface modification beyond the diffraction limit," *Science* **257**, 189–195 (1992).

229. Novotny, L. and Stranick, S. J., "Near-field optical microscopy and spectroscopy with pointed probes," *Annu. Rev. Phys. Chem.* **57**, 303–331 (2006).

230. Lewis, A., Taha, H., Strinkovski, A., Manevitch, A., Khatchatouriants, A., Dekhter, R. and Ammann, E., "Near-field optics: from subwavelength illumination to nanometric shadowing," *Nat. Biotechnol.* **21**, 1378–1386 (2003).

231. Dickenson, N. E., Armendariz, K. P., Huckabay, H. A., Livanec, P. W. and Dunn, R. C., "Near-field scanning optical microscopy: a tool for nanometric exploration of biological membranes," *Anal. Bioanal. Chem.* **396**, 31–43 (2010).

232. Zayats, A. V. and Smolyaninov, I. I., "Near-field photonics: surface plasmon polaritons and localized surface plasmons," *J. Opt. A: Pure Appl. Opt.* **5**, S16–S50 (2003).

233. Want, R., "Near field communication," *IEEE Pervasive Comput.* **10**, 4–7 (2011).

234. Rice, E. M., Bradshaw, D. S., Saadi, K. and Andrews, D. L., "Identifying the development in phase and amplitude of dipole and multipole radiation," *Eur. J. Phys*. **33**, 345–358 (2012).

235. Jackson, J. D., *Classical Electrodynamics*, Wiley, New York (1998).

236. Andrews, D. L., "A unified theory of radiative and radiationless molecular energy transfer," *Chem. Phys.* **135**, 195–201 (1989).

237. Andrews, D. L. and Bradshaw, D. S., "The role of virtual photons in nanoscale photonics," *Ann. Phys.* (Berlin) **526**, 173–186 (2014).

238. Andrews, D. L. and Demidov, A. A., *Resonance Energy Transfer*, Wiley, Chichester (1999).

239. May, V., *Charge and Energy Transfer Dynamics in Molecular Systems*, John Wiley & Sons, Hoboken, NJ (2008).

240. Andrews, D. L. and Sherborne, B. S., "Resonant excitation transfer: A quantum electrodynamical study," *J. Chem. Phys.* **86**, 4011–4017 (1987).

241. Daniels, G. J., Jenkins, R. D., Bradshaw, D. S. and Andrews, D. L., "Resonance energy transfer: The unified theory revisited," *J. Chem. Phys.* **119**, 2264–2274 (2003).

242. Andrews, D. L., "Mechanistic principles and applications of resonance energy transfer," *Can. J. Chem.* **86**, 855–870 (2008).

243. Freeman, A. W., Koene, S. C., Malenfant, P. R. L., Thompson, M. E. and Fréchet, J. M. J., "Dendrimer-containing light-emitting diodes: Toward site-isolation of chromophores," *J. Am. Chem. Soc.* **122**, 12385–12386 (2000).

244. Anthopoulos, T. D., Markham, J. P. J., Namdas, E. B., Lawrence, J. R., Samuel, I. D. W., Lo, S.-C. and Burn, P. L., "Influence of molecular structure on the properties of dendrimer light-emitting diodes," *Org. Electron.* **4**, 71–76 (2003).

245. Furuta, P., Brooks, J., Thompson, M. E. and Fréchet, J. M. J., "Simultaneous light emission from a mixture of dendrimer encapsulated chromophores: A model for single-layer multichromophoric organic light-emitting diodes," *J. Am. Chem. Soc.* **125**, 13165–13172 (2003).

246. Burn, P. L., Lo, S. C. and Samuel, I. D. W., "The development of light-emitting dendrimers for displays," *Adv. Mater.* **19**, 1675–1688 (2007).

247. Youl Yang, K., Cheol Choi, K. and Won Ahn, C., "Surface plasmon-enhanced energy transfer in an organic light-emitting device structure," *Opt. Express* **17**, 11495–11504 (2009).

248. Ghataora, S., Smith, R. M., Athanasiou, M. and Wang, T., "Electrically injected hybrid organic/inorganic III-nitride white light-emitting diodes with nonradiative Förster resonance energy transfer," *ACS Photonics* **5**, 642–647 (2018).

249. Miyakawa, T. and Dexter, D. L., "Cooperative and stepwise excitation of luminescence: Trivalent rare-earth ions in Yb^{3+}-sensitized crystals," *Phys. Rev. B* **1**, 70–80 (1970).

250. Auzel, F., "Upconversion processes in coupled ion systems," *J. Lumin.* **45**, 341–345 (1990).

251. Chua, M. and Tanner, P. A., "Three-body energy transfer processes of lanthanide ions in crystals," *J. Lumin.* **66–67**, 203–207 (1995).

252. Andrews, D. L. and Jenkins, R. D., "A quantum electrodynamical theory of three-center energy transfer for upconversion and downconversion in rare earth doped materials," *J. Chem. Phys.* **114**, 1089–1100 (2001).

253. Leeder, J. M. and Andrews, D. L., "Enhancing optical up-conversion through electrodynamic coupling with ancillary chromophores," *J. Phys. Chem. C* **118**, 23535–23544 (2014).

254. Zhuang, R. and Wang, G., "Sequential energy transfer up-conversion process in Yb^{3+}/Er^{3+}: $SrMoO_4$ crystal," *Opt. Express* **24**, 7543–7557 (2016).

255. Lovett, B. W., Reina, J. H., Nazir, A., Kothari, B. and Briggs, G. A. D., "Resonant transfer of excitons and quantum computation," *Phys. Lett. A* **315**, 136–142 (2003).

256. Govorov, A. O., "Spin and energy transfer in nanocrystals without tunneling," *Phys. Rev. B* **68**, 075315 (2003).

257. Sangu, S., Kobayashi, K., Shojiguchi, A. and Ohtsu, M., "Logic and functional operations using a near-field optically coupled quantum-dot system," *Phys. Rev. B* **69**, 115334 (2004).

258. Bradshaw, D. S. and Andrews, D. L., "Optically controlled resonance energy transfer: Mechanism and configuration for all-optical switching," *J. Chem. Phys.* **128**, 144506 (2008).

259. Bradshaw, D. S. and Andrews, D. L., "All-optical switching between quantum dot nanoarrays," *Superlatt. Microstruct.* **47**, 308–313 (2010).

260. Ashkin, A., "Acceleration and trapping of particles by radiation pressure," *Phys. Rev. Lett.* **24**, 156–159 (1970).

261. Ashkin, A., Dziedzic, J. M., Bjorkholm, J. E. and Chu, S., "Observation of a single-beam gradient force optical trap for dielectric particles," *Opt. Lett.* **11**, 288–290 (1986).

262. Grier, D. G., "A revolution in optical manipulation," *Nature* **424**, 810–816 (2003).

263. Swartzlander, G. A., Peterson, T. J., Artusio-Glimpse, A. B. and Raisanen, A. D., "Stable optical lift," *Nat. Photonics* **5**, 48–51 (2011).

264. Bradshaw, D. S. and Andrews, D. L., "Manipulating particles with light: radiation and gradient forces," *Eur. J. Phys.* **38**, 034008 (2017).

265. Cohen-Tannoudji, C. and Guéry-Odelin, D., *Advances in Atomic Physics. An Overview*, World Scientific, Singapore (2011).

266. Van der Straten, P. and Metcalf, H., *Atoms and Molecules Interacting with Light: Atomic Physics for the Laser Era*, Cambridge University Press, Cambridge (2016).

267. Arita, Y., Mazilu, M. and Dholakia, K., "Laser-induced rotation and cooling of a trapped microgyroscope in vacuum," *Nat. Commun.* **4**, 2374 (2013).

268. Padgett, M. J. and Bowman, R., "Tweezers with a twist," *Nat. Photonics* **5**, 343–348 (2011).

269. Thirunamachandran, T., "Intermolecular interactions in the presence of an intense radiation field," *Mol. Phys.* **40**, 393–399 (1980).

270. Bradshaw, D. S. and Andrews, D. L., "Optically induced forces and torques: Interactions between nanoparticles in a laser beam," *Phys. Rev. A* **72**, 033816 (2005).

271. Salam, A., "Intermolecular interactions in a radiation field via the method of induced moments," *Phys. Rev. A* **73**, 013406 (2006).

272. Simpson, S. H., Zemánek, P., Maragò, O. M., Jones, P. H. and Hanna, S., "Optical binding of nanowires," *Nano Lett.* **17**, 3485–3492 (2017).

273. Andrews, D. L., *Energy Harvesting Materials*, World Scientific, New Jersey (2005).

274. Scholes, G. D., Fleming, G. R., Olaya-Castro, A. and van Grondelle, R., "Lessons from nature about solar light harvesting," *Nat. Chem*. **3**, 763–774 (2011).

275. Tsao, J. Y. et al., "Toward smart and ultra-efficient solid-state lighting," *Adv. Optical Mater.* **2**, 809–836 (2014).

276. Andrews, D. L., "Photon," *Europhys. Lett.* **111**, 40000 (2015).

Further Reading

Al-Amri, M. D., El-Gomati, M. M. and Zubairy, M. S., *Optics in Our Time*, Springer International, Cham, Switzerland (2016).

Andrews, D. L., *Structured Light and its Applications: An Introduction to Phase-Structured Beams and Nanoscale Optical Forces*, Academic Press, Amsterdam (2008).

Andrews, D. L., *Photonics* (four volumes), Wiley, Hoboken, NJ (2015).

Andrews, D. L. and Allcock, P., *Optical Harmonics in Molecular Systems*, Wiley-VCH, Weinheim, Germany (2002).

Andrews, D. L. and Babiker, M., *The Angular Momentum of Light*, Cambridge University Press, Cambridge (2013).

Andrews, D. L. and Bradshaw, D. S., *Optical Nanomanipulation*, Morgan and Claypool, San Rafael, CA (2016).

Ball, D. W., *Maxwell's Equations of Electrodynamics: An Explanation*, SPIE Press, Bellingham, WA (2012).

Bouwmeester, D., Ekert, A. and Zeilinger, A., *The Physics of Quantum Information*, Springer, Berlin (2000).

Boyd, R. W., *Nonlinear Optics*, Academic Press, New York (2008).

Craig, D. P. and Thirunamachandran, T., *Molecular Quantum Electrodynamics: An Introduction to Radiation-Molecule Interactions*, Dover Publications, Mineola, NY (1998).

Datta, A. K. and Munshi, S., *Information Photonics: Fundamentals, Technologies, and Applications*, CRC Press, Boca Raton, FL (2016).

Drummond, P. D and Hillery, M., *The Quantum Theory of Nonlinear Optics*, Cambridge University Press, Cambridge (2014).

Duarte, F. J., *Quantum Optics for Engineers*, CRC Press, Boca Raton, FL (2014).

Grynberg, G., Aspect, A. and Fabre, C., *Introduction to Quantum Optics: From the Semi-Classical Approach to Quantized Light*, Cambridge University Press, Cambridge (2010).

Haus, J. W., *Fundamentals and Applications of Nanophotonics*, Woodhead, Oxford (2016).

Hecht, E., *Optics*, 5th Ed., Pearson, Hoboken, NJ (2016).

Jones, J. A., *Quantum Information, Computation and Communication*, Cambridge University Press, Cambridge (2012).

Li, Y., *Plasmonic Optics: Theory and Applications*, SPIE Press, Bellingham, WA (2017).

Loudon, R., *The Quantum Theory of Light*, 3rd Ed., Oxford University Press, Oxford (2000).

Mandel, L. and Wolf, E., *Optical Coherence and Quantum Optics*, Cambridge University Press, Cambridge (1995).

Milonni, P. W., *The Quantum Vacuum: An Introduction to Quantum Electrodynamics*, Academic Press, San Diego, CA (1993).

Nelson, P., *From Photon to Neuron: Light, Imaging, Vision*, Princeton University Press, Princeton (2017).

Reider, G. A., *Photonics*, Springer, Heidelberg, Germany (2016).

Rieffel, E., Polak, W. H. and Polak, W., *Quantum Computing: A Gentle Introduction*, MIT Press, Cambridge, MA (2014).

Williams, C. P., *Explorations in Quantum Computing*, Springer, London (2011).

Index

David L. Andrews is a Professor at the University of East Anglia, UK, and leads research on fundamental molecular photonics, energy harvesting and transport, opto-mechanical forces, and quantum and nonlinear optics. He has over 350 research papers and 20 books to his name. The current focus of his research group involves the quantum aspects of optical transmission, optical vortices and chirality, frequency conversion, optical nanomanipulation and switching, optically nonlinear mechanisms in fluorescence, and energy-transfer processes. Andrews is a Fellow of SPIE, the Optical Society of America, the Royal Society of Chemistry, and the Institute of Physics. He is also a member of the Board of Directors of SPIE.

David S. Bradshaw is an honorary research associate at the University of East Anglia. He graduated twice from the same university, first receiving a Master's degree in chemical physics (which included a year at the University of Western Ontario, London, Canada) and then a Ph.D. in theoretical chemical physics. Overall, he has co-written 80 research papers, including book chapters, all based on molecular quantum electrodynamics. He has also created a website explaining the key physics in this theory. His long-running research interests include optical trapping, resonance energy transfer, optical binding, and nonlinear optics. Bradshaw is a Member of the Institute of Physics and the Royal Society of Chemistry.